

Distribution Agreement

In presenting this thesis or dissertation as a partial fulfillment of the requirements for an advanced degree from Emory University, I hereby grant to Emory University and its agents the non-exclusive license to archive, make accessible, and display my thesis or dissertation in whole or in part in all forms of media, now or hereafter known, including display on the world wide web. I understand that I may select some access restrictions as part of the online submission of this thesis or dissertation. I retain all ownership rights to the copyright of the thesis or dissertation. I also retain the right to use in future works (such as articles or books) all or part of this thesis or dissertation.

Signature:

Dana Val Shaw Fallaize

Date

Mitochondrial regulation in health and neurodegenerative disease

By

Dana Val Shaw Fallaize
Doctor of Philosophy

Graduate Division of Biological and Biomedical Sciences
Microbiology and Molecular Genetics

Lih-Shen Chin, Ph.D.
Advisor

Lian Li, Ph.D.
Co-advisor

Victor Faundez, M.D, Ph.D.
Committee Member

Daniel Kalman Ph.D.
Committee Member

Martin Moore, Ph.D.
Committee Member

Keith Wilkinson, Ph.D.
Committee Member

Elizabeth Wright, Ph.D.
Committee Member

Accepted:

Lisa A. Tedesco, Ph.D.
Dean of the James T. Laney School of Graduate Studies

Date

Mitochondrial regulation in health and neurodegenerative disease

By

Dana Val Shaw Fallaize
Bachelor of Arts, Molecular Biology, Colgate University, 2007

Advisors: Lih-Shen Chin Ph.D. and Lian Li Ph.D.

An abstract of

A dissertation submitted to Faculty of the
James T. Laney School of Graduate Studies of Emory University
in partial fulfillment of the requirements for the degree of
Doctor of Philosophy

Graduate Division of Biological and Biomedical Sciences
Microbiology and Molecular Genetics Program
2014

Mitochondrial regulation in health and neurodegenerative disease

By: Dana Val Shaw Fallaize

ABSTRACT

Mitochondria are responsible for energy production, calcium buffering, and the regulation of cell death. Mitochondrial dysfunction due to genetic mutations or environmental insults results in the inability to respond to energy needs, accumulation of oxidative stress, cell dysfunction, cell death, and disease. In this study, we examined the role of two proteins, PINK1 and Mgrn1 and their roles in neuroprotection.

Using structured illumination microscopy (SIM), we determined that PINK1 was dual targeted to separate regions of the mitochondria responding to mitochondrial health. We also observed Parkinson's disease linked mutants of PINK1 have aberrant submitochondrial targeting and fail to recruit parkin to damaged mitochondria in neurons.

We determined that loss of Mgrn1 might regulate mitochondrial dynamics. Our data show that loss of Mgrn1-mediated ubiquitination results in mitochondrial fragmentation, accumulation of damaged mitochondria, and increased susceptibility to oxidative stress induced cell death, which may contribute to pathogenesis of spongiform neurodegeneration.

Together the findings presented in this dissertation reveal novel insights into the regulation of mitochondrial dynamics and health related to neurodegenerative diseases. We determined that Mgrn1 may regulate mitochondrial dynamics in response to age-related stresses and PINK1 functions as a molecular switch to trigger two separate signaling cascades related to protection from mitochondrial dysfunction.

Mitochondrial regulation in health and neurodegenerative disease

By

Dana Val Shaw Fallaize
Bachelor of Arts, Molecular Biology, Colgate University, 2007

Advisors: Lian Li Ph.D. and Lih-Shen Chin Ph.D

A dissertation submitted to the Faculty of the
James T. Laney School of Graduate Studies of Emory University
in partial fulfillment of the requirements for the degree of
Doctor of Philosophy in the Graduate Division of Biological and Biomedical Science
Microbiology and Molecular Genetics

2014

Acknowledgements

I would like to thank my advisors, Dr. Lian Li and Dr. Lih-Shen Chin for their mentorship over the last five years. I appreciate that they opened their doors for me when I was searching for a lab to join. I would also like to thank the members of my committee: Dr. Victor Faundez, Dr. Keith Wilkinson, Dr. Elizabeth Wright, Dr. Martin Moore, and Dr. Dan Kalman. Through their encouragement and support, I was able to develop into a mature scientist. I also want to thank my other sources for career and personal development, Emory University's Office of Technology Transfer and Georgia Bio and ELN.

I am grateful to the former and current members of the lab including Jue Chen, Sammy Lee, Jennifer Hurst-Kennedy, Patrick Reynolds, Hong Tang, Haishan Yin, Di Sha, Jeanne McKeon, Crystal Lee, and Cheryl Ho. Without their experimental and emotional support, I doubt that I would have been able to make it this far. They were there for me through the highs and lows of academic science.

I want to thank my parents, Ardan and Tom Shaw, and my in-laws, Beth and Mike Fallaize for their understanding. They tolerated my need to miss family events or leave early to get back to the lab. They've kept me strong and helped me remain focused throughout the years.

And finally, I want to thank my husband for his support over the last 7 years. My husband, Cal Fallaize, has been such a rock for me. I want to thank him for trudging with me to the lab on the weekends or in the middle of the night and being a constant source of reassurance. His patience and love throughout this process is more than I ever could have asked for, and I'll be forever grateful.

Abstract

Acknowledgements

Table of Contents

List of Tables and Figures

Table of Contents

CHAPTER I 1

INTRODUCTION AND BACKGROUND 1

OPENING REMARKS 2

MITOCHONDRIA 3

 Structure 3

FUNCTIONS OF THE MITOCHONDRIA 5

 Cellular respiration 5

 Calcium buffering 6

 Apoptosis 7

CONSEQUENCES OF MITOCHONDRIAL DYSFUNCTION 8

 The role of oxidative stress in aging and disease 10

 The role of mitochondrial DNA in aging and disease 12

MITOCHONDRIAL DYNAMICS 13

 Fusion 15

 Fission 17

 Posttranslational modifications regulate fission and fusion protein activity 18

 Mitophagy 19

NEURODEGENERATIVE DISEASES LINKED TO MITOCHONDRIAL	
DYSFUNCTION.....	20
Parkinson’s disease (PD).....	21
PD genetics linked to mitochondrial dysfunction.....	22
1. PINK1.....	22
2. Parkin.....	23
3. a-synuclein.....	24
4. DJ-1.....	25
Environmental causes of PD.....	25
Human spongiform neurodegenerative disorders.....	27
1. Alzheimer’s disease (AD).....	28
2. Prion diseases.....	29
3. Lysosomal storage disorders.....	31
Animal models of spongiform neurodegeneration.....	33
1. Mahogunin RING finger 1 (Mgrr1) mutant mice.....	33
2. Attractin (Atrn) mutant mice and rats.....	35
3. Manganese superoxide dismutase (SOD2 or MnSOD) mutant mice.....	36
DIAGNOSTICS AND THERAPEUTICS.....	36
Therapeutics in PD.....	37
Therapeutics in spongiform neurodegenerative disorders.....	38
Mitochondrial targets for the development of novel therapeutics against neurodegenerative diseases.....	40
HYPOTHESES AND OVERVIEW.....	41

CHAPTER II.....	70
SUBMITOCHONDRIAL SITES OF PINK1 ACTION REVEALED BY 3D-SIM SUPER-RESOLUTION MICROSCOPY	70
Abstract	72
Introduction	73
Results.....	75
Dual color 3D-SIM super- resolution imaging analysis enables visualization of protein submitochondrial localization	75
PINK1 resides in the cristae membrane/intracristae space of healthy mitochondria and translocates to the OMM upon mitochondrial depolarization	76
PINK1 colocalizes with TRAP1 in the IMM/IMS of healthy mitochondria and colocalizes with parkin on the OMM of dysfunctional mitochondria.....	78
Mitochondrial depolarization-induced PINK1 translocation to the OMM is independent of new PINK1 protein synthesis	79
The ability of PINK1 to translocate to the OMM is impaired by PD-linked PINK1 C92F and W437X mutations	80
PINK1 translocates to the OMM to recruit parkin upon mitochondrial depolarization in neurons and the translocation requires combined action of PINK1 transmembrane and C-terminal domains.....	82
Discussion	83
Materials and methods.....	86
Expression constructs and antibodies	86
Cell transfection and treatment.....	87

PINK1 knockout mice and primary neuronal culture.....	88
Parkin recruitment in neurons.....	88
3D-Structured Illumination Microscopy	89
Image analysis	89
Quantification of colocalization	90
Statistical analysis.....	90
Acknowledgments.....	91
Abbreviations list.....	91
CHAPTER III.....	110
SPONGIFORM NEURODEGENERATION LINKED E3 LIGASE MGRN1 IS LOCALIZED TO MITOCHONDRIA WHERE IT REGULATES MITOCHONDRIAL MORPHOLOGY	110
Abstract	111
Introduction	112
Results.....	115
Mgrn1 mutant mice suffer from spongiform neurodegeneration	115
Mgrn1 is primary localized to mitochondria	116
The putative <i>N</i> -myristoylation motif is required for mitochondrial localization of Mgrn1	117
Mgrn1 regulates mitochondrial morphology.....	119
Mgrn1 is required for mitochondrial health	121
Mitochondria from aged Mgrn1 mutant mice exhibit ultrastructural defects as shown by electron microscopy.....	122

Mgrn1 is cytoprotective against mitochondrial dysfunction	123
Discussion	124
Materials and Methods	127
Expression constructs and antibodies	127
Cell transfection and treatment	128
Mgrn1 mutant mice and primary cell cultures.....	128
Hematoxylin and eosin staining	129
Immunofluorescence confocal microscopy	129
3D-Structured illumination microscopy	130
Purification of mitochondria.....	130
Live imaging of mitochondria	131
Perfusion of mice and electron microscopy	132
Cell viability and apoptosis assays	132
Image analysis	133
Quantification of colocalization	133
Mitochondrial Length.....	133
Mitochondrial membrane potential	134
Statistical analysis.....	134
Acknowledgments.....	135
CHAPTER IV	151
DISCUSSION AND FUTURE DIRECTIONS	151
Summary of Findings	152
PINK1 DISCUSSION AND FUTURE DIRECTIONS	153

3D-SIM analyses provide insights into PINK1 spatiotemporal dynamics	153
3D-SIM can differentiate submitochondrial compartments	153
PINK1 is dual targeted depending on the health of mitochondria	157
PINK1 differentially colocalizes with its substrates depending on mitochondrial health	158
Reduced OMM-translocation of PINK1 as a novel mechanism of PD pathogenesis	160
PD-linked mutants of PINK1 are not translocated to the OMM following loss of membrane potential	160
Translocation-defective PINK1 mutants are unable to recruit parkin to damaged mitochondria	161
PINK1 Future Directions	163
Determine the structural determinants of PINK1 dual targeting	163
What are the physiological triggers of PINK1 translocation?	164
How does PINK1 translocate?	165
Determine the effect of translocation defective PINK1 mutants in cell death and neurodegeneration	166
MGRN1 DISCUSSION	168
Mgrn1 is targeted to the outer mitochondrial membrane via <i>N</i> -myristoylation	168
Mgrn1 is primarily localized to mitochondria	168
<i>N</i> -myristoylation targets Mgrn1 to the OMM	169
Mgrn1 maintains mitochondrial health	170
Loss of Mgrn1 results in mitochondrial fragmentation	170

Loss of Mgrn1 results in mitochondrial dysfunction.....	171
Ubiquitination of Mgrn1 mitochondrial substrate(s) may confer cytoprotection....	172
Mgrn1 Future Directions	173
Identification of mitochondrial substrates of Mgrn1-mediated ubiquitination	173
Does Mgrn1 inhibit mitochondrial fission or promote mitochondrial fusion?.....	174
How do the mitochondrial and endosomal roles of Mgrn1 contribute to neuronal health?.....	175
What is the link between Mgrn1 deficiency and spongiform neurodegenerative diseases?	177
FINAL WORDS.....	178

FIGURES AND TABLES

CHAPTER I: INTRODUCTION AND BACKGROUND

Figure I-1: Compartmentalization is essential to mitochondrial functions.....	45
Figure I-2: Causes and effects of mitochondrial dysfunction.....	46
Table I-1: Neurodegenerative diseases with links to mitochondrial dysfunction.	47
Table I-2: Models of mitochondrial dysfunction causes neurodegeneration	48

CHAPTER II: SUBMITOCHONDRIAL SITES OF PINK1 ACTION REVEALED BY 3D-SIM SUPER-RESOLUTION MICROSCOPY

Figure II-1: Super-resolution imaging of submitochondrial compartments by dual color 3D-SIM fluorescence microscopy.....	96
Figure II-2: PINK1 resides in the cristae membrane/intracristae space under normal conditions and translocates to the OMM following mitochondrial depolarization.....	98
Figure II-3: PINK1 colocalizes with TRAP1 in the IMM/IMS of healthy mitochondria and colocalizes with parkin on the OMM following mitochondrial depolarization.....	100
Figure II-4: Mitochondrial depolarization-induced PINK1 OMM translocation is impaired by PINK1 Δ TM, C92F, and W437X mutations.....	102
Figure II-5: The transmembrane domain and C-terminal region are required for OMM translocation and parkin recruitment in neurons.....	104
Figure II-S1: PINK1 translocates to the OMM following loss of $\Delta\Psi$ but not loss of Δ pH, ATP, or microtubule integrity.....	106

Figure II-S2: Timecourse of mitochondrial depolarization-induced PINK1 translocation to the OMM.....	108
Figure II-S3: Mitochondrial depolarization-induced PINK1 OMM translocation does not require new protein synthesis.....	109

CHAPTER III: SPONGIFORM NEURODEGENERATION LINKED E3 LIGASE MGRN1 IS LOCALIZED TO MITOCHONDRIA WHERE IT REGULATES MITOCHONDRIAL MORPHOLOGY

Figure III-1: Neuropathology of Mgrn1 mutant mice:.....	140
Figure III-2: Endogenous localization of Mgrn1:.....	141
Figure III-3: <i>N</i> -myristoylation targets Mgrn1 to the outer mitochondrial membrane:.....	143
Figure III-4: Overexpression of Mgrn1 promotes mitochondrial elongation:...	145
Figure III-5: Loss of Mgrn1 expression affects mitochondrial morphology.....	146
Figure III-6: Mgrn1 mutant neurons exhibit reduced mitochondrial membrane potential:.....	147
Figure III-7: Mitochondrial ultrastructural defects observed in aged Mgrn1 mutant mouse brains:.....	148
Figure III-8: Mitochondrially localized Mgrn1 is cytoprotective against oxidative stress and mitochondrial dysfunction:.....	149

CHAPTER I

INTRODUCTION AND BACKGROUND

OPENING REMARKS

Mitochondria are essential organelles that carry out important cellular functions including energy production, calcium buffering, and regulation of apoptotic cell death [1]. Mitochondrial functions and dynamics are tightly controlled processes and dysregulation of these activities is linked to several diseases including cancer, autoimmune disorders, and neurodegenerative diseases. Both genetic and environmental exposure to toxins can result in mitochondrial dysfunction and neurodegenerative diseases. Better understanding of the functions and dysfunctions of the proteins regulating mitochondrial health will provide novel insights into the pathogenesis of neurodegenerative diseases.

PINK1 is a mitochondrially-localized kinase and loss-of-function mutations result in early onset Parkinson's disease (PD) [2,3]. PINK1 has two previously characterized substrates: the E3 ubiquitin protein ligase parkin [4] and the mitochondrial chaperone TRAP1 [5]. Dysregulation of PINK1-mediated phosphorylation has been implicated in mitochondrial dysfunction, neuronal dysfunction, cell death, and disease [6-8]. The spatiotemporal dynamics of PINK1 signaling is highly debated and clarification of its localization is critical to understanding PD pathogenesis and mitochondrial quality control.

Loss of the E3 ligase, Mahogunin RING finger 1 (Mgrn1), results in age dependent spongiform neurodegeneration in mice [9]. Mgrn1 deficient mice exhibit mitochondrial dysfunction and accumulation of reactive oxygen species (ROS) preceding the onset of spongiform neurodegeneration, implicating mitochondrial dysfunction as an underlying cause of spongiform neurodegeneration in these animals [10]. This study is the first to identify a mitochondrial role for Mgrn1. Experiments described in the

following chapters investigate the roles of PINK1 and Mgrn1 in regulating mitochondrial signaling, dynamics, and health. These results yield important insights into mitochondrial quality control and how dysfunctions in these processes may lead to neurodegenerative diseases.

MITOCHONDRIA

Mitochondria are important cellular organelles that, in addition to functioning in cellular respiration, play an integral role in calcium buffering [11] and cell death [12]. Loss of mitochondrial function causes accumulation of toxic reactive oxygen species (ROS) leading to protein, organelle, cellular dysfunction, and eventually cell death. Errors in mitochondrial signaling have been strongly implicated in the pathogenesis of diseases including many neurodegenerative disorders such as PD, Alzheimer's disease (AD), prion diseases, Amyotrophic lateral sclerosis (ALS), and Huntington's disease [13] [14]. Understanding mitochondrial function and the consequences of mitochondrial dysfunction will provide novel insights to understand disease pathogenesis.

Structure

Mitochondrial functions are heavily compartmentalized allowing multiple processes to take place in different regions of the mitochondria [15]. Alterations in mitochondrial ultrastructure or incorrect targeting of proteins within the mitochondrial subcompartments can cause defects in mitochondrial signaling and activity. Mitochondria are double membraned organelles and the two mitochondrial membranes separate the

aqueous compartments (Fig 1). The outer mitochondrial membrane OMM separates the mitochondria from the cellular cytosol, while the inner mitochondrial membrane (IMM) divides the mitochondrial aqueous compartments into the intermembrane space (IMS) and the mitochondrial matrix. The IMM folds back and forth to create the mitochondrial cristae, providing increased surface area for the electron transport chain ETC, which is imbedded in the IMM. The cristae junction divides the IMM and IMS into two distinct domains. The section of the IMM that parallels the OMM is called the inner boundary membrane, while the section perpendicular to the OMM and within the cristae fold is the cristae membrane. The region of the IMS between the IMM and OMM is the peripheral intermembrane space. The region between the cristae folds is called the intercristae space, where cytochrome *c*, part of the ETC and an essential signaling component of apoptosis, is localized under normal conditions (Fig. 1) [17].

Although mitochondria contain their own DNA, the mitochondrial genome (mtDNA) only contains genes for 13 polypeptides. The 13 mtDNA-encoded proteins are components of the ETC oxidative phosphorylation (OXPHOS) system and are translated on mitochondrial ribosomes. The remaining mitochondrial proteins, including other protein components required for OXPHOS, are encoded by nuclear DNA, transcribed on cytosolic ribosomes and transported to and/or imported into the mitochondria. Many of these proteins contain a mitochondrial targeting sequence (MTS), which is cleaved once the protein enters the mitochondrial matrix. Proteins can also localize to mitochondria through interacting with mitochondrial membranes or other mitochondrial proteins. Protein localization within the mitochondria is essential to mitochondrial signaling and activity.

FUNCTIONS OF THE MITOCHONDRIA

Cellular respiration

Mitochondria are the essential organelles for OXPHOS, or the process in which the majority of cellular energy is produced. Mitochondria generate energy via the ETC from glucose and fats through the TCA cycle and β -oxidation, respectively. Hydrogen derived from consumed food is oxidized, creating ATP. Briefly, electrons are passed to electron acceptors of increasing strength and release energy with each exchange. Electrons are transferred from $\text{NADH} + \text{H}^+$ to NADH dehydrogenase (complex I) or from succinate to succinate dehydrogenase (complex II). Electrons are then passed to ubiquinone, a mobile carrier, reducing ubiquinone into ubiquinol, which can freely diffuse through the membrane. Ubiquinol then transfers electrons to cytochrome bc_1 complex (complex III). Cytochrome bc_1 passes electrons to another mobile carrier, cytochrome c , which transfers electrons to cytochrome c oxidase (complex IV). Finally, electrons are transported to O_2 to produce H_2O . The energy produced by the free flow of electrons down the ETC is coupled to pump electrons through complexes I, II, and IV against their concentration gradient into the IMS, creating an electrochemical gradient. The energy produced from protons flowing back into the matrix from the IMS via ATP synthase (Complex V) is harnessed to combine adenosine diphosphate (ADP) and free phosphate to form ATP.

Defects in the ETC result in the inability to respond to energy demands and increased production of ROS. Specifically, inhibition of complex I and complex III have been shown to increase ROS production [18,19]. Reduced ATP production can result in increased susceptibility to cell death and neurodegeneration [20,21].

Calcium buffering

Mitochondria are key regulators of intracellular Ca^{2+} [22]. Ca^{2+} is an important second messenger involved in signaling for cell migration, neuronal transmission, muscle contraction, cell growth, and synaptic plasticity. Mitochondria can rapidly take up and slowly release Ca^{2+} providing control over Ca^{2+} levels in the cell and consequently mediate cellular responses [23]. Because mitochondria regulate intracellular Ca^{2+} levels, mitochondrial dysfunction can result in Ca^{2+} imbalance affecting multiple cell processes that rely on Ca^{2+} signaling. Additionally, mitochondrial Ca^{2+} levels are also critical to OXPHOS and the stimulation of ATP synthase [24]. Ca^{2+} is taken up by mitochondria through the mitochondria Ca^{2+} uniporter (MCU) which transports Ca^{2+} against the electrochemical gradient created by the ETC (reviewed in [25]) (Fig. 1). Mitochondrial Ca^{2+} buffering regulates the activity of Ca^{2+} channels [26]. Ca^{2+} flux into the mitochondria is dependent on mitochondrial membrane potential [27]. Ca^{2+} can leave the mitochondria via the permeability transport pore [28].

Ca^{2+} signaling is particularly important for neurons. Ca^{2+} levels are closely tied to neuronal functions such as neuronal transmission and synaptic plasticity [29,30]. As neurons age, their ability to buffer Ca^{2+} is reduced, resulting in increased intracellular

Ca²⁺ levels. Increased intracellular Ca²⁺ can result in aberrant signaling, accumulation of ROS, mitochondrial dysfunction, and apoptosis. In addition, the complicated architecture of neurons coupled with the large energy needs at distal regions of the neuron underscores the necessity of Ca²⁺ sensing for mitochondrial distribution in neurons.

Defects in of Ca²⁺ signaling has been implicated in the pathogenesis of neurodegenerative disorders [31]. As mitochondria are critical regulators of Ca²⁺ buffering, mitochondrial dysfunction can result in increased concentrations of intracellular Ca²⁺, improper calcium signaling in the regulation of enzymatic activity, increased ROS production, oxidative stress, and apoptosis (reviewed in [32]). This has led to the development of the Ca²⁺ hypothesis in brain aging. Altered Ca²⁺ levels are sufficient to cause neuronal cell death and neurodegenerative disease [33,34]. Because Ca²⁺ buffering and signaling are intrinsically linked to mitochondrial function, errors in Ca²⁺ handling can further insult mitochondria and affect cell function and survival.

Apoptosis

Mitochondria are integral to the initiation of intrinsic apoptosis. Mitochondria sense various types of cellular damage including DNA damage, chemotherapeutic agents, UV radiation, and starvation and initiate apoptotic signaling. A complicated cascade of signaling events, involving mitochondrial proteins, tightly regulates apoptosis. Abnormally increased activation of the apoptotic cascade is associated with neurodegenerative diseases [35,36], suggesting dysregulation of anti-apoptotic factors in disease pathogenesis.

BH3-only proteins and Bcl-2 proteins are positive and negative regulators of apoptosis, respectively [37]. Bax/Bak can be either directly [38] or indirectly [39] activated via BH3-only proteins. Bax then translocates from the cytosol to mitochondria [40,41]. Truncated Bid (tBid) translocates to mitochondria to initiate Bax OMM insertion, cause membrane permeabilization, and trigger cytochrome *c* release into the cytoplasm [42]. Cytochrome *c* binds to apoptotic protease-activating factor 1 (Apaf-1) to form a complex that cleaves and activates the initiator caspase 9. Caspase 9 then activates caspases 3 and 7. These activated caspases then go on to promote cell death via various mechanisms including the degradation of DNA [43,44]. Each step of the apoptotic signaling cascade has positive and negative regulators, and an imbalance in these signals can lead to cell death and disease.

CONSEQUENCES OF MITOCHONDRIAL DYSFUNCTION

Mitochondrial dysfunction is heavily implicated in aging, which is the greatest risk factor for developing neurodegenerative diseases [45-47]. Reduction in mitochondrial function results in the inability to respond to energy requirements of the cell, aberrant Ca^{2+} signaling, and improper cell death signaling. In addition to altered or reduced mitochondrial functions, mitochondrial dysfunction also results in the production of toxic ROS that can affect other cellular systems. Increased oxidative stress can affect organelle function such as mitochondria and lysosomes, and also affect protein, lipid, and nucleic acid integrity and function.

Neurons are particularly sensitive to mitochondrial dysfunction, which underscores the role of mitochondrial dysfunction in the pathogenesis of

neurodegenerative diseases. Unlike other cell types that can be replaced through cell division, neurons are post mitotic and non-regenerative. This places increased importance on mechanisms of intracellular signaling that maintain mitochondrial health. Neurons rely strongly on mitochondrial respiration because they have limited capacity for glycolysis [48,49]. In addition, neurons require large amounts of energy; therefore, they have higher rates of respiration and thus, increased rates of ROS production. Although the brain only makes up 2% of human body weight, it consumes 25% of the oxygen, emphasizing the critical role of mitochondrial respiration in the central nervous system (CNS) [50]. Another complication of neuronal biology in respect to mitochondrial function is that the highly polarized and elongated architecture of neurons creates challenges in mitochondrial trafficking. In neurons, mitochondria are formed *de novo* in the perinuclear region around the cell body in neurons, yet there are high-energy demands at distal regions of the neurons such as at axon terminals and dendritic spines [34,51]. Presynaptic and postsynaptic densities require large amounts of energy to release and accept synaptic vesicles and failure of mitochondria to traffic to the synapse results in synaptic dysfunction and neuronal death [52]. Mitochondria are required for neurite outgrowth and growth cone motility during development [53]. Mitochondria must be transported to these areas with high-energy needs for the neuron to function properly, and axons can be up to a meter long. Mitochondrial trafficking defects result in the inability for mitochondria to get to regions of the neuron requiring large amounts of energy, resulting in neuronal dysfunction and death. Due to the strong dependence on mitochondrial function, mitochondrial dysfunction is commonly associated with neurodegenerative diseases.

The role of oxidative stress in aging and disease

Mitochondrial dysfunction is frequently accompanied by the accumulation of ROS and oxidative stress, which are implicated in neurodegenerative disease pathogenesis (Fig. 2). The “oxidative stress theory of aging” or the “free radical theory of aging” states that ROS accumulation causes oxidation of proteins, lipids, and nucleic acids affecting their function(s) over time, contributing to aging. The rate of oxidative damage accumulation is inversely correlated with the maximum life span of mammals [54-56]. Since mitochondria are the major source of endogenous ROS, mitochondrial dysfunction is strongly implicated in the oxidative stress theory of aging. ROS are defined as a group of extremely reactive molecules containing oxygen and accumulation of ROS can be deleterious to multiple cellular processes. Increased rates of ROS production or decreased rates of metabolism will result in accumulation of oxidative stress. Because aging is currently the largest risk factor in for the development of a neurodegenerative disease and patients and animal models of neurodegenerative diseases frequently exhibit signs of oxidative stress, the oxidative stress theory of aging is heavily implicated in the pathogenesis of neurodegenerative diseases.

Accumulation of ROS can have several deleterious effects on the CNS. Decline in cognitive function is strongly associated with oxidative stress [57,58]. Oxidative stress can result in the oxidation of proteins, lipids, and nucleic acids, affecting their cellular functions. Protein oxidation results in protein misfolding, aggregation, and proteasomal inhibition. Lipid peroxidation occurs through the interaction of polyunsaturated fatty

acids and free radicals to produce several byproducts. Lipid peroxidation can affect other cellular systems including the proteasome, mitochondria, protein function, neuronal function, and apoptosis [59-63]. Oxidation of nucleic acids can result in errors in transcription and translocation. Oxidative stress can induce proinflammatory signaling in the brain, leading to inflammation and cell death [64,65]. In neurons, ROS affects myelination due to its high lipid to protein ratio [66]. Oxidative stress can cause synaptic defects, loss of synaptic plasticity, and synaptic degeneration [67]. ROS production from damaged mitochondria can further damage preexisting healthy mitochondria [68-70]. Taken together, oxidative stress can be very deleterious to the structure and functions of nervous tissue.

The redox status in the cell is a balance between ROS production and reduction or degradation of oxidized products [71]. Superoxide and hydrogen peroxide (H_2O_2) are produced as a normal byproduct of the ETC, and the processes that neutralize these molecules are not always efficient. Damaged mitochondria produce increased rates of ROS compared to normal mitochondria via complex I or III dysfunction [72,73]. Exogenous ROS can result from exposure to pollutants, toxins, and radiation. Antioxidant systems exist within the cell to combat accumulation of ROS. Superoxide dismutases (SODs) break down the superoxide anion into oxygen and hydrogen peroxide. Peroxiredoxins catalyze the reduction of hydrogen peroxide, organic hydroperoxides, and peroxynitrites. Catalases convert hydrogen peroxide into water and oxygen. Thioredoxin and glutathione function as protein disulfide reductases. Small molecule antioxidants such as ascorbic acid (vitamin C), tocopherol (vitamin E), uric acid, and glutathione also play a role in reducing ROS. In addition, polyphenol antioxidants scavenge free radicals

[74]. The existence of several antioxidant systems in the cell indicates the need to reduce ROS levels. Imbalances in the generation and metabolism of ROS and oxidized products result in cell dysfunction and death, and are heavily implicated in neurodegenerative disease pathogenesis.

The role of mitochondrial DNA in aging and disease

Defects in mitochondrial DNA (mtDNA) have also been heavily implicated in aging and neurodegeneration. Mitochondrial dysfunction triggered by mutations in or oxidation of mtDNA has been shown to increase with age and in models of neurodegenerative diseases [75-78]. Since mtDNA mostly codes for components of the ETC, mutations in mtDNA frequently affect rates of mitochondrial respiration [79]. Mitochondrial respiratory activity decreases with increased oxidation of mtDNA and increased mutation rate [80]. Mutations in mtDNA have been shown to lead to defects in the CNS and peripheral nervous system (PNS) [81-83]. Mutations in mtDNA or oxidation of mtDNA have been implicated in neurodegenerative diseases such as PD and AD [84-87]. Polymorphisms in mtDNA have been shown to predispose patients for neurodegenerative diseases [88].

Defects in mtDNA are strongly implicated in the pathogenesis of age dependent neurodegenerative disorders. Although mitochondria have several mechanisms for mtDNA repair including base excision repair, mismatch repair, and oxidized DNA processing, they cannot always efficiently repair defects in mtDNA [89,90]. As the activity of the mitochondrial DNA repair machinery decreases with age, the mtDNA

mutation rate increases with age [91]. This results in age-dependent accumulation of mtDNA mutations and mitochondrial defects [84,92]. Knockout mice for mtDNA polymerase have an increased rate of mtDNA mutations and experience premature aging, supporting a role in mitochondrial dysfunction from mtDNA mutations in aging [93]. Mutations in nuclear DNA encoded proteins that affect mtDNA replication are also implicated in mitochondrial dysfunction and neurodegenerative diseases [82]. Loss of the mitochondrial transcription factor TFAM results in reduced copy number of mtDNA, reduced ETC activity, and neuronal cell death [94]. Mice devoid of TFAM expression develop seizures and neurodegeneration [95].

Mitochondrial DNA is exceptionally sensitive to oxidation, which leads to defects in mitochondrial protein transcription and translocation, mitochondrial dysfunction, aging, and neurodegeneration [96,97]. Because mtDNA is not protected by histones, mtDNA is more susceptible to oxidative damaged compared to nuclear DNA [98]. Additionally, because mtDNA resides in the mitochondrial matrix and the majority of cellular ROS is generated by the mitochondria on the IMM, the close proximity of mtDNA to the source of ROS increases the chances for DNA oxidation. MtDNA promoter oxidation results in reduced expression of mitochondrial genes and has also been implicated in reduced transcription factor binding, transcription of mitochondrial genes, mitochondrial respiration, and mitochondrial dysfunction [99].

MITOCHONDRIAL DYNAMICS

Because mitochondrial dysfunction is closely tied to cell death and disease and mitochondria are particularly sensitive to oxidative insults, maintenance of mitochondrial

health is important to cytoprotection, particularly in neurons. In order for mitochondria to protect themselves against stress and respond to energy demands under various conditions, a complex system of self-maintenance has evolved. Although the classical textbook pictorial representation of mitochondria is a static bean-shaped structure, mitochondria are in fact highly dynamic organelles that exist in a reticular network [100]. Mitochondria regularly undergo fission (breaking apart) and fusion (recombining) in processes generally referred to as mitochondrial dynamics. Mitochondrial dynamics regulate mitochondrial health in several ways including maintaining mtDNA, responding to respiratory demands, responding to cellular stress, and initiation of apoptosis. Tight regulation of these processes is required for maintaining homeostasis of the mitochondrial network as well as overall proper cell function and health. Excess mitochondrial fusion or reduction in fission results in an aberrantly elongated network. Conversely, loss of fusion or overabundance of fission results in fragmented mitochondria. Both hyperelongation and fragmentation of the mitochondrial network both negatively affect mitochondrial function and cell health [101]. As mitochondrial dynamics are linked to the life cycle, stress responses, and energy requirements of the cell, dysregulation of mitochondrial dynamics can be highly deleterious. There are several proteins identified in regulation of mitochondrial dynamics that will be discussed in the following section. Post-translational modifications of these proteins have been shown to regulate their activity.

Since mitochondrial fission and fusion are so important to mitochondrial function, dysregulation of mitochondrial dynamics is frequently seen as an underlying cause of disease. Neurodegenerative diseases such as HD, AD, PD, prion diseases, and ALS

present with fragmented mitochondria and mitochondrial dysfunction [102]. Loss-of-function mutations in fusion and fission proteins result in disease and defects in embryonic development. Further understanding of the mechanisms controlling mitochondrial dynamics and how they are altered in disease will provide novel insights into disease pathogenesis.

Fusion

Mitochondrial fusion, or the joining of two individual organelles, mediates mixing of the aqueous and membranous contents of the two fusing mitochondria. Defects in mtDNA including mutations and oxidation of genes and promoters can be repaired through mitochondrial fusion (reviewed in [103]). Mitochondrial fusion is required for robust respiratory function and cytoprotective responses to stress [104-109]. Because mitochondrial fusion is observed during times of stress, it is hypothesized that fusion is important because it allows the complementation of mitochondrial proteins and DNA and equal distribution of metabolites. Low levels of oxidative stress result in a hyperelongated mitochondrial network, suggesting that fusion plays a role in protecting mitochondria from oxidative stress [109,110]. Because fusion is assumed to repair and dilute minor defects in mitochondria, fusion may serve as the first line of defense against mitochondrial damage.

Mitofusins 1 and 2 (Mfn1 and Mfn2), the major mediators in OMM fusion, form homo-oligomeric and hetero-oligomeric coiled-coil complexes on opposing mitochondria to ratchet the two mitochondria together [104,111,112]. Once mitochondria are closely

juxtaposed, mitofusins initiate OMM fusion through GTPase activity [105,112-114]. After the OMMs have fused together, fusion of the two IMMs is mediated through another GTPase, OPA1 [115]. Defects in the proteins regulating mitochondrial fusion result in the accumulation of fragmented, damaged mitochondria [105].

Genetic defects in fusion proteins have been implicated in neurodegenerative disease pathogenesis. Charcot-Marie-Tooth disease Type 2A (CMT2A), an inherited sensory and motor neuropathy, results from loss of function mutations in Mfn2 [116-119]. Patients exhibit muscle weakness, pain, tingling in extremities, and sensory loss. Defects in mitochondrial transport have also been implicated in Mfn2 associated CMT2A pathogenesis, implicating a potential role of Mfn2 in mitochondrial trafficking [120]. Loss of Mfn1 and Mfn2 in double knockout mice is embryonic lethal, and embryonic fibroblasts from these mice exhibit a highly fragmented mitochondrial network [105]. Conditional knockout mice devoid of Mfn2 expression in the liver exhibit ER stress and accumulation of ROS [121]. Hundreds of mutations in OPA1, mostly in the GTPase domain, have been linked to optic atrophy type 1, the disease in which OPA1 received its name [122-125]. In optic atrophy type 1, patients progressively lose retinal ganglion cells and suffer eventual degeneration of the optic nerve and vision loss. While fibroblasts from some optic atrophy patients exhibit fragmented mitochondrial morphology, others exhibit normal mitochondrial morphology [126]. Mice deficient for OPA1 expression die in utero indicating that Opa1 is required for development [127,128]. Mouse models with mutations in OPA1 exhibit age dependent loss of retinal ganglion cells and increased axonal degeneration of the optic nerve [129].

Fission

Mitochondrial fission is the splitting of a single mitochondrion into two daughter mitochondria. Fission is required for development [130], mitophagy, proper mitochondrial distribution during cell division, and apoptosis [131,132]. Aside from regulating the mitochondrial network, mitochondrial fission is implicated in the segregation of damaged mitochondria from the rest of the network, so that they can be cleared by mitophagy without spreading to the healthy mitochondrial pool.

Dynamin related protein 1 (Drp1), also referred to as dynamin like protein 1 (DLP1), mediates the fission of a mitochondrion into two separate and distinct mitochondria. Recently, the ER was shown to mark the site of mitochondrion fission, and mitochondria-ER contact is thought to be the initiating step in mitochondrial fission [133,134]. Drp1 resides in the cytosol under basal conditions and is recruited to mitochondria at the fission site through docking on another protein, Fis1 or mitochondrial fission factor (Mff) [135-137]. While the effect of Fis1 expression on mitochondrial morphology is mixed [136,138,139], depletion of Mff causes mitochondrial elongation and overexpression results in fragmentation [139,140]. Drp1 assembles in a ring shaped structure around the mitochondrial tubule and constricts, pinching the mitochondrion into two separate mitochondria [141]. Overexpression of Drp1 in mammalian cells results in fragmented, clustered mitochondria [135,142] and depletion of Drp1 results in elongated, tubular mitochondria and increased frequency of mtDNA mutations [143].

There is only a single report of a Drp1 mutation in humans. An infant with a point mutation in Drp1 (A395D) died at 37 days of age and exhibited abnormal brain development, optic atrophy, and lactic acidemia and defects in mitochondrial and

peroxisomal fission [144]. When this mutation of Drp1 is expressed in cell culture, cells exhibit mitochondrial and peroxisomal defects, implicating these cellular defects in neonatal lethality [145]. Loss of Drp1 expression in mice is embryonic lethal and causes defects in the synapse formaton [144]. Drp1 deficient mouse embryos exhibited several developmental defects including in the heart, liver, and neuronal systems. Fibroblasts from these mice can be cultured *in vitro* and exhibit highly interconnected mitochondria [144].

Posttranslational modifications regulate fission and fusion protein activity

Fission and fusion are regulated by phosphorylation, ubiquitination, sumoylation, and nitrosylation. Drp1 is phosphorylated by several kinases at Ser616, Ser637, or Ser639 to either promote or downregulate its activity [146-151]. Phosphorylation of Ser616 or Ser637 has been suggested to regulate interactions between Drp1 and OMM proteins and likely allows for Drp1 docking [152]. Drp1 is ubiquitinated by March5 to initiate mitochondrial division and March5 inactivation prevents mitochondrial fission [153,154]. Mulan-mediated sumoylation promotes mitochondrial fission in a Drp1 dependent manner [155]. While nitrosylation of Drp1 does not affect its activity under normal conditions, nitrosylation of Drp1 mediates excessive mitochondrial fission in several disease states [156-158]. Parkin mediated polyubiquitination of mitofusins regulates their proteasomal degradation and mitochondrial fission in mitophagy [159,160]. Drp1 is SUMOylated during apoptosis in a Bak/Bax dependent manner as part of the apoptotic cascade [161]. Mitofusins are ubiquitinated by parkin to promote mitophagy of damaged

mitochondria [160]. Additional proteins that regulate the activity of mitochondrial fission and proteins are being identified. Regulation of the activity of these proteins is especially important to control their activity during and especially important in post mitotic cells such as neurons.

Mitophagy

Mitophagy, or the autophagic degradation of mitochondria, is an essential cellular mechanism to dispose of damaged mitochondria [162]. Loss of mitophagy results in the accumulation of fragmented, damaged mitochondria and therefore, accumulation of ROS [73]. The major players of the canonical mitophagy pathway are PD-linked proteins PINK1 and parkin. Briefly, as mitochondria lose membrane potential as a consequence of mitochondrial damage, PINK1 recruits parkin to damaged mitochondria [163-165] where parkin ubiquitinates several OMM proteins including mitofusins leading to their proteasomal degradation [166-168]. This triggers the recruitment of autophagy factors such as p62 and LC3 to mitochondria [169,170]. Damaged mitochondria are then engulfed by autophagic vesicles and delivered to lysosomes for degradation.

Neurons heavily rely on intracellular mechanisms for maintaining mitochondrial homeostasis and consequently, defects in mitophagy can be extremely deleterious to neurons. Turnover of damaged mitochondria is important to control the rates of ROS production because damaged mitochondria are more prone to producing ROS. Defects in mitophagy cause poor quality control of the mitochondria, accumulation of ROS, and cell death and apoptosis [162,171]. PD-linked mutations in PINK1 and parkin result in loss

of mitophagy, suggesting mitophagy is essential for neuronal function and survival [169]. Dysregulation of mitophagy is implicated in neuronal dysfunction and neurodegenerative diseases.

NEURODEGENERATIVE DISEASES LINKED TO MITOCHONDRIAL DYSFUNCTION

Mitochondrial dysfunction and neurodegeneration are closely intertwined due to the high-energy requirements of neurons and heavy reliance on OXPHOS. Defects in OXPHOS, such as complex I or complex III inhibition result in oxidative stress and cause neurodegeneration in both humans and animal models. In addition, oxidative stress is observed in many neurodegenerative diseases (reviewed in [172]). Defects in the fission/fusion balance have been implicated in the pathogenesis of neurodegenerative diseases such as PD, AD, HD, and ALS. Defects in mitophagy result in the accumulation of damaged mitochondria, which has been strongly implicated in PD and AD pathogenesis [173,174]. Taken together, these findings indicate that tight control of mitochondrial activity and health is required for neuroprotection. Further understanding into the mechanisms by which mitochondrial dysfunction leads to neurodegenerative diseases will provide novel insights into disease pathogenesis. In the following section, I will outline how mitochondrial dysfunction has been implicated in PD and spongiform neurodegenerative diseases.

Parkinson's disease (PD)

Parkinson's disease (PD) is the second most common neurodegenerative disorder and the most common movement disorder [175-177]. PD affects approximately 1% of the population over 60 and 5% of people over 85 years of age [178]. Pathologically, PD is primarily characterized by the loss of dopaminergic neurons in the substantia nigra pars compacta; however, neurodegeneration has been observed in other brain regions as well [179-182]. The accumulation of protein aggregates, Lewy bodies, is the pathological hallmark of PD. Although the causes behind Lewy body formation are unknown, oxidation of proteins is implicated in this process [183]. The pathogenic mechanisms underlying dopaminergic cell loss remain unclear, but mitochondrial dysfunction has been strongly implicated in PD pathogenesis [184-189]. As the population in industrialized nations including the U.S. is aging, the number of people affected by PD is expected to grow substantially in the coming years.

Clinically, PD presents with resting tremor, bradykinesia, and an unsteady gait. The vast majority (~90%) of PD cases are sporadic with no genetic history of PD, while the remaining 10% are associated with heritable mutations. Both sporadic and familial cases of PD are well documented to involve mitochondrial dysfunction in the underlying pathogenesis of PD. Familial cases of PD are linked to mutations in 17 PARK genes, some of which have been shown to have a mitochondrial function [190]. Mutations in two PD-linked genes with roles in mitochondrial function, PINK1 and parkin, are the leading mutations in genetic forms of PD [191]. The PARK genes DJ-1 and α -synuclein have also been implicated to affect mitochondrial function. Environmental and sporadic causes of PD have also been linked to mitochondria. PD patients exhibit reduced complex

I activity [192-194] and toxins affecting mitochondrial respiration have been shown to cause parkinsonism. Exposure to several pesticides that cause mitochondrial dysfunction and oxidative stress is associated with increased incidence of PD and cause PD-like symptoms in animal models.

PD genetics linked to mitochondrial dysfunction

1. PINK1

PINK1 (PARK6) is a serine/threonine kinase that associates with mitochondria via a mitochondrial targeting sequence. Mutations in PINK1 are linked to recessive forms of early onset PD [195-197]. PINK1 knockout mice exhibit reduced complex I activity, increased ROS, and reduced ATP production, indicating that PINK1 is required for proper mitochondrial function [6,191,198]. PINK1 protects against oxidative stress induced cell death and apoptosis in immortalized cells and neurons [5,199,200]. Loss of PINK1 has been associated with alterations in mitochondrial morphology [201] and increased susceptibility to cell death [202].

Currently, PINK1 has two identified substrates of its kinase activity, TRAP1 and parkin, both of which are implicated in mitochondrial health. PINK1 phosphorylates the mitochondrial chaperone TRAP1 in response to oxidative stress, and phosphorylated TRAP1 protects against mitochondrial dysfunction and cell death [5,203,204]. Overexpression of TRAP1 rescues PINK1 loss of function phenotypes such as mitochondrial fragmentation and dysfunction in cellular and fly models suggesting TRAP1 functions downstream of PINK1 in mitochondrial protection [203,205]. TRAP1

can rescue complex I inhibition, dopaminergic cell death, and α -synuclein induced oxidative stress and cytotoxicity in rat cortical neurons [203,204]. Taken together, this suggests that TRAP1 and PINK1-mediated phosphorylation of TRAP1 is essential for maintaining mitochondrial function, protection against mitochondrial stressors, and neuroprotection.

PINK1 also phosphorylates the E3 ubiquitin protein ligase parkin to recruit parkin to damaged mitochondria to initiate mitophagy. PINK1 expression and kinase activity are both required for parkin recruitment [206]. PINK1 binds tightly with parkin to recruit parkin to the OMM and phosphorylation of PINK1 is required for the activation of parkin E3 ligase activity [164,207-211]. PD-linked mutations in PINK1 fail to recruit parkin to mitochondria or stimulate mitophagy, suggesting loss of PINK1/parkin mitophagy may be an underlying cause of genetic forms of PD [207].

2. Parkin

Parkin is an E3 ubiquitin-protein ligase encoded by the PARK2 locus. Mutations in parkin make up 50% of the genetic cases of PD [212]. Loss-of-function mutations in parkin result in autosomal recessive early onset PD [213,214]. Parkin deficient mice exhibit mitochondrial dysfunction suggesting that parkin is implicated in maintaining the overall health of the mitochondrial network [215]. In particular, parkin has been implicated in cellular regulation of autophagy and mitophagy through the ubiquitination of disease linked misfolded proteins [216] and OMM-localized proteins [166,217], respectively. Parkin is recruited to damaged, depolarized mitochondria to initiate mitophagy or the autophagic degradation of these damaged mitochondria [163]. Parkin-

mediated ubiquitination of OMM-localized proteins leads to their proteasomal degradation. Disease linked mutations in parkin result in loss of mitophagy and accumulation of damaged mitochondria [164,207]. Parkin rescues mitochondrial defects caused by PINK1, suggesting that parkin acts downstream in maintaining mitochondrial homeostasis [7,218,219].

3. a-synuclein

PARK1/4 encodes a-synuclein, and while its function is poorly understood, a-synuclein may play a role in synaptic vesicle maintenance. Disease linked mutations of a-synuclein are prone to misfolding and aggregation and are a major component of Lewy bodies in both genetic and sporadic forms of PD [220,221]. The mechanisms by which a-synuclein accumulates are not well understood. A-Synuclein localizes to the cytosol, mitochondria, and ER-mitochondrial contact sites [222-227]. A-Synuclein may promote mitochondrial fission since it is localized to ER-mitochondrial contact sites where mitochondrial fission is initiated and overexpression of wild type a-synuclein caused mitochondrial fragmentation [133,228]. Mitochondrial association of a-synuclein correlates with increased oxidative stress and reduction of mitochondrial function, suggesting a mitochondrial role of a-synuclein mediated PD pathogenesis [226,229]. Overexpressing PD-linked mutants of a-synuclein leads to mitochondrial defects and increased susceptibility to cell death [230-232].

4. DJ-1

DJ-1 is encoded by the PARK7 gene and mutations in DJ-1 result in autosomal recessive early onset PD [233]. DJ-1 is partially localized to mitochondria; however, the precise mitochondrial role of DJ-1 has yet to be defined [234]. DJ-1 depletion is associated with mitochondrial fragmentation and increased mitochondrial Ca^{2+} levels, suggesting DJ-1 has a role in maintaining mitochondrial homeostasis [235]. Loss of DJ-1 is associated with increased ROS levels [236]. Mild oxidation of DJ-1 results in activation of its protease activity, which confers cytoprotection to the cell, suggesting DJ-1 may sense and protect neurons from oxidative damage [237]. PD-linked mutations in DJ-1 result in loss of protease activity and cytoprotection [237]. Although the particular function of DJ-1 at mitochondria is not well defined, the role of DJ-1 in protection from oxidative stress induced cell death suggests a mechanism of cytoprotection during mitochondrial dysfunction.

Environmental causes of PD

Since a very small population of those affected by neurodegenerative diseases, including PD, are genetically inherited, it is important to elucidate the underlying mechanisms that can result in sporadic cases of PD. Exposure to various environmental toxins can result in mitochondrial dysfunction and is associated with an increased risk for developing a neurodegenerative disease. Animal models exposed to these compounds recapitulate major aspects of PD. Several chemicals that induce mitochondrial

dysfunction via complex I inhibition cause parkinsonism and is used in animal models of PD, underscoring the role of mitochondrial dysfunction in PD pathogenesis.

The compound 1-methyl-4-phenyl-1,2,3,6-tetrahydropyridine (MPTP) caused PD-like symptoms in young drug users exposed to MPTP as a drug impurity [238]. Since then, MPTP has been well established as an acute toxicant model of PD. MPTP crosses the blood brain barrier and is metabolized into MPP⁺ which is taken up specifically by dopaminergic neurons via the dopamine transporter; therefore, only dopaminergic neurons are affected by MPP⁺ exposure [239]. MPP⁺ inhibits complex I of the ETC resulting in elevated ROS production [240,241]. Nonhuman primates given MPTP exhibit many of the clinical and pathological hallmarks of PD such as loss of dopaminergic neurons, bradykinesia, and rigidity [242-246]. Mice exposed to MPTP also exhibit degeneration of dopaminergic neurons, but the level of sensitivity is dependent on the particular strain and age of the animal [247,248]. Interestingly, MPTP treated animals and MPTP exposed humans do not develop the intracellular protein inclusions typical of PD [180], which may be because of the rapid onset of disease. Genetic models of PD exhibit increased susceptibility to MPTP further confirming both genetic links and mitochondrial dysfunction to PD [249,250].

Rotenone is a widely used insecticide that easily crosses the blood brain barrier and bioaccumulates in lipids [251]. Rotenone inhibits complex I by binding the ubiquinone binding site of NADH hydrogenase, preventing the transfer of electrons. Compared to MPTP models, acute treatment with rotenone has little effect on producing PD symptoms, only when animal models are chronically dosed with rotenone do PD-like symptoms develop [252]. Rotenone inhibits complex I in all regions of the brain causing

widespread neurodegeneration, unlike MPTP which only affects dopaminergic neurons. Rotenone animal models exhibit striatal oxidative damage, typical PD protein inclusions, and degeneration of the nigrostriatal pathway [252,253]. Rats exposed to rotenone exhibit similar clinical signs of PD patients including slow movements, rigidity, resting tremor, and altered posture [253]. Rotenone treated neurons exhibit increased susceptibility to oxidative damage and cytotoxicity [254,255].

Paraquat is a widely used naturally occurring herbicide in which exposure causes increased risk for developing PD [256,257]. Because of structural similarities between paraquat and MPTP, paraquat has been hypothesized to also inhibit complex I [258]. However, unlike MPTP, paraquat passes the blood brain barrier via neutral amino acid transport into striatal neuronal cells. Exposure to paraquat results in the PD-typical degeneration of dopaminergic neurons in the substantia nigra and typical PD-associated protein inclusions [259]. Paraquat-treated *Drosophila* models also show loss of dopaminergic neurons, and PD genetic models exhibit increased susceptibility to paraquat-induced neurotoxicity [260].

Human spongiform neurodegenerative disorders

Spongiform neurodegeneration is the hallmark of prion diseases and is also seen as a pathological consequence of AD, diffuse Lewy body disease, human immunodeficiency virus (HIV) associated encephalitis, and lysosomal storage disorders. Spongiform neurodegeneration is characterized by intracellular and extracellular vacuolation of tissue along with neuronal and glial cell death. Since a range of diseases

can cause similar tissue pathology, it suggests that a common mechanism may be involved in the pathogenesis of spongiform neurodegeneration. Mitochondrial abnormalities and dysfunction and increased oxidative stress have been observed occur prior to onset of disease.

1. Alzheimer's disease (AD)

AD, currently the 6th leading cause of death in the United States, is the world's most common neurodegenerative disorder and is characterized by progressive dementia [261]. AD causes loss of neurons and synapses in the cerebral cortex and other regions of the brain resulting in shrinkage and loss of brain mass in AD patients. In patients, a reduction in cortical thickness correlates to the degree of dementia [262]. Genetic mouse models of AD exhibit defects in dendritic spines and synapses [263]. There is a large correlation between mitochondrial dysfunction, loss of synapses and dendritic spines, and the cognitive decline seen in AD patients [264]. In addition, AD patients exhibit mitochondrial dysfunction and oxidative stress prior to disease onset, indicating a potential causal relationship [265-267]. Taken together, mitochondrial dysfunction and oxidative stress are indicated in cellular and tissue pathology and behavioral symptoms of AD.

Pathologically, postmortem AD brain presents with intracellular neurofibrillary tangles (NFT) and extracellular amyloid plaques that accumulate in affected areas of the brain, and both of these pathogenic structures can result in mitochondrial dysfunction [268-270]. Tau localizes to microtubules and is involved in the axonal transport of organelles including mitochondria [271]. Hyperphosphorylated, aggregated tau can

dissociate from microtubules and block mitochondrial transport [272,273]. Mitochondrial dysfunction can also lead to tau hyperphosphorylation, creating a toxic positive feedback loop [274,275]. Hyperphosphorylated tau interacts with Drp1, suggesting a mechanism by which tau can affect mitochondrial dynamics [276].

Genetic causes of AD have been linked to mitochondrial dysfunction. Ab and the amyloid precursor protein are both localized to mitochondria in mitochondrial import channels [265,277]. Mitochondrial association of Ab is associated with mitochondrial dysfunction in AD patient brains and cell culture models [266,278]. Presenillin genes, also implicated in AD, code for the catalytic subunit of γ -secretase and are involved in the cleavage of APP into Ab [279,280]. PS-1 and PS-2 localize to mitochondria [281,282] and mitochondria-associated-ER membranes [283,284] and affect mitochondrial respiration and mitochondrial membrane potential [285]. AD genetic mouse models exhibit mitochondrial defects that precede the development of neurodegeneration [285-287], further supporting a role of mitochondrial dysfunction in AD pathogenesis.

2. Prion diseases

Prion diseases, or transmissible spongiform encephalopathies, are caused by misfolding of the prion protein (PRNP). Although the propagation of pathogenic prion isoforms has been studied extensively, the cellular mechanisms by which prion misfolding causes spongiform neurodegeneration occurs remains unclear. Human prion diseases include Creutzfeldt-Jakob disease (CJD), Kuru, Gerstmann-Straussler-Scheinker syndrome (GSS), and Fatal Familial Insomnia [288] [105,288]. Each disease has

strikingly different clinical presentations, but all display widespread spongiform change throughout the brain and neuronal and glial cell death. Prion diseases are rapidly progressive, untreatable, cause dementia, and are ultimately fatal.

Healthy prion (PrP^c) maintains an α -helical conformation, while the pathogenic “scrapie” form (PrP^{sc}) results from a conformational switch into a β -sheet and misfolds and aggregates. PrP^{sc} serves as a template for misfolding of additional PrP^c . Initial exposure to PrP^{sc} can be caused by an inherited mutation, *de novo* mutation, or ingesting prion-infected tissue. In addition, there have been several reported cases in which people have contracted prion diseases through surgical procedures with contaminated equipment [289].

Increased oxidative stress is observed in patients with prion diseases and animal models of prion diseases [290,291]. In addition, oxidation of PrP^c has been implicated in pathogenic prion misfolding (reviewed in [292]). Extensive oxidative damage to nucleic acids correlates with disease progression, PrP^{sc} deposition, and neuronal cell death [290,293]. Mouse models of prion diseases exhibit protein and lipid oxidation, reduced SOD and glutathione peroxidase activity, reduced metabolism of free radicals, and reduced ATP output [294-297]. Oxidative stress has been shown to lead to further mitochondrial dysfunction in scrapie-infected mice, resulting in a positive feedback loop [298].

PrP^c may have antioxidant functions; therefore, loss of PrP^c through the conformational switch to PrP^{sc} may contribute to prion-associated oxidative stress. PrP^c antioxidant activity is dependent on copper binding, and infection with PrP^{sc} decreases copper binding and increases susceptibility to oxidative stress induced cell death

[299,300]. Cortical neurons from prion knockout mice have reduced survival and increased susceptibility to oxidative stress induced cell death that can be rescued by treatment with the antioxidant, vitamin E [301]. PrP knockout mice were also shown to have reduced SOD1 activity [301]. Overexpression of PrP^c in the dopaminergic cell line, SH-SY5Y, is cytoprotective against the mitochondrial toxin, paraquat [302]. PrP^c overexpression protects mitochondria from fragmentation and loss of membrane potential triggered by paraquat treatment, ultimately preventing apoptotic cell death [302,303].

Prion diseases are associated with mitochondrial defects. PrP (106-126), a fragment associated with GSS, causes loss of mitochondrial membrane potential and initiation of the mitochondria-dependent apoptotic cascade [304]. Ultrastructural analysis revealed intramitochondrial crystalloids [305] and abnormal accumulation of mitochondria in neuronal processes of GSS patient brain [306]. In a case of FFI, degenerating mitochondria were seen accompanying neuroaxonal dystrophy [307]. Animal models of prion diseases exhibit degenerating mitochondria, mitochondrial dysfunction, reduced ATPase activity, IMM and OMM abnormalities, reduction in mitochondrial mass, and apoptosis [296,298,308,309].

3. Lysosomal storage disorders

Lysosomal storage disorders (LSDs) are caused by deficiencies in lysosomal enzymes and include approximately 50 different diseases. Some LSDs present with spongiform neurodegeneration [310,311]. Reduction in lysosomal activity in LSDs causes the accumulation of toxic substrates. Patients with LSDs suffer mental retardation, progressive neurodegeneration, and premature death [312]. Because lysosomes have

reduced function and damaged mitochondria are degraded by lysosomes, accumulation of damaged mitochondria is also frequently seen in patients and animal models of LSDs [313]. As damaged mitochondria are normally segregated from the rest of the mitochondrial network and marked for for mitophagic degradation, the loss of lysosomal activity in LSDs results in accumulation of damaged mitochondria and mitochondria in autophagosomes and lysosomes [313].

General cellular pathologies observed in patients and animal models of LSDs include mitochondrial fragmentation, loss of membrane potential, and ATP production [314,315], reduced Ca^{2+} buffering, and increased cytochrome *c* oxidase activity [256,316,317]. Oxidative stress has been linked to increased apoptosis in patients with LSDs [318-320]. Defects in mitophagy are observed in LSDs such as reduced parkin translocation to damaged mitochondria, reduced ubiquitination of OMM-localized proteins, accumulation of mitochondrial proteins in lysosomes, and reduced mitochondrial turnover is also seen in LSDs [314,321]. Interestingly, parkinsonism associated with the LSD Gaucher Disease is attributed to similar cellular pathologies between the two disorders such as a-synuclein accumulation, reduced ATP production, reduced mitochondrial membrane potential, and defects in autophagy [322].

Animal models of spongiform neurodegeneration

1. Mahogunin RING finger 1 (Mgrn1) mutant mice

Mice homozygous for a null mutation of the *Mahogunin* gene (*Mgrn1^{md-nc}*) results in a darker coat color [9,323,324], reduced embryonic viability, abnormal patterning of the left-right axis [325], and develop age-dependent spongiform neurodegeneration [9]. *Mahogunin* encodes a 64 kDa protein that contains a RING finger E3 ubiquitin-protein ligase domain. Neurodegeneration in *Mgrn1* mutant mice begins in the cortex, and eventually spreads to the hippocampus, cerebellum, thalamus, caudate-putamen, and brain stem over the course of disease progression [9]. Spongiform neurodegeneration, astrocytosis, extracellular vacuolation, and neuronal cell death in *Mgrn1* mutant mice is primarily seen in the grey matter [9]. While the pattern of neurodegeneration in *Mgrn1* mutant mice closely resembles the neurodegeneration associated with prion diseases, *Mgrn1* mutant mice develop spongiform neurodegeneration without the accumulation of proteinase resistant prion protein and *Mgrn1* expression has no effect on prion pathogenesis [9,326]. Mahogunin has four isoforms determined by alternative splicing [327]. Two isoforms contain a nuclear localization sequence, and are shown to localize to the nucleus [327]. Two other isoforms display a punctate pattern that we have previously shown by our lab to partially colocalize with TSG101 on early endosomes [328].

There are only a few identified substrates of *Mgrn1*-mediated ubiquitination. We have previously shown that *Mgrn1* ubiquitinates TSG101 and depletion of *Mgrn1* expression in HeLa cells results in delayed trafficking of EGFR and swollen endosomes and lysosomes [328]. *Mgrn1* also mediates ubiquitination of the melanocortin 2 receptor,

leading to its trafficking and degradation [329]. Mgrn1 indirectly mediates ubiquitination of α -tubulin via an unidentified E3 ligase. Mgrn1-mediated ubiquitination of α -tubulin regulates the order of α -tubulin and spindle assembly [330]. Pigment type switching requires Mgrn1 E3 ligase activity; however, the precise mechanism underlying Mgrn1-dependent pigment type switching remains unclear [331]. The role of Mgrn1-mediated ubiquitination on neuroprotection is just beginning to be elucidated.

Mgrn1 mutant mice exhibit increased oxidative modification of proteins and mitochondrial dysfunction prior to the onset of neurodegeneration, indicating a potential causal relationship [329]. Currently there is not an identified mitochondrial substrate for Mgrn1-mediated ubiquitination and therefore, the mechanism by which Mgrn1 mutant mice suffer from mitochondrial dysfunction and oxidative stress remains unclear.

Since Mgrn1 mutant mice exhibit neurodegeneration independent of PrP^{sc} accumulation, it has been proposed that Mgrn1 functions downstream of PrP^{sc} propagation, accumulation, and aggregation. Cytosolically exposed prion, PrP^{cm}, has been shown to interact with and sequester Mgrn1 around these swollen endosome compartments, where it is assumed Mgrn1 cannot ubiquitinate its substrates [332]. Additionally, siRNA-mediated depletion of Mgrn1 yields similar cellular consequences to overexpressing PrP^{cm}, including delayed endosome-to-lysosome trafficking and swollen endocytic compartments [332]. These results suggest the importance of Mgrn1 localization, function, and the potential role in pathogenic prion in downregulating Mgrn1-mediated ubiquitination in disease pathogenesis. Determination of additional substrates may provide novel insights into the cellular pathways affected by loss of Mgrn1 function.

2. Attractin (Atrn) mutant mice and rats

Loss of function of Attractin (Atrn) in either the *mahogany* mouse or the *Zitter* rat results in changes in coat color [333], myelin defects, and spongiform neuropathology [333-337]. Atrn is localized to various membranes including mitochondria, lysosomes, Golgi apparatus, endoplasmic reticulum, and the plasma membrane of neurons [338]. Atrn depletion causes increased susceptibility to mitochondrial inhibitors, which suggests that Atrn may have a role in mitochondrial function [339]. Knockdown of Atrn results in increased susceptibility to the mitochondrial complex I inhibitor MPP+, while overexpression of Atrn increases neuroprotection [339]. Atrn has been hypothesized to have a cellular role as an antioxidant [339].

There are two models of Atrn deficiency: *Mahogany* mice and *Zitter* rats. *Mahogany* mice also exhibit mitochondrial dysfunction and increased oxidative stress [10]. *Zitter* mutant rats exhibit membranous abnormalities in mitochondria, lysosomes, and endoplasmic reticulum of oligodendrocytes and Schwann cells [338,340,341]. Mitochondrial defects correlate with loss of synapses and astrocytes in *Zitter* rats, suggesting mitochondrial dysfunction underlies neuronal dysfunction [342]. Fibroblasts and neurons derived from *zitter* rats have increased accumulation of ROS and increased sensitivity to oxidative stress induced cell death, which may indicate defects in ROS metabolism [343,344]. Chronic treatment with the antioxidant, Vitamin E, ameliorates dopaminergic neuron loss in *Zitter* rats further confirming the role of oxidative stress in the neurodegeneration [337].

3. Manganese superoxide dismutase (SOD2 or MnSOD) mutant mice

SOD2 is a cellular antioxidant located in the mitochondrial matrix that converts superoxide radicals into H_2O_2 , which reduces mitochondrial and cellular ROS. SOD2 knockout mice exhibit spongiform neurodegeneration, suggesting mitochondrial antioxidants play a key role in neuroprotection [345-347]. SOD2 knockout mice exhibit widespread spongiform neurodegeneration primarily in the cortex and brainstem [347]. SOD2 deficiency results in growth defects and neonatal lethality [345,346]. Loss of SOD2 function increases susceptibility of cells to oxidative stress mediated cell death [346]. Mitochondria in affected brain regions of SOD2 knockout mice are swollen and have disrupted cristae structure, suggesting mitochondrial pathology may be related to the development of spongiform change [346,347]. Treating SOD2 knockout mice with antioxidants ameliorates apoptotic cell death phenotypes [348]. Reduced SOD2 activity in heterozygous mice correlates with oxidative modification of proteins and DNA, and susceptibility to MPTP and other mitochondrial toxins [349].

DIAGNOSTICS AND THERAPEUTICS

Diagnoses of neurodegenerative diseases are challenging. Currently, there are no accepted biomarkers or approved tests to detect the presence of neurodegenerative diseases. The lack of reliable tests means that diagnoses solely rely on the classification of symptoms. Neurodegenerative diseases are associated with age, so for many conditions like PD and AD, initial symptoms are often dismissed as a consequence of aging. In most cases, it is not until the patient has developed severe symptoms, meaning

they have suffered from the disease for years, that they receive a diagnosis and diagnoses can only be confirmed postmortem. This presents a challenge to the development and successes of therapeutics. Therapeutic options for neurodegenerative diseases are limited and not effective in all patients. Current available treatments do not alter the course of disease and have a limited window of effectiveness. This indicates a high unmet need for the development of additional therapeutics. In addition, with a growing aging population, the number of people afflicted with neurodegenerative diseases is expected to rise in the coming years.

Therapeutics in PD

The major PD treatment is L-levodopa (L-dopa) given in tandem with carbidopa and is marketed as Sinemet by Bristol-Myers-Squibb. L-dopa can cross the blood brain barrier and is a precursor of dopamine synthesis. Once in the brain, L-dopa is converted to dopamine via dopa decarboxylase. Carbidopa given in tandem with L-dopa increases the bioavailability of L-dopa in the brain [350]. L-dopa/carbidopa therapy can alleviate some symptoms such as bradykinesia, rigidity, and gait stability; however, there are several drawbacks to L-dopa/carbidopa as a PD therapeutic. Patients with PD can live with the disease for decades, and the fact that L-dopa/carbidopa only has a limited window of effectiveness makes this therapy ineffective for the majority of the time a patient suffers from PD. Moreover, L-dopa/carbidopa does not address all symptoms, even in patients that respond well to L-dopa/carbidopa treatment. After a few years of L-dopa/carbidopa treatment, patients become less responsive most likely due to continued

loss of dopaminergic neurons or the desensitization of dopamine receptors. In patients with later stages of PD, L-dopa/carbidopa treatment can have an on-off effect in which the drug's effectiveness is cyclical. During the "on" period, patients have reduced symptoms while during the "off" period; patients present with akinesia and induce dyskinesias. In addition to the less than ideal effects of L-dopa/carbidopa treatments, there are many PD patients that do not respond to this therapy at all.

Deep brain stimulation (DBS) is another therapeutic option for some PD patients [13,351]. DBS addresses multiple PD-linked symptoms including on/off changes and dyskinesias failed to be addressed by L-dopa therapy. A thin electrode is implanted into the brain and electrical pulses are delivered to this electrode via a medical device similar to a pacemaker. These electrical impulses are able to stimulate certain brain regions while blocking others. While positive results can be achieved using DBS, many patients are not candidates for this therapy. Patients who do not respond to L-dopa/carbidopa generally do not see improvements with DBS. In addition, patients with dementia are also not candidates for this therapy. The precise mechanism by which DBS improves motor symptoms in patients with PD is poorly understood.

Therapeutics in spongiform neurodegenerative disorders

As with PD, there are limited therapeutic options for patients with spongiform neurodegenerative disorders and the treatments currently available are not completely effective. In addition, although spongiform neurodegenerative diseases have a similar pathology that suggests a common underlying cause, our understanding is lacking on

what precisely leads to spongiform change in the CNS, so therapeutics have yet to be developed addressing the group of diseases as a whole.

An aging population indicates a growth in the number of people affected by AD, and without effective therapeutics, this will create a tremendous international financial and occupational burden. Current therapies for AD are limited [352]. The mainstay treatments for AD are acetylcholinesterase inhibitors and include donepezil (Aricept), rivastigmine (Exelon), and galantamine (Razadyne) and are geared towards treating cognitive and behavioral symptoms. All current AD treatments have only mild effects on cognitive and behavioral symptoms and are only effective in early stages of the disease. As with PD, patients with AD can live for decades after diagnosis meaning treatments aren't effective during the majority of time patients suffer from AD.

The only treatments available for patients with prion diseases are palliative and aimed towards providing a safe environment for patients that are easily agitated [353]. Efforts to prevent the spread of prion diseases include monitoring of beef for human consumption, restriction on blood donations, and single use surgical tools. An experimental treatment of pentosan sulfate was given to a teenager with variant CJD, and while he and several other patients experienced a longer survival time, it did not halt or alter disease progression [354]. A much larger study would need to be performed in order to truly investigate if pentosan polysulphate affects disease trajectory.

Patients with LSDs are challenged with a difficult prognosis and limited treatment options. The majority of efforts to develop new treatments are focused on bone marrow transplants, stem cell therapies, enzyme replacement therapies for diseases that are

lacking a particular enzyme, substrate reduction therapy, chemical chaperone therapy, or gene therapy [355]. With the current therapies available, LSDs remain fatal diseases.

Mitochondrial targets for the development of novel therapeutics against neurodegenerative diseases

There are several ways that novel therapeutics may modulate the mitochondrial network to protect against neurodegeneration. Because mitochondria are fragmented in neurodegenerative diseases, mechanisms to promote mitochondrial fusion or prevent mitochondrial fission may be effective to protect against cell death. Potentially, decreasing Drp1 docking and/or activity or increasing the GTPase activity of mitofusins would be beneficial therapeutic targets. Defects in mitophagy and the subsequent accumulation of damaged mitochondria are underlying causes of neurodegenerative diseases, like PD and AD. Therapeutics could be developed to assist PINK1 and parkin in identifying and tagging damaged mitochondria to facilitate mitophagy.

Mechanisms to reduce the accumulation of oxidative stress may also prove to be promising as novel therapeutics for the prevention or treatment of neurodegenerative diseases. There is evidence to suggest that antioxidants may ameliorate neurodegenerative disease phenotypes. The antioxidant α -tocopherol has been shown to be neuroprotective and importantly, slow disease progression and increased survival time in AD patient trials [356,357]. Antioxidant treatments of AD model mice have had varied effects depending on the specific antioxidant and model [358,359]. In addition, attempts to upregulate the expression or activity of endogenous antioxidant systems such as SOD

proteins may reduce oxidative stress and improve patient condition [360,361]. Caloric restriction and intermittent fasting are associated with delayed aging, extended life span, improved health, and delayed neurodegeneration [362-365]. In addition, activation of sirtuins, protein acetylases that are upregulated following calorie restriction, improves cognitive function, delays neurodegeneration, and extends lifespan [366,367]. Sirtuins are thought to be neuroprotective because they regulate transcription factors involved in the stress response [368]. Upregulation of autophagy in patients with neurodegenerative diseases has been hypothesized to rid cells of oxidized misfolded proteins that would normally impair other cellular processes [369-372].

Advances in therapeutics to combat the common intracellular defects observed in neurodegenerative diseases have shown promising results in animal models. Not only do they alleviate symptoms, but in some cases these therapeutics have altered the course of disease. Regulating mitochondrial health and protecting from oxidative stress should be a large area of focus for the development of novel therapeutics for the treatment and/or prevention of neurodegenerative diseases.

HYPOTHESES AND OVERVIEW

Mitochondrial health and activity is complicated and tightly regulated and dysregulation of this machinery through altered expression of proteins, mutations, or protein inactivation through misfolding has been strongly implicated in the pathogenesis of neurodegenerative diseases. The number of identified disease linked proteins implicated in mitochondria function, health, and disease has been increasing.

Understanding the effects of loss or dysfunction of mitochondrial proteins in neurodegenerative disease pathogenesis is important due to increasing links between mitochondrial dysfunction and neurodegenerative disease pathogenesis. PINK1 has been implicated in regulating mitochondrial dynamics and turnover of damaged mitochondria. While the role of PINK1 in maintaining mitochondrial homeostasis has been characterized extensively, the use of different and problematic methods has resulted in confusion in the literature regarding PINK1 submitochondrial localization. The spatiotemporal dynamics of PINK1 mitochondrial signaling are still under debate. Loss of spongiform neurodegenerative disease linked protein, Mgrn1, results in mitochondrial dysfunction in mice that precedes the onset of spongiform neurodegeneration; however the mechanism by which Mgrn1 regulates mitochondrial health remains undefined [10].

In chapter II, we tested the hypothesis that PINK1 is dual targeted to the IMM or OMM depending on the health of the mitochondria and that PINK1 submitochondrial targeting is essential to proper PINK1 signaling. Our findings demonstrate that PINK1 resides in the IMM in healthy mitochondria, where it extensively colocalizes with its substrate TRAP1, and when mitochondria are depolarized, PINK1 is localized to the OMM where it colocalizes with its substrate parkin. Since TRAP1 and parkin are involved in maintaining mitochondrial homeostasis and the degradation of damaged mitochondria, respectively, this suggests that PINK1 acts as a “molecular switch” to signal to the cell the level of damage in the mitochondria. Under low levels of damage, PINK1 can phosphorylate the mitochondrial chaperone, TRAP1, which protects against mitochondrial dysfunction and oxidative stress induced cell death [5,203]. Following depolarization of mitochondria, PINK1 is translocated to the OMM where it colocalizes

with the E3 parkin, a regulator of mitophagy. In addition, I determined that PD-linked mutants of PINK1 are defective in OMM-translocation in response to loss of membrane potential. These mutants are also unable to recruit parkin to damaged mitochondria in neurons. This suggests that the improper submitochondrial targeting of PINK1 mutants contribute to pathogenesis in PINK1 associated autosomal recessive PD.

In chapter III, we address the role of Mgrn1 in mitochondrial health. We determined that a large pool of Mgrn1 was localized to mitochondria via *N*-myristoylation. In addition, the *N*-myristoylation mutant, Mgrn1G2A, remained cytosolic and mislocalized. In addition, we determined that Mgrn1 was specifically targeted to the OMM. Although Mgrn1 mutant mice were previously shown to have accumulation of ROS, oxidative modification of proteins, and mitochondrial dysfunction [10], the precise mechanisms by which Mgrn1 regulates mitochondrial health remained undefined. We observed fragmented mitochondria in primary cortical neurons cultured from Mgrn1 mutant mice compared to wild type controls. In addition, these mitochondria had reduced membrane potential, underscoring the level of mitochondrial damage. We provide evidence that Mgrn1 is cytoprotective and *N*-myristoylation and E3 ligase activity of Mgrn1 are required for cytoprotective function against mitochondrial insults.

Together, our findings further emphasize mitochondrial dysfunction as an underlying cause in the pathogenesis of neurodegenerative diseases. Specifically, PINK1 initiates two separate signaling cascades depending on the level of mitochondrial damage to try to save the mitochondria and reduce the damage that the mitochondria has on the cell. Mgrn1 was shown to be a potential regulator of mitochondrial dynamics and loss of Mgrn1 results in dysregulation of the mitochondrial network. As accumulation of ROS is

associated with the pathogenesis of both PD and spongiform neurodegenerative diseases and ROS is produced by damaged mitochondria, this underscores the role of PINK1 and Mgrn1 in disease pathogenesis. Specifically, PINK1 mediates mitochondrial repair or mitochondrial autophagy depending on the health of the mitochondria while Mgrn1 promotes mitochondrial fusion as a mechanism to repair damaged mitochondria. These findings have further enriched our understandings of the biological functions of two mitochondrially-localized proteins and their roles in neurodegenerative disease pathogenesis.

Figures and Legends

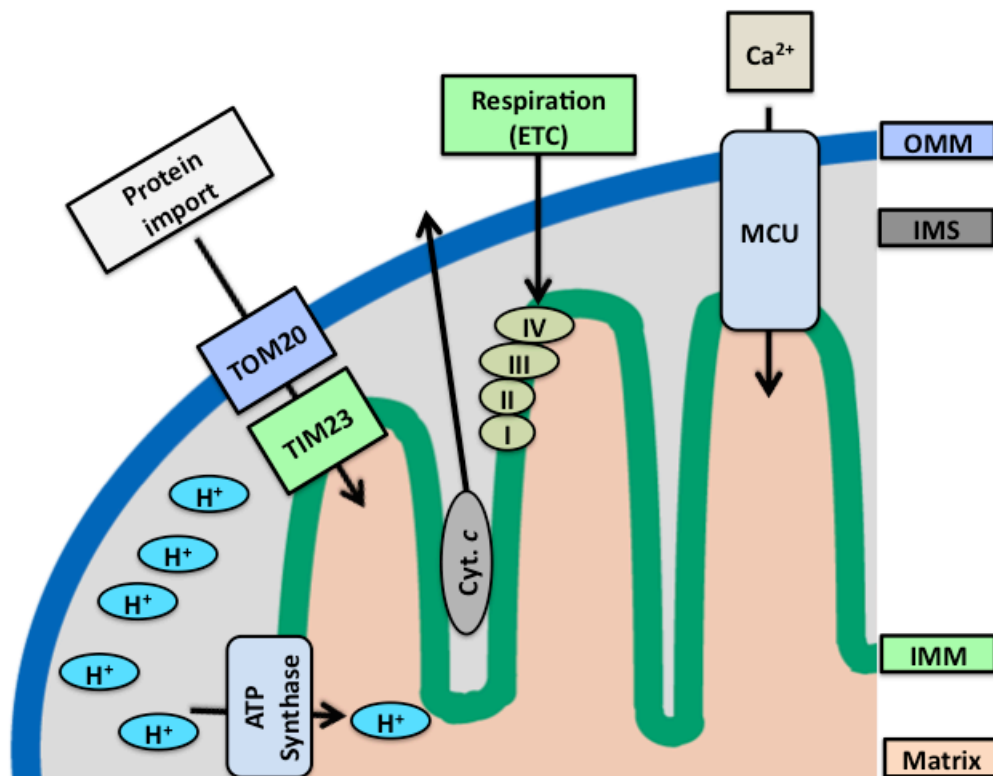


Figure I-1: Compartmentalization is essential to mitochondria functions

Mitochondria have two membranes: the OMM and IMM, which separate the two aqueous compartments, the IMS and the matrix from the remainder of the cell. Mitochondrial respiration through the ETC occurs through passing electrons to progressively stronger electron acceptors. Using the energy generated from the transfer of electrons through the ETC, mitochondrial membrane potential is created by pumping H⁺ into the IMS against the concentration gradient. Then H⁺ can be pumped back into the matrix via ATP synthase and the energy produced generates ATP. Mitochondrial import occurs through

membrane pores, TOM20 and TIM23. Proteins with mitochondrial targeting sequences can be imported into the mitochondrial matrix. I-IV, mitochondrial electron transport chain; ATP, adenosine triphosphate; Ca^{2+} , calcium ions, Cyt *c*, cytochrome *c*; ETC, electron transport chain; OMM, outer mitochondrial membrane; IMS, intermembrane space; IMM, inner mitochondrial membrane; MCU, mitochondrial calcium uniporter; H^+ , hydrogen ions.

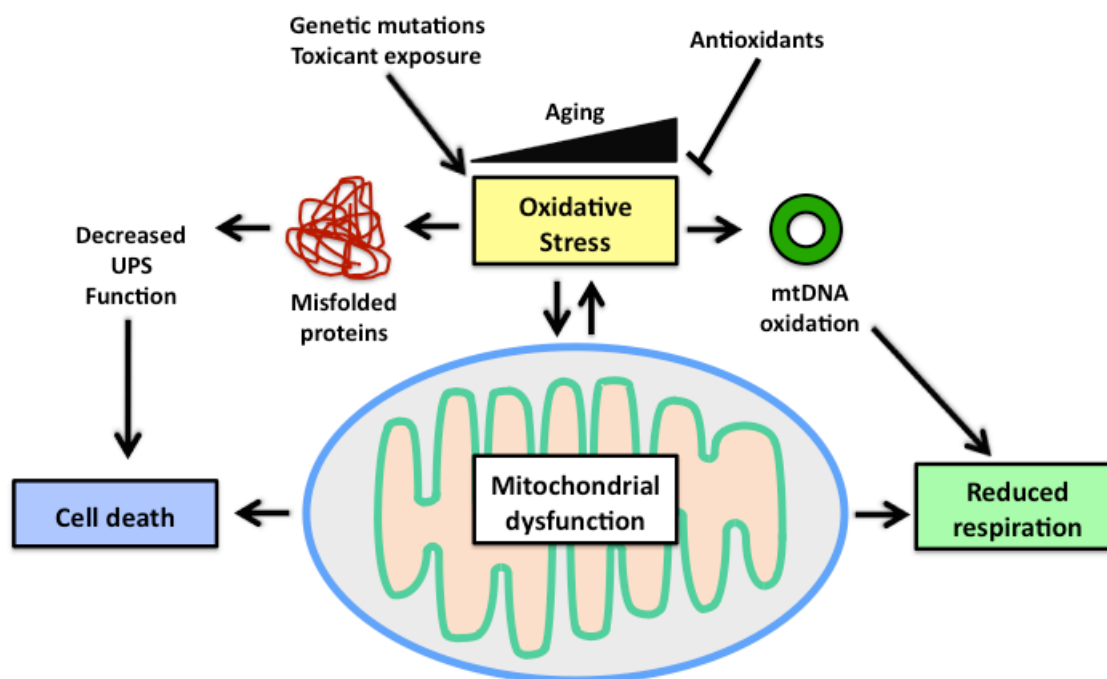


Figure I-2: Causes and effects of mitochondrial dysfunction

Mitochondrial dysfunction can cause multiple problems for the cell and damaged mitochondria produce excess ROS. Exposure to environmental toxicants or mutations in genes that regulate mitochondrial function has been shown to increase the accumulation

of reactive oxygen species (ROS). On the other hand, antioxidants can reduce the amount of free ROS. Accumulation of oxidative stress can oxidize proteins leading to protein dysfunction, misfolding, and aggregation and damage the proteasomal degradation pathway. Accumulation of ROS can also oxidize mtDNA resulting in aberrant or lower expression of mitochondrially-encoded genes, such as the players of the ETC. Oxidative stress can cause further dysfunction of mitochondria. Mitochondrial dysfunction or UPS dysfunction caused the accumulation of oxidized protein aggregates can both result in cell dysfunction and death. mtDNA, mitochondrial DNA; UPS, ubiquitin-proteasome system.

Table I-1: Neurodegenerative diseases with links to mitochondrial dysfunction

<u>Disease</u>	<u>Mitochondrial defects</u>	<u>Causes</u>	<u>Mitochondrial link</u>
Alzheimer's disease	mitochondrial fragmentation, mtDNA mutations and oxidation, reduced mtDNA, altered ultrastructure, increased nitrosylated Drp1	APP	mitochondrial dynamics
		tau	inhibits mitochondrial trafficking
Parkinson's disease	reduced OXPHOS, increased sensitivity to oxidative stress, altered morphology, altered ultrastructure, disrupted trafficking, increased ROS disrupted Ca ²⁺ homeostasis	a-Syn	accumulation blocks fusion
		PINK1	initiates mitophagy and protects against oxidative stress induced cell death
		parkin	targets damaged mitochondria for mitophagy

		DJ-1	protects against oxidative stress induced cell death
		MPTP	complex I inhibitor
		rotenone	complex I inhibitor
		paraquat	complex I inhibitor
Amyolateral sclerosis	disrupted trafficking, clustering, fragmentation, disrupted Ca ²⁺ homeostasis	TDP-43	affects mitochondrial dynamics
		SOD1	antioxidant function
Huntington's disease	reduced Ca ²⁺ buffering, reduced DY, reduced OXPPOS, increased fission, increased Drp1 expression, reduced Mfn expression	Huntingtin	directly interacts with Drp1
Prion diseases	reduced OXPPOS, fragmentation, ultrastructure defects, ROS	PrP ^{sc}	loss of PrP ^c results in mitochondrial dysfunction and increased oxidative stress

Table I-2: Models of mitochondrial dysfunction results in neurodegeneration

Gene	mitochondrial function	neurodegeneration
Mfn2	regulates OMM fusion	Charcot-Marie-Tooth Type 2A, axonal degeneration of motor nerves
OPA1	regulates IMM fusion	Autosomal Dominant Optic Atrophy, retinal ganglion and optic nerve degeneration
Drp1	regulates mitochondrial fission	neonatal lethality, abnormal brain development

Mgrn1	? E3 ligase	spongiform neurodegeneration
Atrn	?	spongiform neurodegeneration
SOD2	mitochondrial superoxide dismutase	spongiform neurodegeneration

References

1. Nunnari, J. and A. Suomalainen, Mitochondria: in sickness and in health. 2012. *Cell*, **148**(6): 1145-59.
2. Bonifati, V., et al., Early-onset parkinsonism associated with PINK1 mutations: frequency, genotypes, and phenotypes. 2005. *Neurology*, **65**(1): 87-95.
3. Hatano, Y., et al., Novel PINK1 mutations in early-onset parkinsonism. 2004. *Ann Neurol*, **56**(3): 424-7.
4. Kim, Y., et al., PINK1 controls mitochondrial localization of Parkin through direct phosphorylation. 2008. *Biochem Biophys Res Commun*, **377**(3): 975-80.
5. Pridgeon, J.W., et al., PINK1 protects against oxidative stress by phosphorylating mitochondrial chaperone TRAP1. 2007. *PLoS Biol*, **5**(7): e172.
6. Gautier, C.A., et al., Loss of PINK1 causes mitochondrial functional defects and increased sensitivity to oxidative stress. 2008. *Proc Natl Acad Sci U S A*, **105**(32): 11364-9.
7. Exner, N., et al., Loss-of-function of human PINK1 results in mitochondrial pathology and can be rescued by parkin. 2007. *J Neurosci*, **27**(45): 12413-8.
8. Lutz, A.K., et al., Loss of parkin or PINK1 function increases Drp1-dependent mitochondrial fragmentation. 2009. *J Biol Chem*, **284**(34): 22938-51.
9. He, L., et al., Spongiform degeneration in mahoganoid mutant mice. 2003. *Science*, **299**(5607): 710-2.
10. Sun, K., et al., Mitochondrial dysfunction precedes neurodegeneration in mahogunin (Mgrn1) mutant mice. 2007. *Neurobiol Aging*, **28**(12): 1840-52.
11. Duchen, M.R., Mitochondria and Ca²⁺ in cell physiology and pathophysiology. 2000. *Cell Calcium*, **28**(5-6): 339-48.
12. Green, D.R. and G.P. Amarante-Mendes, The point of no return: mitochondria, caspases, and the commitment to cell death. 1998. *Results Probl Cell Differ*, **24**: 45-61.
13. Deuschl, G., et al., A randomized trial of deep-brain stimulation for Parkinson's disease. 2006. *N Engl J Med*, **355**(9): 896-908.

14. Streck, E.L., et al., Neurodegeneration, mitochondrial dysfunction, and oxidative stress. 2013. *Oxid Med Cell Longev*, **2013**: 826046.
15. Cardoso, A.R., et al., Mitochondrial compartmentalization of redox processes. 2012. *Free Radic Biol Med*, **52**(11-12): 2201-8.
16. Delettre, C., et al., Nuclear gene OPA1, encoding a mitochondrial dynamin-related protein, is mutated in dominant optic atrophy. 2000. *Nat Genet*, **26**(2): 207-10.
17. Ow, Y.P., et al., Cytochrome c: functions beyond respiration. 2008. *Nat Rev Mol Cell Biol*, **9**(7): 532-42.
18. Hirst, J., et al., The production of reactive oxygen species by complex I. 2008. *Biochem Soc Trans*, **36**(Pt 5): 976-80.
19. Chen, Q., et al., Production of reactive oxygen species by mitochondria: central role of complex III. 2003. *J Biol Chem*, **278**(38): 36027-31.
20. Eguchi, Y., et al., Intracellular ATP levels determine cell death fate by apoptosis or necrosis. 1997. *Cancer Res*, **57**(10): 1835-40.
21. Luo, Y., et al., Compromised mitochondrial function leads to increased cytosolic calcium and to activation of MAP kinases. 1997. *Proc Natl Acad Sci U S A*, **94**(18): 9705-10.
22. Gunter, T.E., et al., Calcium and mitochondria. 2004. *FEBS Lett*, **567**(1): 96-102.
23. Thayer, S.A. and R.J. Miller, Regulation of the intracellular free calcium concentration in single rat dorsal root ganglion neurones in vitro. 1990. *J Physiol*, **425**: 85-115.
24. Das, A.M. and D.A. Harris, Control of mitochondrial ATP synthase in heart cells: inactive to active transitions caused by beating or positive inotropic agents. 1990. *Cardiovasc Res*, **24**(5): 411-7.
25. Rizzuto, R., et al., Mitochondria as sensors and regulators of calcium signalling. 2012. *Nat Rev Mol Cell Biol*, **13**(9): 566-78.
26. Hoth, M., et al., Mitochondrial control of calcium-channel gating: a mechanism for sustained signaling and transcriptional activation in T lymphocytes. 2000. *Proc Natl Acad Sci U S A*, **97**(19): 10607-12.
27. Pradhan, R.K., et al., Characterization of membrane potential dependency of mitochondrial Ca²⁺ uptake by an improved biophysical model of mitochondrial Ca²⁺ uniporter. 2010. *PLoS One*, **5**(10): e13278.
28. Bernardi, P. and V. Petronilli, The permeability transition pore as a mitochondrial calcium release channel: a critical appraisal. 1996. *J Bioenerg Biomembr*, **28**(2): 131-8.
29. Ivannikov, M.V., et al., Synaptic vesicle exocytosis in hippocampal synaptosomes correlates directly with total mitochondrial volume. 2013. *J Mol Neurosci*, **49**(1): 223-30.
30. Berridge, M.J., Neuronal calcium signaling. 1998. *Neuron*, **21**(1): 13-26.
31. Mattson, M.P., Calcium and neurodegeneration. 2007. *Aging Cell*, **6**(3): 337-50.
32. Supnet, C. and I. Bezprozvanny, Neuronal calcium signaling, mitochondrial dysfunction, and Alzheimer's disease. 2010. *J Alzheimers Dis*, **20 Suppl 2**: S487-98.

33. Toescu, E.C. and A. Verkhratsky, Role of calcium in normal aging and neurodegeneration. 2007. *Aging Cell*, **6**(3): 265.
34. Toescu, E.C. and M. Vreugdenhil, Calcium and normal brain ageing. 2010. *Cell Calcium*, **47**(2): 158-64.
35. Yuan, J. and B.A. Yankner, Apoptosis in the nervous system. 2000. *Nature*, **407**(6805): 802-9.
36. Martin, L.J., Neuronal cell death in nervous system development, disease, and injury (Review). 2001. *Int J Mol Med*, **7**(5): 455-78.
37. Wei, M.C., et al., Proapoptotic BAX and BAK: a requisite gateway to mitochondrial dysfunction and death. 2001. *Science*, **292**(5517): 727-30.
38. Kim, H., et al., Hierarchical regulation of mitochondrion-dependent apoptosis by BCL-2 subfamilies. 2006. *Nat Cell Biol*, **8**(12): 1348-58.
39. Willis, S.N., et al., Apoptosis initiated when BH3 ligands engage multiple Bcl-2 homologs, not Bax or Bak. 2007. *Science*, **315**(5813): 856-9.
40. Hsu, Y.T., et al., Cytosol-to-membrane redistribution of Bax and Bcl-X(L) during apoptosis. 1997. *Proc Natl Acad Sci U S A*, **94**(8): 3668-72.
41. Wolter, K.G., et al., Movement of Bax from the cytosol to mitochondria during apoptosis. 1997. *J Cell Biol*, **139**(5): 1281-92.
42. Lovell, J.F., et al., Membrane binding by tBid initiates an ordered series of events culminating in membrane permeabilization by Bax. 2008. *Cell*, **135**(6): 1074-84.
43. Liu, X., et al., DFF, a heterodimeric protein that functions downstream of caspase-3 to trigger DNA fragmentation during apoptosis. 1997. *Cell*, **89**(2): 175-84.
44. Enari, M., et al., A caspase-activated DNase that degrades DNA during apoptosis, and its inhibitor ICAD. 1998. *Nature*, **391**(6662): 43-50.
45. Collier, T.J., et al., Ageing as a primary risk factor for Parkinson's disease: evidence from studies of non-human primates. 2011. *Nat Rev Neurosci*, **12**(6): 359-66.
46. Pereira, M.D., et al., Oxidative stress in neurodegenerative diseases and ageing. 2012. *Oxid Med Cell Longev*, **2012**: 796360.
47. Hung, C.W., et al., Ageing and neurodegenerative diseases. 2010. *Ageing Res Rev*, **9 Suppl 1**: S36-46.
48. Bolanos, J.P., et al., Glycolysis: a bioenergetic or a survival pathway? 2010. *Trends Biochem Sci*, **35**(3): 145-9.
49. Herrero-Mendez, A., et al., The bioenergetic and antioxidant status of neurons is controlled by continuous degradation of a key glycolytic enzyme by APC/C-Cdh1. 2009. *Nat Cell Biol*, **11**(6): 747-52.
50. Mink, J.W., et al., Ratio of central nervous system to body metabolism in vertebrates: its constancy and functional basis. 1981. *Am J Physiol*, **241**(3): R203-12.
51. Li, Z., et al., The importance of dendritic mitochondria in the morphogenesis and plasticity of spines and synapses. 2004. *Cell*, **119**(6): 873-87.
52. Verstreken, P., et al., Synaptic mitochondria are critical for mobilization of reserve pool vesicles at *Drosophila* neuromuscular junctions. 2005. *Neuron*, **47**(3): 365-78.

53. Steketee, M.B., et al., Mitochondrial dynamics regulate growth cone motility, guidance, and neurite growth rate in perinatal retinal ganglion cells in vitro. 2012. *Invest Ophthalmol Vis Sci*, **53**(11): 7402-11.
54. Sohal, R.S., et al., Hydrogen peroxide production by liver mitochondria in different species. 1990. *Mech Ageing Dev*, **53**(3): 209-15.
55. Ku, H.H., et al., Relationship between mitochondrial superoxide and hydrogen peroxide production and longevity of mammalian species. 1993. *Free Radic Biol Med*, **15**(6): 621-7.
56. Barja, G., et al., Low mitochondrial free radical production per unit O₂ consumption can explain the simultaneous presence of high longevity and high aerobic metabolic rate in birds. 1994. *Free Radic Res*, **21**(5): 317-27.
57. Rosa, E.F., et al., Oxidative stress induced by intense and exhaustive exercise impairs murine cognitive function. 2007. *J Neurophysiol*, **98**(3): 1820-6.
58. Berr, C., et al., Cognitive decline is associated with systemic oxidative stress: the EVA study. *Etude du Vieillissement Arteriel*. 2000. *J Am Geriatr Soc*, **48**(10): 1285-91.
59. Zarkovic, K., 4-hydroxynonenal and neurodegenerative diseases. 2003. *Mol Aspects Med*, **24**(4-5): 293-303.
60. Shamoto-Nagai, M., et al., In parkinsonian substantia nigra, alpha-synuclein is modified by acrolein, a lipid-peroxidation product, and accumulates in the dopamine neurons with inhibition of proteasome activity. 2007. *J Neural Transm*, **114**(12): 1559-67.
61. Lee, J., et al., Modulation of lipid peroxidation and mitochondrial function improves neuropathology in Huntington's disease mice. 2011. *Acta Neuropathol*, **121**(4): 487-98.
62. Morel, P., et al., Effects of 4-hydroxynonenal, a lipid peroxidation product, on dopamine transport and Na⁺/K⁺ ATPase in rat striatal synaptosomes. 1998. *Neurochem Int*, **33**(6): 531-40.
63. Tamagno, E., et al., Multiple signaling events in amyloid beta-induced, oxidative stress-dependent neuronal apoptosis. 2003. *Free Radic Biol Med*, **35**(1): 45-58.
64. Chan, P.H., Reactive oxygen radicals in signaling and damage in the ischemic brain. 2001. *J Cereb Blood Flow Metab*, **21**(1): 2-14.
65. Barth, B.M., et al., Proinflammatory cytokines provoke oxidative damage to actin in neuronal cells mediated by Rac1 and NADPH oxidase. 2009. *Mol Cell Neurosci*, **41**(2): 274-85.
66. Bongarzone, E.R., et al., Oxidative damage to proteins and lipids of CNS myelin produced by in vitro generated reactive oxygen species. 1995. *J Neurosci Res*, **41**(2): 213-21.
67. Mattson, M.P. and D. Liu, Energetics and oxidative stress in synaptic plasticity and neurodegenerative disorders. 2002. *Neuromolecular Med*, **2**(2): 215-31.
68. Sanz, A. and R.K. Stefanatos, The mitochondrial free radical theory of aging: a critical view. 2008. *Curr Aging Sci*, **1**(1): 10-21.
69. de Grey, A.D., A proposed refinement of the mitochondrial free radical theory of aging. 1997. *Bioessays*, **19**(2): 161-6.

70. Harman, D., Free radical theory of aging: dietary implications. 1972. *Am J Clin Nutr*, **25**(8): 839-43.
71. Sohal, R.S. and R. Weindruch, Oxidative stress, caloric restriction, and aging. 1996. *Science*, **273**(5271): 59-63.
72. Kudin, A.P., et al., Characterization of superoxide production sites in isolated rat brain and skeletal muscle mitochondria. 2005. *Biomed Pharmacother*, **59**(4): 163-8.
73. Kurihara, Y., et al., Mitophagy plays an essential role in reducing mitochondrial production of reactive oxygen species and mutation of mitochondrial DNA by maintaining mitochondrial quantity and quality in yeast. 2012. *J Biol Chem*, **287**(5): 3265-72.
74. Carocho, M. and I.C. Ferreira, A review on antioxidants, prooxidants and related controversy: natural and synthetic compounds, screening and analysis methodologies and future perspectives. 2013. *Food Chem Toxicol*, **51**: 15-25.
75. Kruman, II, et al., Cell cycle activation linked to neuronal cell death initiated by DNA damage. 2004. *Neuron*, **41**(4): 549-61.
76. Linnane, A.W., et al., Mitochondrial DNA mutations as an important contributor to ageing and degenerative diseases. 1989. *Lancet*, **1**(8639): 642-5.
77. Lin, M.T., et al., Somatic mitochondrial DNA mutations in early Parkinson and incidental Lewy body disease. 2012. *Ann Neurol*, **71**(6): 850-4.
78. Grazina, M., et al., Genetic basis of Alzheimer's dementia: role of mtDNA mutations. 2006. *Genes Brain Behav*, **5 Suppl 2**: 92-107.
79. Kraytsberg, Y., et al., Mitochondrial DNA deletions are abundant and cause functional impairment in aged human substantia nigra neurons. 2006. *Nat Genet*, **38**(5): 518-20.
80. Wei, Y.H., et al., Oxidative damage and mutation to mitochondrial DNA and age-dependent decline of mitochondrial respiratory function. 1998. *Ann N Y Acad Sci*, **854**: 155-70.
81. Taylor, R.W. and D.M. Turnbull, Mitochondrial DNA mutations in human disease. 2005. *Nat Rev Genet*, **6**(5): 389-402.
82. Luoma, P., et al., Parkinsonism, premature menopause, and mitochondrial DNA polymerase gamma mutations: clinical and molecular genetic study. 2004. *Lancet*, **364**(9437): 875-82.
83. Swerdlow, R.H., et al., Matrilinial inheritance of complex I dysfunction in a multigenerational Parkinson's disease family. 1998. *Ann Neurol*, **44**(6): 873-81.
84. Corral-Debrinski, M., et al., Mitochondrial DNA deletions in human brain: regional variability and increase with advanced age. 1992. *Nat Genet*, **2**(4): 324-9.
85. Mecocci, P., et al., Oxidative damage to mitochondrial DNA is increased in Alzheimer's disease. 1994. *Ann Neurol*, **36**(5): 747-51.
86. Ikebe, S., et al., Point mutations of mitochondrial genome in Parkinson's disease. 1995. *Brain Res Mol Brain Res*, **28**(2): 281-95.

87. Ozawa, T., et al., Quantitative determination of deleted mitochondrial DNA relative to normal DNA in parkinsonian striatum by a kinetic PCR analysis. 1990. *Biochem Biophys Res Commun*, **172**(2): 483-9.
88. Wallace, D.C., et al., Diseases resulting from mitochondrial DNA point mutations. 1992. *J Inher Metab Dis*, **15**(4): 472-9.
89. Gredilla, R., et al., Differential age-related changes in mitochondrial DNA repair activities in mouse brain regions. 2010. *Neurobiol Aging*, **31**(6): 993-1002.
90. Gredilla, R., et al., Mitochondrial DNA repair and association with aging--an update. 2010. *Exp Gerontol*, **45**(7-8): 478-88.
91. Chen, D., et al., Age-dependent decline of DNA repair activity for oxidative lesions in rat brain mitochondria. 2002. *J Neurochem*, **81**(6): 1273-84.
92. Melov, S., et al., Multi-organ characterization of mitochondrial genomic rearrangements in ad libitum and caloric restricted mice show striking somatic mitochondrial DNA rearrangements with age. 1997. *Nucleic Acids Res*, **25**(5): 974-82.
93. Trifunovic, A., et al., Premature ageing in mice expressing defective mitochondrial DNA polymerase. 2004. *Nature*, **429**(6990): 417-23.
94. Ekstrand, M.I., et al., Progressive parkinsonism in mice with respiratory-chain-deficient dopamine neurons. 2007. *Proc Natl Acad Sci U S A*, **104**(4): 1325-30.
95. Sorensen, L., et al., Late-onset corticohippocampal neurodepletion attributable to catastrophic failure of oxidative phosphorylation in MILON mice. 2001. *J Neurosci*, **21**(20): 8082-90.
96. Mecocci, P., et al., Oxidative damage to mitochondrial DNA shows marked age-dependent increases in human brain. 1993. *Ann Neurol*, **34**(4): 609-16.
97. Sohal, R.S. and A. Dubey, Mitochondrial oxidative damage, hydrogen peroxide release, and aging. 1994. *Free Radic Biol Med*, **16**(5): 621-6.
98. Ozawa, T., Genetic and functional changes in mitochondria associated with aging. 1997. *Physiol Rev*, **77**(2): 425-64.
99. Ghosh, R. and D.L. Mitchell, Effect of oxidative DNA damage in promoter elements on transcription factor binding. 1999. *Nucleic Acids Res*, **27**(15): 3213-8.
100. Lewis, M.R. and W.H. Lewis, Mitochondria in Tissue Culture. 1914. *Science*, **39**(1000): 330-3.
101. Chan, D., et al., Mitochondrial dynamics in cell life and death. 2006. *Cell Death Differ*, **13**(4): 680-4.
102. Knott, A.B., et al., Mitochondrial fragmentation in neurodegeneration. 2008. *Nat Rev Neurosci*, **9**(7): 505-18.
103. Chen, H., et al., Mitochondrial fusion is required for mtDNA stability in skeletal muscle and tolerance of mtDNA mutations. 2010. *Cell*, **141**(2): 280-9.
104. Chen, H., et al., Disruption of fusion results in mitochondrial heterogeneity and dysfunction. 2005. *J Biol Chem*, **280**(28): 26185-92.
105. Chen, H., et al., Mitofusins Mfn1 and Mfn2 coordinately regulate mitochondrial fusion and are essential for embryonic development. 2003. *J Cell Biol*, **160**(2): 189-200.

106. Chen, H., et al., Mitochondrial fusion protects against neurodegeneration in the cerebellum. 2007. *Cell*, **130**(3): 548-62.
107. Chen, Y., et al., Mitochondrial fusion is essential for organelle function and cardiac homeostasis. 2011. *Circ Res*, **109**(12): 1327-31.
108. Rambold, A.S., et al., Fuse or die: Shaping mitochondrial fate during starvation. 2011. *Commun Integr Biol*, **4**(6): 752-4.
109. Tondera, D., et al., SLP-2 is required for stress-induced mitochondrial hyperfusion. 2009. *EMBO J*, **28**(11): 1589-600.
110. Ryan, M.T. and D. Stojanovski, Mitofusins 'bridge' the gap between oxidative stress and mitochondrial hyperfusion. 2012. *EMBO Rep*, **13**(10): 870-1.
111. Detmer, S.A. and D.C. Chan, Complementation between mouse Mfn1 and Mfn2 protects mitochondrial fusion defects caused by CMT2A disease mutations. 2007. *J Cell Biol*, **176**(4): 405-14.
112. Koshihara, T., et al., Structural basis of mitochondrial tethering by mitofusin complexes. 2004. *Science*, **305**(5685): 858-62.
113. Detmer, S.A. and D.C. Chan, Functions and dysfunctions of mitochondrial dynamics. 2007. *Nat Rev Mol Cell Biol*, **8**(11): 870-9.
114. Santel, A. and M.T. Fuller, Control of mitochondrial morphology by a human mitofusin. 2001. *J Cell Sci*, **114**(Pt 5): 867-74.
115. Song, Z., et al., Mitofusins and OPA1 mediate sequential steps in mitochondrial membrane fusion. 2009. *Mol Biol Cell*, **20**(15): 3525-32.
116. Lawson, V.H., et al., Clinical and electrophysiologic features of CMT2A with mutations in the mitofusin 2 gene. 2005. *Neurology*, **65**(2): 197-204.
117. Vallat, J.M., et al., Histopathological findings in hereditary motor and sensory neuropathy of axonal type with onset in early childhood associated with mitofusin 2 mutations. 2008. *J Neuropathol Exp Neurol*, **67**(11): 1097-102.
118. Zuchner, S., et al., Mutations in the mitochondrial GTPase mitofusin 2 cause Charcot-Marie-Tooth neuropathy type 2A. 2004. *Nat Genet*, **36**(5): 449-51.
119. Boaretto, F., et al., Severe CMT type 2 with fatal encephalopathy associated with a novel MFN2 splicing mutation. 2010. *Neurology*, **74**(23): 1919-21.
120. Baloh, R.H., et al., Altered axonal mitochondrial transport in the pathogenesis of Charcot-Marie-Tooth disease from mitofusin 2 mutations. 2007. *J Neurosci*, **27**(2): 422-30.
121. Sebastian, D., et al., Mitofusin 2 (Mfn2) links mitochondrial and endoplasmic reticulum function with insulin signaling and is essential for normal glucose homeostasis. 2012. *Proc Natl Acad Sci U S A*, **109**(14): 5523-8.
122. Zanna, C., et al., OPA1 mutations associated with dominant optic atrophy impair oxidative phosphorylation and mitochondrial fusion. 2008. *Brain*, **131**(Pt 2): 352-67.
123. Pesch, U.E., et al., OPA1 mutations in patients with autosomal dominant optic atrophy and evidence for semi-dominant inheritance. 2001. *Hum Mol Genet*, **10**(13): 1359-68.
124. Toomes, C., et al., Spectrum, frequency and penetrance of OPA1 mutations in dominant optic atrophy. 2001. *Hum Mol Genet*, **10**(13): 1369-78.
125. Delettre, C., et al., Mutation spectrum and splicing variants in the OPA1 gene. 2001. *Hum Genet*, **109**(6): 584-91.

126. Olichon, A., et al., Effects of OPA1 mutations on mitochondrial morphology and apoptosis: relevance to ADOA pathogenesis. 2007. *J Cell Physiol*, **211**(2): 423-30.
127. Alavi, M.V., et al., A splice site mutation in the murine Opa1 gene features pathology of autosomal dominant optic atrophy. 2007. *Brain*, **130**(Pt 4): 1029-42.
128. Davies, V.J., et al., Opa1 deficiency in a mouse model of autosomal dominant optic atrophy impairs mitochondrial morphology, optic nerve structure and visual function. 2007. *Hum Mol Genet*, **16**(11): 1307-18.
129. White, K.E., et al., OPA1 deficiency associated with increased autophagy in retinal ganglion cells in a murine model of dominant optic atrophy. 2009. *Invest Ophthalmol Vis Sci*, **50**(6): 2567-71.
130. Jagasia, R., et al., DRP-1-mediated mitochondrial fragmentation during EGL-1-induced cell death in *C. elegans*. 2005. *Nature*, **433**(7027): 754-60.
131. Bossy-Wetzell, E., et al., Mitochondrial fission in apoptosis, neurodegeneration and aging. 2003. *Curr Opin Cell Biol*, **15**(6): 706-16.
132. Frank, S., et al., The role of dynamin-related protein 1, a mediator of mitochondrial fission, in apoptosis. 2001. *Dev Cell*, **1**(4): 515-25.
133. Friedman, J.R., et al., ER tubules mark sites of mitochondrial division. 2011. *Science*, **334**(6054): 358-62.
134. Murley, A., et al., ER-associated mitochondrial division links the distribution of mitochondria and mitochondrial DNA in yeast. 2013. *Elife*, **2**: e00422.
135. Pitts, K.R., et al., The dynamin-like protein DLP1 is essential for normal distribution and morphology of the endoplasmic reticulum and mitochondria in mammalian cells. 1999. *Mol Biol Cell*, **10**(12): 4403-17.
136. Yoon, Y., et al., The mitochondrial protein hFis1 regulates mitochondrial fission in mammalian cells through an interaction with the dynamin-like protein DLP1. 2003. *Mol Cell Biol*, **23**(15): 5409-20.
137. Germain, M., et al., Endoplasmic reticulum BIK initiates DRP1-regulated remodelling of mitochondrial cristae during apoptosis. 2005. *EMBO J*, **24**(8): 1546-56.
138. Stojanovski, D., et al., Levels of human Fis1 at the mitochondrial outer membrane regulate mitochondrial morphology. 2004. *J Cell Sci*, **117**(Pt 7): 1201-10.
139. Otera, H., et al., Mff is an essential factor for mitochondrial recruitment of Drp1 during mitochondrial fission in mammalian cells. 2010. *J Cell Biol*, **191**(6): 1141-58.
140. Gandre-Babbe, S. and A.M. van der Blik, The novel tail-anchored membrane protein Mff controls mitochondrial and peroxisomal fission in mammalian cells. 2008. *Mol Biol Cell*, **19**(6): 2402-12.
141. Shaw, J.M. and J. Nunnari, Mitochondrial dynamics and division in budding yeast. 2002. *Trends Cell Biol*, **12**(4): 178-84.
142. Smirnova, E., et al., A human dynamin-related protein controls the distribution of mitochondria. 1998. *J Cell Biol*, **143**(2): 351-8.
143. Malena, A., et al., Inhibition of mitochondrial fission favours mutant over wild-type mitochondrial DNA. 2009. *Hum Mol Genet*, **18**(18): 3407-16.

144. Ishihara, N., et al., Mitochondrial fission factor Drp1 is essential for embryonic development and synapse formation in mice. 2009. *Nat Cell Biol*, **11**(8): 958-66.
145. Chang, C.R., et al., A lethal de novo mutation in the middle domain of the dynamin-related GTPase Drp1 impairs higher order assembly and mitochondrial division. 2010. *J Biol Chem*, **285**(42): 32494-503.
146. Taguchi, N., et al., Mitotic phosphorylation of dynamin-related GTPase Drp1 participates in mitochondrial fission. 2007. *J Biol Chem*, **282**(15): 11521-9.
147. Qi, X., et al., Aberrant mitochondrial fission in neurons induced by protein kinase C $\{\delta\}$ under oxidative stress conditions in vivo. 2011. *Mol Biol Cell*, **22**(2): 256-65.
148. Wang, W., et al., Mitochondrial fission triggered by hyperglycemia is mediated by ROCK1 activation in podocytes and endothelial cells. 2012. *Cell Metab*, **15**(2): 186-200.
149. Chang, C.R. and C. Blackstone, Drp1 phosphorylation and mitochondrial regulation. 2007. *EMBO Rep*, **8**(12): 1088-9; author reply 1089-90.
150. Cribbs, J.T. and S. Strack, Reversible phosphorylation of Drp1 by cyclic AMP-dependent protein kinase and calcineurin regulates mitochondrial fission and cell death. 2007. *EMBO Rep*, **8**(10): 939-44.
151. Chou, C.H., et al., GSK3 β -mediated Drp1 phosphorylation induced elongated mitochondrial morphology against oxidative stress. 2012. *PLoS One*, **7**(11): e49112.
152. van der Blik, A.M., et al., Mechanisms of mitochondrial fission and fusion. 2013. *Cold Spring Harb Perspect Biol*, **5**(6).
153. Fang, L., et al., Inactivation of MARCH5 prevents mitochondrial fragmentation and interferes with cell death in a neuronal cell model. 2012. *PLoS One*, **7**(12): e52637.
154. Karbowski, M., et al., The mitochondrial E3 ubiquitin ligase MARCH5 is required for Drp1 dependent mitochondrial division. 2007. *J Cell Biol*, **178**(1): 71-84.
155. Braschi, E., et al., MAPL is a new mitochondrial SUMO E3 ligase that regulates mitochondrial fission. 2009. *EMBO Rep*, **10**(7): 748-54.
156. Haun, F., et al., S-nitrosylation of dynamin-related protein 1 mediates mutant huntingtin-induced mitochondrial fragmentation and neuronal injury in Huntington's disease. 2013. *Antioxid Redox Signal*, **19**(11): 1173-84.
157. Cho, D.H., et al., S-nitrosylation of Drp1 mediates beta-amyloid-related mitochondrial fission and neuronal injury. 2009. *Science*, **324**(5923): 102-5.
158. Nakamura, T., et al., S-nitrosylation of Drp1 links excessive mitochondrial fission to neuronal injury in neurodegeneration. 2010. *Mitochondrion*, **10**(5): 573-8.
159. Youle, R.J. and D.P. Narendra, Mechanisms of mitophagy. 2011. *Nat Rev Mol Cell Biol*, **12**(1): 9-14.
160. Gegg, M.E., et al., Mitofusin 1 and mitofusin 2 are ubiquitinated in a PINK1/parkin-dependent manner upon induction of mitophagy. 2010. *Hum Mol Genet*, **19**(24): 4861-70.

161. Wasiak, S., et al., Bax/Bak promote sumoylation of DRP1 and its stable association with mitochondria during apoptotic cell death. 2007. *J Cell Biol*, **177**(3): 439-50.
162. Kim, I., et al., Selective degradation of mitochondria by mitophagy. 2007. *Arch Biochem Biophys*, **462**(2): 245-53.
163. Narendra, D., et al., Parkin is recruited selectively to impaired mitochondria and promotes their autophagy. 2008. *J Cell Biol*, **183**(5): 795-803.
164. Matsuda, N., et al., PINK1 stabilized by mitochondrial depolarization recruits Parkin to damaged mitochondria and activates latent Parkin for mitophagy. 2010. *J Cell Biol*, **189**(2): 211-21.
165. Narendra, D.P., et al., PINK1 is selectively stabilized on impaired mitochondria to activate Parkin. 2010. *PLoS Biol*, **8**(1): e1000298.
166. Chan, N.C., et al., Broad activation of the ubiquitin-proteasome system by Parkin is critical for mitophagy. 2011. *Hum Mol Genet*, **20**(9): 1726-37.
167. Tanaka, A., et al., Proteasome and p97 mediate mitophagy and degradation of mitofusins induced by Parkin. 2010. *J Cell Biol*, **191**(7): 1367-80.
168. Yoshii, S.R., et al., Parkin mediates proteasome-dependent protein degradation and rupture of the outer mitochondrial membrane. 2011. *J Biol Chem*, **286**(22): 19630-40.
169. Lee, J.Y., et al., Disease-causing mutations in parkin impair mitochondrial ubiquitination, aggregation, and HDAC6-dependent mitophagy. 2010. *J Cell Biol*, **189**(4): 671-9.
170. Narendra, D., et al., p62/SQSTM1 is required for Parkin-induced mitochondrial clustering but not mitophagy; VDAC1 is dispensable for both. 2010. *Autophagy*, **6**(8): 1090-106.
171. Lemasters, J.J., Selective mitochondrial autophagy, or mitophagy, as a targeted defense against oxidative stress, mitochondrial dysfunction, and aging. 2005. *Rejuvenation Res*, **8**(1): 3-5.
172. Schapira, A.H., Complex I: inhibitors, inhibition and neurodegeneration. 2010. *Exp Neurol*, **224**(2): 331-5.
173. Boland, B., et al., Autophagy induction and autophagosome clearance in neurons: relationship to autophagic pathology in Alzheimer's disease. 2008. *J Neurosci*, **28**(27): 6926-37.
174. Nixon, R.A., Endosome function and dysfunction in Alzheimer's disease and other neurodegenerative diseases. 2005. *Neurobiol Aging*, **26**(3): 373-82.
175. de Rijk, M.C., et al., Prevalence of parkinsonism and Parkinson's disease in Europe: the EUROPARKINSON Collaborative Study. European Community Concerted Action on the Epidemiology of Parkinson's disease. 1997. *J Neurol Neurosurg Psychiatry*, **62**(1): 10-5.
176. Lang, A.E. and A.M. Lozano, Parkinson's disease. First of two parts. 1998. *N Engl J Med*, **339**(15): 1044-53.
177. Lang, A.E. and A.M. Lozano, Parkinson's disease. Second of two parts. 1998. *N Engl J Med*, **339**(16): 1130-43.
178. Lang, A.E. and A.M. Lozano, Parkinson's disease. First of two parts. 1998. *N Engl J Med*, **339**(15): 1044-53.

179. Braak, H., et al., Stages in the development of Parkinson's disease-related pathology. 2004. *Cell & Tissue Research*, **318**(1): 121-34.
180. Dauer, W. and S. Przedborski, Parkinson's disease: mechanisms and models. 2003. *Neuron*, **39**(6): 889-909.
181. Goedert, M., et al., 100 years of Lewy pathology. 2013. *Nat Rev Neurol*, **9**(1): 13-24.
182. Hawkes, C.H., et al., A timeline for Parkinson's disease. 2010. *Parkinsonism Relat Disord*, **16**(2): 79-84.
183. Hashimoto, M., et al., Oxidative stress induces amyloid-like aggregate formation of NACP/alpha-synuclein in vitro. 1999. *Neuroreport*, **10**(4): 717-21.
184. Schapira, A.H., et al., Mitochondrial complex I deficiency in Parkinson's disease. 1989. *Lancet*, **1**(8649): 1269.
185. Abou-Sleiman, P.M., et al., Expanding insights of mitochondrial dysfunction in Parkinson's disease. 2006. *Nature Reviews Neuroscience*, **7**(3): 207-19.
186. Schapira, A.H., Mitochondrial dysfunction in Parkinson's disease. 2007. *Cell Death & Differentiation*, **14**(7): 1261-6.
187. Schon, E.A. and S. Przedborski, Mitochondria: the next (neurode)generation. 2011. *Neuron*, **70**(6): 1033-53.
188. Bossy-Wetzler, E., et al., Molecular pathways to neurodegeneration. 2004. *Nat Med*, **10 Suppl**: S2-9.
189. Cookson, M.R. and O. Bandmann, Parkinson's disease: insights from pathways. 2010. *Human Molecular Genetics*, **19**(R1): R21-7.
190. Shulman, J.M., et al., Parkinson's disease: genetics and pathogenesis. 2011. *Annu Rev Pathol*, **6**: 193-222.
191. Deas, E., et al., PINK1 function in health and disease. 2009. *EMBO Mol Med*, **1**(3): 152-65.
192. Bindoff, L.A., et al., Mitochondrial function in Parkinson's disease. 1989. *Lancet*, **2**(8653): 49.
193. Parker, W.D., Jr., et al., Abnormalities of the electron transport chain in idiopathic Parkinson's disease. 1989. *Ann Neurol*, **26**(6): 719-23.
194. Shoffner, J.M., et al., Mitochondrial oxidative phosphorylation defects in Parkinson's disease. 1991. *Ann Neurol*, **30**(3): 332-9.
195. Poole, A.C., et al., The PINK1/Parkin pathway regulates mitochondrial morphology. 2008. *Proc Natl Acad Sci U S A*, **105**(5): 1638-43.
196. Valente, E.M., et al., Hereditary early-onset Parkinson's disease caused by mutations in PINK1. 2004. *Science*, **304**(5674): 1158-60.
197. Valente, E.M., et al., PINK1 mutations are associated with sporadic early-onset parkinsonism. 2004. *Ann Neurol*, **56**(3): 336-41.
198. Morais, V.A., et al., PINK1 loss-of-function mutations affect mitochondrial complex I activity via NdufA10 ubiquinone uncoupling. 2014. *Science*, **344**(6180): 203-7.
199. Tang, B., et al., Association of PINK1 and DJ-1 confers digenic inheritance of early-onset Parkinson's disease. 2006. *Hum Mol Genet*, **15**(11): 1816-25.

200. Petit, A., et al., Wild-type PINK1 prevents basal and induced neuronal apoptosis, a protective effect abrogated by Parkinson disease-related mutations. 2005. *J Biol Chem*, **280**(40): 34025-32.
201. Deas, E., et al., Mitophagy and Parkinson's disease: the PINK1-parkin link. 2011. *Biochim Biophys Acta*, **1813**(4): 623-33.
202. Parganlija, D., et al., Loss of PINK1 Impairs Stress-Induced Autophagy and Cell Survival. 2014. *PLoS One*, **9**(4): e95288.
203. Zhang, L., et al., TRAP1 rescues PINK1 loss-of-function phenotypes. 2013. *Hum Mol Genet*, **22**(14): 2829-41.
204. Butler, E.K., et al., The mitochondrial chaperone protein TRAP1 mitigates alpha-Synuclein toxicity. 2012. *PLoS Genet*, **8**(2): e1002488.
205. Costa, A.C., et al., Drosophila Trap1 protects against mitochondrial dysfunction in a PINK1/parkin model of Parkinson's disease. 2013. *Cell Death Dis*, **4**: e467.
206. Vives-Bauza, C., et al., PINK1-dependent recruitment of Parkin to mitochondria in mitophagy. 2010. *Proc Natl Acad Sci U S A*, **107**(1): 378-83.
207. Geisler, S., et al., The PINK1/Parkin-mediated mitophagy is compromised by PD-associated mutations. 2010. *Autophagy*, **6**(7): 871-8.
208. Kane, L.A., et al., PINK1 phosphorylates ubiquitin to activate Parkin E3 ubiquitin ligase activity. 2014. *J Cell Biol*.
209. Kazlauskaitė, A., et al., Parkin is activated by PINK1-dependent phosphorylation of ubiquitin at Serine65. 2014. *Biochem J*.
210. Kondapalli, C., et al., PINK1 is activated by mitochondrial membrane potential depolarization and stimulates Parkin E3 ligase activity by phosphorylating Serine 65. 2012. *Open Biol*, **2**(5): 120080.
211. Shiba-Fukushima, K., et al., PINK1-mediated phosphorylation of the Parkin ubiquitin-like domain primes mitochondrial translocation of Parkin and regulates mitophagy. 2012. *Sci Rep*, **2**: 1002.
212. Abbas, N., et al., A wide variety of mutations in the parkin gene are responsible for autosomal recessive parkinsonism in Europe. French Parkinson's Disease Genetics Study Group and the European Consortium on Genetic Susceptibility in Parkinson's Disease. 1999. *Hum Mol Genet*, **8**(4): 567-74.
213. Matsumine, H., et al., Localization of a gene for an autosomal recessive form of juvenile Parkinsonism to chromosome 6q25.2-27. 1997. *Am J Hum Genet*, **60**(3): 588-96.
214. Kitada, T., et al., Mutations in the parkin gene cause autosomal recessive juvenile parkinsonism. 1998. *Nature*, **392**(6676): 605-8.
215. Palacino, J.J., et al., Mitochondrial dysfunction and oxidative damage in parkin-deficient mice. 2004. *J Biol Chem*, **279**(18): 18614-22.
216. Olzmann, J.A. and L.S. Chin, Parkin-mediated K63-linked polyubiquitination: a signal for targeting misfolded proteins to the aggresome-autophagy pathway. 2008. *Autophagy*, **4**(1): 85-7.
217. Sarraf, S.A., et al., Landscape of the PARKIN-dependent ubiquitylome in response to mitochondrial depolarization. 2013. *Nature*, **496**(7445): 372-6.

218. Park, J., et al., Mitochondrial dysfunction in *Drosophila* PINK1 mutants is complemented by parkin. 2006. *Nature*, **441**(7097): 1157-61.
219. Yang, Y., et al., Mitochondrial pathology and muscle and dopaminergic neuron degeneration caused by inactivation of *Drosophila* Pink1 is rescued by Parkin. 2006. *Proc Natl Acad Sci U S A*, **103**(28): 10793-8.
220. Giasson, B.I., et al., A panel of epitope-specific antibodies detects protein domains distributed throughout human alpha-synuclein in Lewy bodies of Parkinson's disease. 2000. *J Neurosci Res*, **59**(4): 528-33.
221. Klein, C. and A. Westenberger, Genetics of Parkinson's disease. 2012. *Cold Spring Harb Perspect Med*, **2**(1): a008888.
222. Auluck, P.K., et al., alpha-Synuclein: membrane interactions and toxicity in Parkinson's disease. 2010. *Annu Rev Cell Dev Biol*, **26**: 211-33.
223. Fortin, D.L., et al., Lipid rafts mediate the synaptic localization of alpha-synuclein. 2004. *J Neurosci*, **24**(30): 6715-23.
224. Cole, N.B., et al., Mitochondrial translocation of alpha-synuclein is promoted by intracellular acidification. 2008. *Exp Cell Res*, **314**(10): 2076-89.
225. Devi, L., et al., Mitochondrial import and accumulation of alpha-synuclein impair complex I in human dopaminergic neuronal cultures and Parkinson disease brain. 2008. *J Biol Chem*, **283**(14): 9089-100.
226. Parihar, M.S., et al., Mitochondrial association of alpha-synuclein causes oxidative stress. 2008. *Cell Mol Life Sci*, **65**(7-8): 1272-84.
227. Guardia-Laguarta, C., et al., alpha-Synuclein is localized to mitochondria-associated ER membranes. 2014. *J Neurosci*, **34**(1): 249-59.
228. Nakamura, K., et al., Direct membrane association drives mitochondrial fission by the Parkinson disease-associated protein alpha-synuclein. 2011. *J Biol Chem*, **286**(23): 20710-26.
229. Hsu, L.J., et al., alpha-synuclein promotes mitochondrial deficit and oxidative stress. 2000. *Am J Pathol*, **157**(2): 401-10.
230. Tanaka, Y., et al., Inducible expression of mutant alpha-synuclein decreases proteasome activity and increases sensitivity to mitochondria-dependent apoptosis. 2001. *Hum Mol Genet*, **10**(9): 919-26.
231. Smith, W.W., et al., Endoplasmic reticulum stress and mitochondrial cell death pathways mediate A53T mutant alpha-synuclein-induced toxicity. 2005. *Hum Mol Genet*, **14**(24): 3801-11.
232. Lin, X., et al., Leucine-rich repeat kinase 2 regulates the progression of neuropathology induced by Parkinson's-disease-related mutant alpha-synuclein. 2009. *Neuron*, **64**(6): 807-27.
233. Bonifati, V., et al., DJ-1 (PARK7), a novel gene for autosomal recessive, early onset parkinsonism. 2003. *Neurol Sci*, **24**(3): 159-60.
234. Zhang, L., et al., Mitochondrial localization of the Parkinson's disease related protein DJ-1: implications for pathogenesis. 2005. *Hum Mol Genet*, **14**(14): 2063-73.
235. Ottolini, D., et al., The Parkinson disease-related protein DJ-1 counteracts mitochondrial impairment induced by the tumour suppressor protein p53 by enhancing endoplasmic reticulum-mitochondria tethering. 2013. *Hum Mol Genet*, **22**(11): 2152-68.

236. Giaime, E., et al., Loss of DJ-1 does not affect mitochondrial respiration but increases ROS production and mitochondrial permeability transition pore opening. 2012. PLoS One, **7**(7): e40501.
237. Chen, J., et al., Parkinson disease protein DJ-1 converts from a zymogen to a protease by carboxyl-terminal cleavage. 2010. Hum Mol Genet, **19**(12): 2395-408.
238. Langston, J.W. and P.A. Ballard, Jr., Parkinson's disease in a chemist working with 1-methyl-4-phenyl-1,2,5,6-tetrahydropyridine. 1983. N Engl J Med, **309**(5): 310.
239. Javitch, J.A., et al., Parkinsonism-inducing neurotoxin, N-methyl-4-phenyl-1,2,3,6-tetrahydropyridine: uptake of the metabolite N-methyl-4-phenylpyridine by dopamine neurons explains selective toxicity. 1985. Proc Natl Acad Sci U S A, **82**(7): 2173-7.
240. Nicklas, W.J., et al., Inhibition of NADH-linked oxidation in brain mitochondria by 1-methyl-4-phenyl-pyridine, a metabolite of the neurotoxin, 1-methyl-4-phenyl-1,2,5,6-tetrahydropyridine. 1985. Life Sci, **36**(26): 2503-8.
241. Tipton, K.F. and T.P. Singer, Advances in our understanding of the mechanisms of the neurotoxicity of MPTP and related compounds. 1993. J Neurochem, **61**(4): 1191-206.
242. Chiueh, C.C., et al., Neurochemical and behavioral effects of 1-methyl-4-phenyl-1,2,3,6-tetrahydropyridine (MPTP) in rat, guinea pig, and monkey. 1984. Psychopharmacol Bull, **20**(3): 548-53.
243. Langston, J.W., et al., MPTP-induced parkinsonism in human and non-human primates--clinical and experimental aspects. 1984. Acta Neurol Scand Suppl, **100**: 49-54.
244. Langston, J.W., et al., Selective nigral toxicity after systemic administration of 1-methyl-4-phenyl-1,2,5,6-tetrahydropyridine (MPTP) in the squirrel monkey. 1984. Brain Res, **292**(2): 390-4.
245. Crossman, A.R., et al., Regional brain uptake of 2-deoxyglucose in N-methyl-4-phenyl-1,2,3,6-tetrahydropyridine (MPTP)-induced parkinsonism in the macaque monkey. 1985. Neuropharmacology, **24**(6): 587-91.
246. Doudet, D., et al., MPTP primate model of Parkinson's disease: a mechanographic and electromyographic study. 1985. Brain Res, **335**(1): 194-9.
247. Heikkila, R.E., et al., Dopaminergic neurotoxicity of 1-methyl-4-phenyl-1,2,5,6-tetrahydropyridine (MPTP) in the mouse: relationships between monoamine oxidase, MPTP metabolism and neurotoxicity. 1985. Life Sci, **36**(3): 231-6.
248. Chiueh, C.C., et al., Neurochemical and behavioral effects of systemic and intranigral administration of N-methyl-4-phenyl-1,2,3,6-tetrahydropyridine in the rat. 1984. Eur J Pharmacol, **100**(2): 189-94.
249. Haque, M.E., et al., Inactivation of Pink1 gene in vivo sensitizes dopamine-producing neurons to 1-methyl-4-phenyl-1,2,3,6-tetrahydropyridine (MPTP) and can be rescued by autosomal recessive Parkinson disease genes, Parkin or DJ-1. 2012. J Biol Chem, **287**(27): 23162-70.

250. Kim, R.H., et al., Hypersensitivity of DJ-1-deficient mice to 1-methyl-4-phenyl-1,2,3,6-tetrahydropyridine (MPTP) and oxidative stress. 2005. *Proc Natl Acad Sci U S A*, **102**(14): 5215-20.
251. Cannon, J.R., et al., A highly reproducible rotenone model of Parkinson's disease. 2009. *Neurobiol Dis*, **34**(2): 279-90.
252. Sherer, T.B., et al., Subcutaneous rotenone exposure causes highly selective dopaminergic degeneration and alpha-synuclein aggregation. 2003. *Exp Neurol*, **179**(1): 9-16.
253. Betarbet, R., et al., Chronic systemic pesticide exposure reproduces features of Parkinson's disease. 2000. *Nat Neurosci*, **3**(12): 1301-6.
254. Hensley, K., et al., Interaction of alpha-phenyl-N-tert-butyl nitron and alternative electron acceptors with complex I indicates a substrate reduction site upstream from the rotenone binding site. 1998. *J Neurochem*, **71**(6): 2549-57.
255. Greene, J.G. and J.T. Greenamyre, Bioenergetics and glutamate excitotoxicity. 1996. *Prog Neurobiol*, **48**(6): 613-34.
256. Day, B.J., et al., A mechanism of paraquat toxicity involving nitric oxide synthase. 1999. *Proc Natl Acad Sci U S A*, **96**(22): 12760-5.
257. Costello, S., et al., Parkinson's disease and residential exposure to maneb and paraquat from agricultural applications in the central valley of California. 2009. *Am J Epidemiol*, **169**(8): 919-26.
258. Cocheme, H.M. and M.P. Murphy, Complex I is the major site of mitochondrial superoxide production by paraquat. 2008. *J Biol Chem*, **283**(4): 1786-98.
259. Manning-Bog, A.B., et al., The herbicide paraquat causes up-regulation and aggregation of alpha-synuclein in mice: paraquat and alpha-synuclein. 2002. *J Biol Chem*, **277**(3): 1641-4.
260. Botella, J.A., et al., Modelling Parkinson's disease in *Drosophila*. 2009. *Neuromolecular Med*, **11**(4): 268-80.
261. Jiang, T., et al., Epidemiology and etiology of Alzheimer's disease: from genetic to non-genetic factors. 2013. *Curr Alzheimer Res*, **10**(8): 852-67.
262. Putcha, D., et al., Hippocampal hyperactivation associated with cortical thinning in Alzheimer's disease signature regions in non-demented elderly adults. 2011. *J Neurosci*, **31**(48): 17680-8.
263. Palop, J.J. and L. Mucke, Synaptic depression and aberrant excitatory network activity in Alzheimer's disease: two faces of the same coin? 2010. *Neuromolecular Med*, **12**(1): 48-55.
264. Palop, J.J., et al., A network dysfunction perspective on neurodegenerative diseases. 2006. *Nature*, **443**(7113): 768-73.
265. Manczak, M., et al., Mitochondria are a direct site of A beta accumulation in Alzheimer's disease neurons: implications for free radical generation and oxidative damage in disease progression. 2006. *Hum Mol Genet*, **15**(9): 1437-49.
266. Devi, L., et al., Accumulation of amyloid precursor protein in the mitochondrial import channels of human Alzheimer's disease brain is associated with mitochondrial dysfunction. 2006. *J Neurosci*, **26**(35): 9057-68.

267. Nunomura, A., et al., Oxidative damage is the earliest event in Alzheimer disease. 2001. *J Neuropathol Exp Neurol*, **60**(8): 759-67.
268. Sennvik, K., et al., Levels of alpha- and beta-secretase cleaved amyloid precursor protein in the cerebrospinal fluid of Alzheimer's disease patients. 2000. *Neurosci Lett*, **278**(3): 169-72.
269. Terry, R.D. and P. Davies, Dementia of the Alzheimer type. 1980. *Annu Rev Neurosci*, **3**: 77-95.
270. Tiraboschi, P., et al., The importance of neuritic plaques and tangles to the development and evolution of AD. 2004. *Neurology*, **62**(11): 1984-9.
271. Trinczek, B., et al., Tau regulates the attachment/detachment but not the speed of motors in microtubule-dependent transport of single vesicles and organelles. 1999. *J Cell Sci*, **112 (Pt 14)**: 2355-67.
272. Stamer, K., et al., Tau blocks traffic of organelles, neurofilaments, and APP vesicles in neurons and enhances oxidative stress. 2002. *J Cell Biol*, **156**(6): 1051-63.
273. Mandelkow, E.M. and E. Mandelkow, Biochemistry and cell biology of tau protein in neurofibrillary degeneration. 2012. *Cold Spring Harb Perspect Med*, **2**(7): a006247.
274. Melov, S., et al., Mitochondrial oxidative stress causes hyperphosphorylation of tau. 2007. *PLoS One*, **2**(6): e536.
275. Escobar-Khondiker, M., et al., Annonacin, a natural mitochondrial complex I inhibitor, causes tau pathology in cultured neurons. 2007. *J Neurosci*, **27**(29): 7827-37.
276. Manczak, M. and P.H. Reddy, Abnormal interaction of oligomeric amyloid-beta with phosphorylated tau: implications to synaptic dysfunction and neuronal damage. 2013. *J Alzheimers Dis*, **36**(2): 285-95.
277. Berge, E.O., et al., Identification and characterization of retinoblastoma gene mutations disturbing apoptosis in human breast cancers. 2010. *Mol Cancer*, **9**: 173.
278. Anandatheerthavarada, H.K., et al., Mitochondrial targeting and a novel transmembrane arrest of Alzheimer's amyloid precursor protein impairs mitochondrial function in neuronal cells. 2003. *J Cell Biol*, **161**(1): 41-54.
279. De Strooper, B., et al., Deficiency of presenilin-1 inhibits the normal cleavage of amyloid precursor protein. 1998. *Nature*, **391**(6665): 387-90.
280. Edbauer, D., et al., Reconstitution of gamma-secretase activity. 2003. *Nat Cell Biol*, **5**(5): 486-8.
281. Ankarcrona, M. and K. Hultenby, Presenilin-1 is located in rat mitochondria. 2002. *Biochem Biophys Res Commun*, **295**(3): 766-70.
282. Hansson, C.A., et al., Nicastrin, presenilin, APh-1, and PEN-2 form active gamma-secretase complexes in mitochondria. 2004. *J Biol Chem*, **279**(49): 51654-60.
283. Area-Gomez, E., et al., Upregulated function of mitochondria-associated ER membranes in Alzheimer disease. 2012. *EMBO J*, **31**(21): 4106-23.
284. Schon, E.A. and E. Area-Gomez, Is Alzheimer's disease a disorder of mitochondria-associated membranes? 2010. *J Alzheimers Dis*, **20 Suppl 2**: S281-92.

285. Behbahani, H., et al., Differential role of Presenilin-1 and -2 on mitochondrial membrane potential and oxygen consumption in mouse embryonic fibroblasts. 2006. *J Neurosci Res*, **84**(4): 891-902.
286. Schuessel, K., et al., Aging sensitizes toward ROS formation and lipid peroxidation in PS1M146L transgenic mice. 2006. *Free Radic Biol Med*, **40**(5): 850-62.
287. Strazielle, C., et al., Regional brain metabolism with cytochrome c oxidase histochemistry in a PS1/A246E mouse model of autosomal dominant Alzheimer's disease: correlations with behavior and oxidative stress. 2009. *Neurochem Int*, **55**(8): 806-14.
288. Zhang, C., et al., Differential occurrence of mutations in mitochondrial DNA of human skeletal muscle during aging. 1998. *Hum Mutat*, **11**(5): 360-71.
289. Thomas, J.G., et al., Iatrogenic Creutzfeldt-Jakob disease via surgical instruments. 2013. *J Clin Neurosci*, **20**(9): 1207-12.
290. Van Everbroeck, B., et al., Extracellular protein deposition correlates with glial activation and oxidative stress in Creutzfeldt-Jakob and Alzheimer's disease. 2004. *Acta Neuropathol*, **108**(3): 194-200.
291. Petersen, R.B., et al., Redox metals and oxidative abnormalities in human prion diseases. 2005. *Acta Neuropathol*, **110**(3): 232-8.
292. Aguzzi, A. and M. Polymenidou, Mammalian prion biology: one century of evolving concepts. 2004. *Cell*, **116**(2): 313-27.
293. Guentchev, M., et al., Oxidative damage to nucleic acids in human prion disease. 2002. *Neurobiol Dis*, **9**(3): 275-81.
294. Wong, B.S., et al., Oxidative impairment in scrapie-infected mice is associated with brain metals perturbations and altered antioxidant activities. 2001. *J Neurochem*, **79**(3): 689-98.
295. Lee, D.W., et al., Alteration of free radical metabolism in the brain of mice infected with scrapie agent. 1999. *Free Radic Res*, **30**(6): 499-507.
296. Park, J.H., et al., Association of endothelial nitric oxide synthase and mitochondrial dysfunction in the hippocampus of scrapie-infected mice. 2011. *Hippocampus*, **21**(3): 319-33.
297. Yun, S.W., et al., Oxidative stress in the brain at early preclinical stages of mouse scrapie. 2006. *Exp Neurol*, **201**(1): 90-8.
298. Choi, S.I., et al., Mitochondrial dysfunction induced by oxidative stress in the brains of hamsters infected with the 263 K scrapie agent. 1998. *Acta Neuropathol*, **96**(3): 279-86.
299. Brown, D.R., et al., The cellular prion protein binds copper in vivo. 1997. *Nature*, **390**(6661): 684-7.
300. Brown, D.R., et al., Effects of copper on survival of prion protein knockout neurons and glia. 1998. *J Neurochem*, **70**(4): 1686-93.
301. Brown, D.R., et al., Prion protein-deficient cells show altered response to oxidative stress due to decreased SOD-1 activity. 1997. *Exp Neurol*, **146**(1): 104-12.
302. Dupiereux, I., et al., Protective effect of prion protein via the N-terminal region in mediating a protective effect on paraquat-induced oxidative injury in neuronal cells. 2008. *J Neurosci Res*, **86**(3): 653-9.

303. Kim, B.H., et al., The cellular prion protein (PrPC) prevents apoptotic neuronal cell death and mitochondrial dysfunction induced by serum deprivation. 2004. *Brain Res Mol Brain Res*, **124**(1): 40-50.
304. O'Donovan, C.N., et al., Prion protein fragment PrP-(106-126) induces apoptosis via mitochondrial disruption in human neuronal SH-SY5Y cells. 2001. *J Biol Chem*, **276**(47): 43516-23.
305. Liberski, P.P. and H. Budka, Ultrastructural pathology of Gerstmann-Straussler-Scheinker disease. 1995. *Ultrastruct Pathol*, **19**(1): 23-36.
306. Alzualde, A., et al., A novel PRNP Y218N mutation in Gerstmann-Straussler-Scheinker disease with neurofibrillary degeneration. 2010. *J Neuropathol Exp Neurol*, **69**(8): 789-800.
307. Liberski, P.P., et al., Ultrastructural pathology of prion diseases revisited: brain biopsy studies. 2005. *Neuropathol Appl Neurobiol*, **31**(1): 88-96.
308. Walis, A., et al., Ultrastructural changes in the optic nerves of rodents with experimental Creutzfeldt-Jakob Disease (CJD), Gerstmann-Straussler-Scheinker disease (GSS) or scrapie. 2003. *J Comp Pathol*, **129**(2-3): 213-25.
309. Siskova, Z., et al., Morphological and functional abnormalities in mitochondria associated with synaptic degeneration in prion disease. 2010. *Am J Pathol*, **177**(3): 1411-21.
310. Topcu, M., et al., Leigh syndrome in a 3-year-old boy with unusual brain MR imaging and pathologic findings. 2000. *AJNR Am J Neuroradiol*, **21**(1): 224-7.
311. Baslow, M.H., Canavan's spongiform leukodystrophy: a clinical anatomy of a genetic metabolic CNS disease. 2000. *J Mol Neurosci*, **15**(2): 61-9.
312. Nixon, R.A., et al., Neurodegenerative lysosomal disorders: a continuum from development to late age. 2008. *Autophagy*, **4**(5): 590-9.
313. Osellame, L.D. and M.R. Duchen, Quality control gone wrong: mitochondria, lysosomal storage disorders and neurodegeneration. 2014. *Br J Pharmacol*, **171**(8): 1958-72.
314. de Pablo-Latorre, R., et al., Impaired parkin-mediated mitochondrial targeting to autophagosomes differentially contributes to tissue pathology in lysosomal storage diseases. 2012. *Hum Mol Genet*, **21**(8): 1770-81.
315. Settembre, C., et al., Systemic inflammation and neurodegeneration in a mouse model of multiple sulfatase deficiency. 2007. *Proc Natl Acad Sci U S A*, **104**(11): 4506-11.
316. Jennings, J.J., Jr., et al., Mitochondrial aberrations in mucopolipidosis Type IV. 2006. *J Biol Chem*, **281**(51): 39041-50.
317. Takamura, A., et al., Enhanced autophagy and mitochondrial aberrations in murine G(M1)-gangliosidosis. 2008. *Biochem Biophys Res Commun*, **367**(3): 616-22.
318. Wei, H., et al., ER and oxidative stresses are common mediators of apoptosis in both neurodegenerative and non-neurodegenerative lysosomal storage disorders and are alleviated by chemical chaperones. 2008. *Hum Mol Genet*, **17**(4): 469-77.
319. Fu, R., et al., Oxidative stress in Niemann-Pick disease, type C. 2010. *Mol Genet Metab*, **101**(2-3): 214-8.

320. Vitner, E.B., et al., Common and uncommon pathogenic cascades in lysosomal storage diseases. 2010. *J Biol Chem*, **285**(27): 20423-7.
321. Palmer, D.N., et al., Mitochondrial ATP synthase subunit c storage in the ceroid-lipofuscinoses (Batten disease). 1992. *Am J Med Genet*, **42**(4): 561-7.
322. Osellame, L.D. and M.R. Duchen, Defective quality control mechanisms and accumulation of damaged mitochondria link Gaucher and Parkinson diseases. 2013. *Autophagy*, **9**(10): 1633-1635.
323. Miller, K.A., et al., Genetic studies of the mouse mutations mahogany and mahoganoid. 1997. *Genetics*, **146**(4): 1407-15.
324. Bagher, P., et al., Characterization of Mahogunin Ring Finger-1 expression in mice. 2006. *Pigment Cell Res*, **19**(6): 635-43.
325. Cota, C.D., et al., Mice with mutations in Mahogunin ring finger-1 (*Mgrn1*) exhibit abnormal patterning of the left-right axis. 2006. *Dev Dyn*, **235**(12): 3438-47.
326. Silvius, D., et al., Levels of the Mahogunin Ring Finger 1 E3 ubiquitin ligase do not influence prion disease. 2013. *PLoS One*, **8**(1): e55575.
327. Jiao, J., et al., Transgenic analysis of the physiological functions of Mahogunin Ring Finger-1 isoforms. 2009. *Genesis*, **47**(8): 524-34.
328. Kim, B.Y., et al., Spongiform neurodegeneration-associated E3 ligase Mahogunin ubiquitylates TSG101 and regulates endosomal trafficking. 2007. *Mol Biol Cell*, **18**(4): 1129-42.
329. Cooray, S.N., et al., The E3 ubiquitin ligase Mahogunin ubiquitinates the melanocortin 2 receptor. 2011. *Endocrinology*, **152**(11): 4224-31.
330. Srivastava, D. and O. Chakrabarti, Mahogunin-mediated alpha-tubulin ubiquitination via noncanonical K6 linkage regulates microtubule stability and mitotic spindle orientation. 2014. *Cell Death Dis*, **5**: e1064.
331. Gunn, T.M., et al., MGRN1-dependent pigment-type switching requires its ubiquitination activity but not its interaction with TSG101 or NEDD4. 2013. *Pigment Cell Melanoma Res*, **26**(2): 263-8.
332. Chakrabarti, O. and R.S. Hegde, Functional depletion of mahogunin by cytosolically exposed prion protein contributes to neurodegeneration. 2009. *Cell*, **137**(6): 1136-47.
333. Gunn, T.M., et al., The mouse mahogany locus encodes a transmembrane form of human attractin. 1999. *Nature*, **398**(6723): 152-6.
334. He, L., et al., A biochemical function for attractin in agouti-induced pigmentation and obesity. 2001. *Nat Genet*, **27**(1): 40-7.
335. Rehm, S., et al., A new rat mutant with defective overhairs and spongy degeneration of the central nervous system: clinical and pathologic studies. 1982. *Lab Anim Sci*, **32**(1): 70-3.
336. Kondo, A., et al., Early myelination in zitter rat: morphological, immunocytochemical and morphometric studies. 1992. *Brain Res Dev Brain Res*, **67**(2): 217-28.
337. Ueda, S., et al., Degeneration of dopaminergic neurons in the substantia nigra of zitter mutant rat and protection by chronic intake of Vitamin E. 2005. *Neurosci Lett*, **380**(3): 252-6.

338. Nakadate, K., et al., Progressive dopaminergic neurodegeneration of substantia nigra in the zitter mutant rat. 2006. *Acta Neuropathol*, **112**(1): 64-73.
339. Paz, J., et al., The neuroprotective role of attractin in neurodegeneration. 2007. *Neurobiol Aging*, **28**(9): 1446-56.
340. Kondo, A., et al., An ultrastructural study of oligodendrocytes in zitter rat: a new animal model for hypomyelination in the CNS. 1991. *J Neurocytol*, **20**(11): 929-39.
341. Kondo, A., et al., The zitter rat: membranous abnormality in the Schwann cells of myelinated nerve fibers. 1993. *Brain Res*, **613**(1): 173-9.
342. Kondo, A., et al., Spongy degeneration in the zitter rat: ultrastructural and immunohistochemical studies. 1995. *J Neurocytol*, **24**(7): 533-44.
343. Muto, Y. and K. Sato, Pivotal role of attractin in cell survival under oxidative stress in the zitter rat brain with genetic spongiform encephalopathy. 2003. *Brain Res Mol Brain Res*, **111**(1-2): 111-22.
344. Ueda, S., et al., Vulnerability of monoaminergic neurons in the brainstem of the zitter rat in oxidative stress. 2002. *Prog Brain Res*, **136**: 293-302.
345. Li, Y., et al., Dilated cardiomyopathy and neonatal lethality in mutant mice lacking manganese superoxide dismutase. 1995. *Nat Genet*, **11**(4): 376-81.
346. Lebovitz, R.M., et al., Neurodegeneration, myocardial injury, and perinatal death in mitochondrial superoxide dismutase-deficient mice. 1996. *Proc Natl Acad Sci U S A*, **93**(18): 9782-7.
347. Melov, S., et al., A novel neurological phenotype in mice lacking mitochondrial manganese superoxide dismutase. 1998. *Nat Genet*, **18**(2): 159-63.
348. Hinerfeld, D., et al., Endogenous mitochondrial oxidative stress: neurodegeneration, proteomic analysis, specific respiratory chain defects, and efficacious antioxidant therapy in superoxide dismutase 2 null mice. 2004. *J Neurochem*, **88**(3): 657-67.
349. Andreassen, O.A., et al., Mice with a partial deficiency of manganese superoxide dismutase show increased vulnerability to the mitochondrial toxins malonate, 3-nitropropionic acid, and MPTP. 2001. *Exp Neurol*, **167**(1): 189-95.
350. Smith, Y., et al., Parkinson's disease therapeutics: new developments and challenges since the introduction of levodopa. 2012. *Neuropsychopharmacology*, **37**(1): 213-46.
351. Bronstein, J.M., et al., Deep brain stimulation for Parkinson disease: an expert consensus and review of key issues. 2011. *Arch Neurol*, **68**(2): 165.
352. Wolfe, M.S., Therapeutic strategies for Alzheimer's disease. 2002. *Nat Rev Drug Discov*, **1**(11): 859-66.
353. Trevitt, C.R. and J. Collinge, A systematic review of prion therapeutics in experimental models. 2006. *Brain*, **129**(Pt 9): 2241-65.
354. Rainov, N.G., et al., Experimental treatments for human transmissible spongiform encephalopathies: is there a role for pentosan polysulfate? 2007. *Expert Opin Biol Ther*, **7**(5): 713-26.
355. Bruni, S., et al., Update on treatment of lysosomal storage diseases. 2007. *Acta Myol*, **26**(1): 87-92.

356. Sano, M., et al., A controlled trial of selegiline, alpha-tocopherol, or both as treatment for Alzheimer's disease. The Alzheimer's Disease Cooperative Study. 1997. *N Engl J Med*, **336**(17): 1216-22.
357. Pavlik, V.N., et al., Vitamin E use is associated with improved survival in an Alzheimer's disease cohort. 2009. *Dement Geriatr Cogn Disord*, **28**(6): 536-40.
358. Sung, S., et al., Early vitamin E supplementation in young but not aged mice reduces Abeta levels and amyloid deposition in a transgenic model of Alzheimer's disease. 2004. *FASEB J*, **18**(2): 323-5.
359. Nakashima, H., et al., Effects of alpha-tocopherol on an animal model of tauopathies. 2004. *Free Radic Biol Med*, **37**(2): 176-86.
360. Joshi, G. and J.A. Johnson, The Nrf2-ARE pathway: a valuable therapeutic target for the treatment of neurodegenerative diseases. 2012. *Recent Pat CNS Drug Discov*, **7**(3): 218-29.
361. Uttara, B., et al., Oxidative stress and neurodegenerative diseases: a review of upstream and downstream antioxidant therapeutic options. 2009. *Curr Neuropharmacol*, **7**(1): 65-74.
362. Weindruch, R., The retardation of aging by caloric restriction: studies in rodents and primates. 1996. *Toxicol Pathol*, **24**(6): 742-5.
363. Goodrick, C.L., et al., Effects of intermittent feeding upon growth and life span in rats. 1982. *Gerontology*, **28**(4): 233-41.
364. Graff, J., et al., A dietary regimen of caloric restriction or pharmacological activation of SIRT1 to delay the onset of neurodegeneration. 2013. *J Neurosci*, **33**(21): 8951-60.
365. Chen, D., et al., The role of calorie restriction and SIRT1 in prion-mediated neurodegeneration. 2008. *Exp Gerontol*, **43**(12): 1086-93.
366. Kanfi, Y., et al., The sirtuin SIRT6 regulates lifespan in male mice. 2012. *Nature*, **483**(7388): 218-21.
367. Braidy, N., et al., Sirtuins in cognitive ageing and Alzheimer's disease. 2012. *Curr Opin Psychiatry*, **25**(3): 226-30.
368. Giannakou, M.E. and L. Partridge, The interaction between FOXO and SIRT1: tipping the balance towards survival. 2004. *Trends Cell Biol*, **14**(8): 408-12.
369. Bauer, P.O., et al., Harnessing chaperone-mediated autophagy for the selective degradation of mutant huntingtin protein. 2010. *Nat Biotechnol*, **28**(3): 256-63.
370. Cuervo, A.M., et al., Impaired degradation of mutant alpha-synuclein by chaperone-mediated autophagy. 2004. *Science*, **305**(5688): 1292-5.
371. Caccamo, A., et al., Molecular interplay between mammalian target of rapamycin (mTOR), amyloid-beta, and Tau: effects on cognitive impairments. 2010. *J Biol Chem*, **285**(17): 13107-20.
372. Spilman, P., et al., Inhibition of mTOR by rapamycin abolishes cognitive deficits and reduces amyloid-beta levels in a mouse model of Alzheimer's disease. 2010. *PLoS One*, **5**(4): e9979.

CHAPTER II

**SUBMITOCHONDRIAL SITES OF PINK1 ACTION REVEALED BY 3D-SIM
SUPER-RESOLUTION MICROSCOPY**

**Submitochondrial sites of PINK1 action revealed by 3D-SIM super-resolution
microscopy**

Dana Fallaize, Lih-Shen Chin*, Lian Li*⁺

Department of Pharmacology and Center for Neurodegenerative Disease, Emory
University School of Medicine, Atlanta, GA 30322, USA

Running head: PINK1 submitochondrial localization by 3D-SIM

Number of characters: 20,000 characters (not counting spaces)

*To whom correspondence should be addressed. Tel: +1 4047270361; Fax: +1
4047270365; Email: chinl@pharm.emory.edu; lianli@pharm.emory.edu

⁺To whom the editorial and production offices should communicate with.

Abstract

Mutations in the mitochondrial kinase PINK1 cause early onset Parkinson disease (PD), but the submitochondrial site(s) of PINK1 action remains unclear. Here, we show that three-dimensional structured illumination microscopy (3D-SIM) enables visualization of protein submitochondrial localization. Dual color 3D-SIM super-resolution imaging analysis reveals that PINK1 resides in the cristae membrane domain of the inner mitochondrial membrane (IMM.) but not in the outer mitochondrial membrane (OMM) of healthy mitochondria and that PINK1 colocalizes with its substrate TRAP1. In response to mitochondrial depolarization, PINK1, but not TRAP1, translocates to the OMM. PINK1 translocation is dependent on the loss of mitochondrial membrane potential but not the loss of pH gradient or ATP. In the OMM of depolarized mitochondria, PINK1 colocalizes with parkin, supporting the proposed role of PINK1 in recruiting parkin for mitophagy. The ability of PINK1 to translocate to the OMM is impaired by PD-linked PINK1 C92F and W437X mutations, indicating the involvement of disrupted PINK1 translocation in PD pathogenesis.

Introduction

Parkinson disease (PD) is the most common neurodegenerative movement disorder [1-3]. While PD is best known for the loss of dopaminergic neurons in the substantia nigra, increasing evidence indicates that the disease also involves neurodegeneration in other brain regions, including cerebral cortex [4-7]. The pathogenic mechanisms that cause neurodegeneration in PD remain unclear, but mitochondrial dysfunction has been strongly implicated in PD pathogenesis [8-13]. Human genetic studies have identified a number of homozygous mutations in mitochondrial serine/threonine kinase PINK1 that cause autosomal recessive, early-onset PD [14-17]. In addition, heterozygous mutations in PINK1 have been implicated as a significant risk factor in the development of late-onset PD [18-22]. These findings underscore the importance of determining the sites and mechanisms of PINK1 action.

Mitochondria contain two membranes: the outer mitochondrial membrane (OMM) and the inner mitochondrial membrane (IMM.), which separate two aqueous compartments: the intermembrane space (IMS) and the matrix. Compartmentalization provided by the double membrane structure is fundamental to many aspects of mitochondrial function, including redox control, energy production, metabolism, and programmed cell death [23,24]. Because the resolution of confocal microscopy is not sufficient to resolve submitochondrial compartments, most published studies of PINK1 submitochondrial localization relied on the use of subcellular and submitochondrial fractionation, a method which is prone to artifacts resulting from impurities in the preparation of fractions [25-28]. A few PINK1 localization studies [29-31] used

immunogold labeling electron microscopy, which suffers from potential artifacts resulting from the harsh chemical fixation, embedding, and sectioning procedures. These methodological limitations may contribute to the conflicting conclusions on PINK1 submitochondrial localization: several studies, including ours, showed that PINK1 is localized in the IMM and IMS [28-30,32-34], whereas others reported that PINK1 resides on the OMM with its kinase domain facing the cytosol [26,28,31,35,36]. Thus, the submitochondrial localization of PINK1 remains contentious and unresolved.

Three-dimensional structured illumination microscopy (3D-SIM) is a recently developed, super-resolution fluorescence imaging technique, which improves resolution through reconstruction of multiple images, produced with periodic illumination patterns in different orientations [37,38]. Here, we show that 3D-SIM is a useful tool for studying protein submitochondrial localization. Dual color 3D-SIM super-resolution imaging analysis reveals that PINK1 resides in the IMM and IMS but not in the OMM under normal physiological conditions and that PINK1 colocalizes with mitochondrial molecular chaperone TRAP1, a PINK1 substrate identified in our previous study [32]. When mitochondria are depolarized, PINK1, but not TRAP1, translocates to the OMM and colocalizes with E3 ubiquitin-protein ligase parkin, a PINK1 substrate with a key role in mitophagy [31,33,39]. Furthermore, our study has identified the structural determinants of PINK1 translocation to the OMM and obtained evidence linking the impairment of PINK1 translocation to PD pathogenesis.

Results

Dual color 3D-SIM super- resolution imaging analysis enables visualization of protein submitochondrial localization

Mitochondria have a complex architecture with four distinct compartments: the OMM, IMM, IMS, and matrix (Fig. 1 A). Due to the presence of the cristae junction, the IMM is divided into two structurally distinct subdomains: the inner boundary membrane, which parallels the OMM, and the cristae membrane, which invaginates into the matrix [40,41]. Likewise, the IMS is divided into two subcompartments: the peripheral IMS, which lies between the OMM and the inner boundary membrane, and the intracristae space, which is bordered by the cristae membrane (Fig. 1 A). To determine if 3D-SIM is capable of resolving submitochondrial compartments, we performed dual color 3D-SIM fluorescence imaging analysis of HeLa cells with mitochondria labeled by the mitochondrial matrix marker mito-dsRed and antibodies against the OMM marker TOM20, the IMM marker TIM23, or the IMS marker cytochrome *c* (Fig. 1 B-E). Dual color 3D-SIM images showed that the TOM20-positive OMM surrounds the mitochondrial matrix labeled by mito-dsRed, and there is no overlap between these two submitochondrial compartments (Fig. 1, B and C). We observed that the TIM23-positive IMM wraps along and protrudes into the mito-dsRed-labeled matrix, often in a striated pattern, which is indicative of the cristae membrane (Fig. 1 D). The TIM23-positive, cristae membrane is enclosed inside the TOM20-positive OMM (Fig. 1 E). The TIM23-positive, inner boundary membrane appears in close proximity or colocalizes with the

TOM20-positive OMM at a number of sites (arrows in Fig. 1 E), which likely represent the so-called mitochondrial contact sites seen in electron microscopic images [42,43]. We found that cytochrome *c*-positive IMS also wraps along and protrudes into the mito-dsRed-labeled matrix in a striated pattern, which is indicative of the intracristae space (Fig. 1 F). The cytochrome *c*-positive, intracristae space exhibits substantial overlap with the TIM23-positive, cristae membrane (Fig. 1 G), but shows a spatial separation from the TOM20-positive OMM (Fig. 1 H). Together, these results demonstrate, for the first time, the capability of 3D-SIM to resolve submitochondrial compartments, and they indicate that 3D-SIM is a useful tool for studying protein submitochondrial localization.

PINK1 resides in the cristae membrane/intracristae space of healthy mitochondria and translocates to the OMM upon mitochondrial depolarization

Next, we performed dual color 3D-SIM super-resolution fluorescence imaging analyses to examine the submitochondrial localization of PINK1. Because of the lack of a reliable anti-PINK1 antibody for immunostaining of endogenous PINK1, we imaged HeLa cells expressing C-terminal GFP-tagged PINK1 (PINK1-GFP) with various markers of submitochondrial compartments (Fig. 2 A). We found that mitochondria displayed a tubular morphology under basal conditions and PINK1-GFP fluorescence was confined inside the boundary defined by the TOM20 immunofluorescence, indicating that PINK1 is not localized to the OMM of healthy mitochondria. The PINK1-GFP fluorescence had a striated pattern along the mito-dsRed-labeled matrix and showed substantial overlap with the TIM23 and cytochrome *c* immunofluorescence (Fig. 2 A), indicating that PINK1

is localized to the cristae membrane and intracristae space of healthy mitochondria. Given the critical involvement of the cristae membrane and intracristae space compartments in the control of many mitochondrial activities such as respiration, metabolism, and redox control [44] our results support a role of PINK1 in these compartments to regulate mitochondrial function under normal physiological conditions. Our dual color 3D-SIM imaging analysis revealed that treatment of cells with the mitochondrial uncoupler carbonyl cyanide m-chlorophenylhydrazone (CCCP) caused fragmentation of mitochondria into spherical organelles and redistribution of PINK1-GFP fluorescence from the cristae membrane and intracristae space to the OMM (Fig. 2 B), indicating PINK1 translocation to the OMM of damaged mitochondria. Because CCCP is a protonophore that dissipates mitochondrial membrane potential ($\Delta\Psi$) and pH gradient (ΔpH) leading to impaired ATP production, we examined the effects of additional ionophores and other drugs to determine the cause of PINK1 redistribution (Fig. S1). We found that the K^+ ionophore valinomycin, which dissipates $\Delta\Psi$ but not ΔpH , was capable of inducing PINK1 redistribution to the OMM, whereas the H^+/K^+ antiporter, nigericin, which reduces ΔpH but not $\Delta\Psi$, was unable to cause PINK1 redistribution (Fig. S1 and Fig. 2 C). In addition, the mitochondrial complex III inhibitor antimycin A, which causes increased ROS generation and mitochondrial depolarization, could also trigger PINK1 redistribution. In contrast, the ATP synthase inhibitor, oligomycin, or the microtubule-depolymerizing drug, nocodazole, could not induce PINK1 redistribution (Fig. S1 and Fig. 2 C). These results indicate that PINK1 translocates to the OMM following loss of mitochondrial membrane potential but not on loss of pH gradient, ATP, or microtubule integrity.

PINK1 colocalizes with TRAP1 in the IMM/IMS of healthy mitochondria and colocalizes with parkin on the OMM of dysfunctional mitochondria

Our finding of PINK1 localization in the cristae membrane and intracristae space of healthy mitochondria (Fig. 2 A) suggests a signaling role of PINK1-mediated phosphorylation in these compartments. We previously identified the mitochondrial molecular chaperone, TRAP1, as a substrate of PINK1-mediated phosphorylation [32], but the submitochondrial localization of TRAP1, like PINK1, has also been controversial. While our subcellular fractionation analysis showed that TRAP1 is localized to the IMM and IMS [32], others reported that TRAP1 resides in the matrix [45]. We therefore performed dual color 3D-SIM imaging analyses to determine TRAP1 submitochondrial localization. We found that TRAP1 resides in the cristae membrane and intracristae space and that TRAP1 colocalizes with PINK1 in healthy mitochondria under basal conditions (Fig. 3, A and C). However, unlike PINK1, TRAP1 does not undergo mitochondrial depolarization-induced translocation to the OMM (Fig. 3, B and E). These data support a physiological role of the PINK1-TRAP1 signaling pathway in regulating the activities of healthy mitochondria.

PINK1 has been proposed to recruit parkin from the cytosol to mitochondria for initiating mitophagy [46-50], but the specifics of PINK1-mediated parkin recruitment remain unclear. Our dual color 3D-SIM super-resolution imaging analyses revealed that, in contrast to previous reports that overexpression of PINK1 caused parkin translocation to mitochondria with normal membrane potential [31,33], parkin failed to translocate to mitochondria under basal conditions even with high levels of PINK1 overexpression (Fig. 3 A) because PINK1 is restricted to the IMM/IMS and cannot interact with cytosolic

parkin. When mitochondria were depolarized by CCCP, PINK1 translocation to the OMM of damaged mitochondria was observed concurrently with parkin recruitment to the OMM, where these two proteins showed extensive colocalization (Fig. 3, B, D and E). Taken together, these results demonstrate that increased PINK1 protein expression levels alone are insufficient to trigger parkin recruitment to mitochondria, and they indicate that mitochondrial depolarization-induced PINK1 translocation from the IMM/IMS to the OMM is required for parkin recruitment to mitochondria.

Our 3D-SIM imaging analyses revealed that ectopic parkin expression in HeLa cells, which lack endogenous parkin, induced perinuclear clustering of CCCP-depolarized mitochondria (Fig. 3 B), consistent with published studies [31,33]. However, different from the previous report that parkin was localized to the outside boundaries of clustered mitochondria [31], we found that parkin was enriched in the mitochondrion - mitochondrion contacts (Fig. 3 B). Our results demonstrate the power of dual color 3D-SIM super-resolution imaging in visualization of protein spatial distributions and support a direct role of parkin in promoting the clustering of dysfunctional mitochondria.

Mitochondrial depolarization-induced PINK1 translocation to the OMM is independent of new PINK1 protein synthesis

To further characterize mitochondrial depolarization-induced PINK1 translocation, we investigated the spatiotemporal dynamics of PINK1 redistribution following CCCP treatment. Due to rapid movement of mitochondria and the time required to acquire a dual color 3D-SIM image, we were unable to resolve submitochondrial compartments in live cells (data not shown). Our time course analysis using fixed cells showed that

PINK1 began to appear in the OMM of fragmented mitochondria around 15-30 min of CCCP treatment and reached the maximum by 60 min and then sustained to at least 2 hour (Fig. S2). The increase in the OMM-localized PINK1 was accompanied by a gradual disappearance of the IMM/IMS-localized PINK1 with continued CCCP treatment (Fig. S2). By 60 min, PINK1 was almost solely localized on the OMM and there was very little PINK1 inside the mitochondria (Fig. S2).

To determine whether mitochondrial depolarization-induced PINK1 translocation to the OMM is due to the recruitment of newly synthesized PINK1, we pretreated cells with the protein synthesis inhibitor, emetine, for 1 hour followed by co-incubation with CCCP for an additional 2 hours. 3D-SIM imaging analysis revealed that 3 hour emetine treatment failed to block PINK1 redistribution to the OMM of depolarized mitochondria (Fig. S3). A similar result was also obtained by repeating the experiments using another protein synthesis inhibitor, cycloheximide (Fig. S3). These results indicate that mitochondrial depolarization-induced PINK1 translocation to the OMM is independent of new PINK1 protein synthesis, suggesting that OMM-localized PINK1 could come from preexisting pools of cytosolic PINK1 or IMM/IMS-localized PINK1.

The ability of PINK1 to translocate to the OMM is impaired by PD-linked PINK1 C92F and W437X mutations

PINK1 contains a hydrophobic region (residues 94-110) that has been proposed to act as a transmembrane domain or a stop-transfer signal to prevent full translocation of PINK1 into the mitochondrial matrix [26,35]. Our 3D-SIM imaging analysis of transfected HeLa cells revealed that, different from previous reports [26,35], deletion of PINK1

hydrophobic transmembrane domain (PINK1 Δ TM) did not cause PINK1 to mislocalize to the mitochondrial matrix under either the basal or CCCP-treated conditions (Fig. 4, F and G). We found that the PINK1 Δ TM mutant remained in the IMM/IMS and was incapable of translocating to the OMM following CCCP treatment (Fig. 4, D and E), indicating that the PINK1 transmembrane domain is required for mitochondrial depolarization-induced PINK1 OMM translocation.

Our 3D-SIM imaging analysis showed that, although PD-linked PINK1 C92F mutation did not change the IMM/IMS localization of PINK1 under basal conditions, the mutation significantly reduced the mitochondrial depolarization-induced PINK1 translocation to the OMM (Fig. 4, H, I, N). In contrast, PD-linked PINK1 L347P mutation, which is known to disrupt PINK1 kinase function [32], had no effect on PINK1 submitochondrial localization in either healthy or CCCP-depolarized mitochondria (Fig 4, J, K, N), indicating that PINK1 kinase activity is not required for mitochondrial depolarization-induced PINK1 OMM translocation. We found that PD-linked PINK1 W437X, a truncation mutation causing loss of the C-terminal region, completely abolished the ability of PINK1 to translocate to the OMM following CCCP treatment without affecting the IMM/IMS localization of PINK1 under basal conditions (Fig. 4, L-N), indicating an essential role of the PINK1 C-terminal region in PINK1 translocation to the OMM. Our finding that mitochondrial depolarization-induced PINK1 translocation to the OMM is disrupted by PD-linked PINK1 C92F and W437X mutations provides evidence linking the impairment of PINK1 OMM translocation to PD pathogenesis.

PINK1 translocates to the OMM to recruit parkin upon mitochondrial depolarization in neurons and the translocation requires combined action of PINK1 transmembrane and C-terminal domains

Next, we performed dual color 3D-SIM imaging analyses of mitochondria in primary mouse cortical neurons and found that the resolution provided by 3D-SIM is also able to differentiate the OMM from the interior structures of the mitochondria in neurons (Fig 5 A, B). We observed that PINK1-GFP expressed in cortical neurons translocates to the OMM of depolarized mitochondria following CCCP treatment and this translocation is abolished by PINK1 Δ TM or PINK1 W437X mutation (Fig. 5 C-F). These results are consistent with our findings in HeLa cells (Fig 4) and demonstrate that both the transmembrane and C-terminal domains of PINK1 are necessary but neither one is sufficient for PINK1 localization in the OMM of CCCP-depolarized mitochondria, indicating that combined action of these two domains are required for mitochondrial depolarization-induced PINK1 translocation to the OMM.

To investigate the relationship between PINK1 OMM translocation and parkin recruitment to mitochondria, we transfected *PINK1*^{-/-} mouse cortical neurons with mCherry-parkin and WT or mutant PINK1-GFP or GFP control. Dual color 3D-SIM imaging analysis revealed that in PINK1 WT-transfected *PINK1*^{-/-} neurons, mitochondrial depolarization-induced PINK1 OMM translocation was associated with parkin recruitment to the OMM, as shown by the extensive colocalization between these two proteins (Fig. 5, J). In contrast, parkin remained in the cytosol in GFP-transfected *PINK1*^{-/-} neurons following CCCP treatment (Fig. 5 I), indicating that PINK1 is required for parkin recruitment to the OMM. Furthermore, the OMM translocation-defective

PINK1 Δ TM and PINK1 W437X mutants were unable to facilitate parkin recruitment to the OMM of CCCP-depolarized mitochondria (Fig. 5, K and L). The ability of PINK1 WT, but not PINK1 Δ TM or PINK1 W437X mutants, to recruit parkin to depolarized mitochondria was also confirmed by confocal fluorescence microscopic analysis (data not shown). There is a significantly less colocalization between Δ TM and W437X and parkin compared to PINK1 WT (Fig. 5 M). In addition, parkin recruitment is abolished by Δ TM and W437X while we saw 70% of neurons overexpressing PINK1 WT recruited parkin to damaged mitochondria (Fig 5 N). Together, these data indicate that mitochondrial depolarization-induced PINK1 OMM translocation is required for parkin recruitment to the OMM of depolarized mitochondria.

Discussion

The identification of PINK1 mutations in recessive early onset PD underscores the importance of PINK1 function in neuroprotection [14-17]. Dysregulation of PINK1-mediated phosphorylation results in mitochondrial dysfunction suggesting that PINK1 regulates mitochondrial health and mitochondrial dysfunction associated with PINK1 loss may result in neuronal dysfunction and death [51-53]. And while PINK1 mitochondrial signaling has been studied extensively, the use of unreliable methods to study the submitochondrial localization of PINK1 has resulted in conflicting data. Due to the importance of mitochondrial compartmentalization in mitochondrial functions and the unclear submitochondrial localization of PINK1, it is imperative to properly characterize

the submitochondrial localization of PINK1 in order to understand its role in signaling. Our studies reveal that PINK1 is dual targeted depending on the health of mitochondria.

The mechanisms underlying the maintenance of mitochondrial homeostasis are tightly regulated. Our findings in this study suggest that PINK1 plays an integral part in the regulation of mitochondrial signaling in response to mitochondrial damage. PINK1 dual targeting allows for differential colocalization, interaction, and phosphorylation of its substrates, TRAP1 and parkin based on the degree of mitochondrial damage. PINK1-mediated phosphorylation of TRAP1 protects against mitochondrial dysfunction and oxidative stress induced cell death while PINK1-mediated phosphorylation of parkin initiates removal of damaged mitochondria [32,54-56]. Potentially, the spatiotemporal dynamics of PINK1 may act as a “molecular switch” to trigger two separate signaling cascades to maintain proper mitochondrial function and cell health. Under low levels of mitochondrial damage, PINK1 phosphorylates TRAP1 and phosphorylated TRAP1 can protect against mitochondrial dysfunction. Following extreme damage to the mitochondria in which mitochondria become depolarized, PINK1 phosphorylates parkin to trigger mitophagy to prevent further cellular damage.

There are several current models of PINK1 spatiotemporal dynamics and how they relate to signaling in mitochondrial health and disease. One model suggests that PINK1 is imported into the mitochondria where it is rapidly degraded and mitochondrial depolarization blocks mitochondrial protein import resulting in accumulation of newly synthesized PINK1 on the OMM. This model suggests a role on the exterior of the mitochondria, by PINK1-mediated phosphorylation of parkin to initiate mitophagy, but no role of PINK1 inside the mitochondria [25,57]. Another model suggests that PINK1

remains stuck in the TOM/TIM complexes with the kinase domain facing the cytoplasm. This model suggests that following depolarization of mitochondria, the N-terminal region of PINK1 is cleaved and rapidly degraded while the remaining C-terminal region either remains embedded in the OMM or is translocated back to the cytosol [26]. Our results do not support either of these models. We clearly show that in healthy mitochondria, PINK1 resides in detectable levels in the IMM/IMS negating both models. Moreover, we observe extensive colocalization between PINK1 and our previously identified substrate, TRAP1 in the IMM/IMS. Our previous study shows PINK1 kinase activity is required for TRAP1 cytoprotective activity indicating the significance of PINK1-mediated phosphorylation inside the mitochondria [32]. Because PINK1 plays an integral role in maintaining mitochondrial health and cytoprotection through PINK1-mediated phosphorylation, PINK1 is likely not as rapidly degraded as once thought. Interestingly, blocking the synthesis of new PINK1 protein does not affect PINK1 OMM-localization also negating the previously proposed dual targeting model.

Another challenge our data presents to the previously proposed models is the spatiotemporal dynamics of OMM-translocation defective mutants. These mutants are observed in the IMM/IMS of healthy mitochondria and their submitochondrial localization does not change following mitochondrial depolarization. If the previously proposed dual targeting model was correct, there would have to be defects in both degradation of these mutants and also recruitment and embedding into the OMM in order for these PINK1 mutants to remain in the IMM/IMS. The fact that mutations in the transmembrane domain or C-terminal region would have to cause defects in both of those processes, we find this model unlikely. Instead, we propose a different model in which

the PINK1 inside the mitochondria is somehow specifically translocated to the OMM. Further studies are needed to confirm this model and to determine the mechanism for PINK1 translocation and mechanisms by which PINK1 OMM translocation may occur.

Our findings suggest that PINK1 OMM-translocation is required for parkin recruitment to damaged mitochondria. Our identification of PD-linked mutants that are both defective in OMM-translocation and parkin recruitment suggests dysregulated PINK1 translocation is a novel mechanism of PD pathogenesis. Our new understanding the role of PINK1 spatiotemporal dynamics in disease can provide us further insight into the role of mitochondrial dynamics in the pathogenesis of PD. For instance, determining the submitochondrial localization of PINK1 in patient samples will indicate whether the mitochondria are depolarized. In addition, dysfunction of PINK1 translocation in patient fibroblasts when mitochondria are depolarized may suggest PINK1 OMM-translocation dysfunction is related to neurodegeneration. Further studies to elucidate the mechanism(s) underlying PINK1 dual targeting and the effect of mistargeting on mitochondrial signaling should advance our understanding of the role PINK1 submitochondrial localization in mitochondrial health and PD pathogenesis.

Materials and methods

Expression constructs and antibodies

The expression constructs encoding C-terminal GFP-tagged human PINK1 WT, PD-linked PINK1 L347P and W437X mutants were generated by using standard molecular

biological techniques. Plasmids containing PINK1 C92F and Δ TM mutant cDNAs were provided by R. Youle (National Institutes of Health, Bethesda, MD) and the cDNAs were subcloned to generate constructs for expression of C-terminal GFP-tagged PINK1 C92F and Δ TM mutants. The validity of all constructs was confirmed by DNA sequencing. The vector for mitochondrial matrix-targeted mito-dsRed (pDsRed2-Mito) was obtained from Clontech (Mountain View, CA) and the plasmid mCherry-parkin from Addgene (Cambridge, MA). The following antibodies were used in this study: anti-TOM20 (FL-145) and anti-TRAP1 (TR1 or HSP75; Santa Cruz Biotechnology), anti-cytochrome *c* (Clone 6H2.B4) and anti-TIM23 (BD biosciences). All secondary antibodies (FITC and TRITC) were purchased from Jackson ImmunoResearch Laboratories, Inc.

Cell transfection and treatment

HeLa cells were cultured in Dulbecco's Modified Eagle Medium supplemented with 5% fetal bovine serum, 100 IU/ml penicillin, and 100 mg/ml streptomycin. HeLa cells were transfected with the indicated plasmids using Lipofectamine 2000 (Invitrogen) by following the manufacturer's instructions. For analysis of the effects of various treatments on PINK1 submitochondrial localization, cells were either untreated or treated for two hours with 10 μ M CCCP, 10 μ M valinomycin, 10 μ M oligomycin, 15 μ M nocodazole, 80 μ M antimycin A, or 10 μ M nigericin. All chemicals were purchased from Sigma-Aldrich. For analysis of protein synthesis inhibition on mitochondrial depolarization-induced PINK1 OMM translocation, cells were pretreated with either 10 μ M emetine or 100 μ M cyclohexamide for one hour followed by addition of CCCP and co-incubation of emetine or cyclohexamide with 10 μ M CCCP for 2 hours.

PINK1 knockout mice and primary neuronal culture

A breeding colony of PINK1 knockout mice on 129/SvEv background was established from breeding pairs provided by G. Auburger (University Medical School, Frankfurt am Main, Germany) as described [58]. Primary cortical cultures were prepared from wild type or PINK1 knockout mouse embryos as described previously [59,60]. Briefly, cortices were dissected from embryonic day 18 (E18) mouse embryos and cortical neurons were dissociated and plated on poly-L-lysine coated coverslips or MatTek glass bottom dishes. Neurons were cultured in Neurobasal Media (Invitrogen) supplemented with 0.5 μ M L-glutamine, B27 (Invitrogen), 100 IU/ml penicillin, and 100 mg/ml streptomycin. Neurons were transfected with the indicated constructs on day *in vitro* 4 using Lipofectamine 2000 (Invitrogen). Culture media were changed to the supplemented Neurobasal media lacking B27 at 24 hours after transfection, and neurons were treated with 10 μ M CCCP for three hours.

Parkin recruitment in neurons

To evaluate parkin recruitment by various PINK1 mutants, cells were transfected with various PINK1-GFP constructs and mcherry-parkin using Lipo2000 (Invitrogen) according to the manufacturer's instructions for 24 hours, treated with 10 μ M CCCP lacking B27 for 3 hours followed by fixation with 4% paraformaldehyde at 37 degrees. Fixed neurons were stained with TOM20 as a marker for mitochondria (647). Neurons were imaged for PINK1-GFP signal (488), mcherry-parkin signal (561) and TOM20 (647) using confocal microscopy as described above. Neurons with parkin enriched in

mitochondria puncta were scored as positive and neurons with diffuse parkin were scored as negative.

3D-Structured Illumination Microscopy

Cells were fixed with 4% paraformaldehyde in culture media for 10 min, permeabilized with a solution containing 0.1% saponin (Sigma-Aldrich) and 2% horse serum in 1× PBS, stained with the indicated primary antibodies followed by secondary antibodies conjugated to FITC or TRITC, and then mounted in ProLong Gold antifade reagent (Invitrogen) according to the manufacturer's instructions. Images were captured at room temperature using a CFI Apochromat TIRF 100x/1.49 NA oil immersion objective lens on an N-SIM microscope (Nikon Instruments) equipped with CCD camera (DU-897), Perfect Focus System, and SIM Illuminator using 488 nm and 561 nm lasers. All images were acquired and reconstructed using NIS Elements software (Nikon). Image stacks were acquired in 100 nm intervals for 8-15 Z planes. In each plane, 15 images were acquired with a rotating illumination pattern (5 phases, 3 angles) in two color channels (488 nm and 561 nm) independently. The series of images were reconstructed using NIS-Elements software to yield three-dimensional images with resolution beyond the limit of diffraction. Brightness was adjusted using NIS-Elements software and figures were compiled using Photoshop CS4 software (Adobe Systems).

Image analysis

All image analysis was performed using the ImageJ software (National Institutes of Health). For line scans, a straight line was drawn through the mitochondria between the

two arrowheads indicated on the images, and the fluorescence intensity profiles of each color channel was determined by using the Plot Profile function in ImageJ. The value of fluorescence intensity was normalized to that of the single brightest point in each channel and is expressed as arbitrary unit. Graphs were made in SigmaPlot 11.0 (Systat Software, Inc.), and images were annotated to indicate where the line was drawn using Photoshop CS4 software.

Quantification of colocalization

Quantification of the colocalization of PINK1 with TRAP1 or parkin was performed on unprocessed images. The background was subtracted from the images by setting the threshold of each channel to the background value, and the percentage of PINK1 overlapping with TRAP1 or parkin was determined by Mander's coefficients using the JACOP plugin for ImageJ [61,62]. The percentages of overlap were averaged from a total of 90 randomly selected mitochondria from three independent experiments. Graphs were generated with SigmaPlot 11.0 software and figures made using Photoshop CS4 software.

Statistical analysis

Data were subjected to statistical analyses by one- or two-way analysis of variance with a Tukey's *post hoc* test using the SigmaPlot software (Systat Software, Inc.) Results are expressed as mean \pm SEM. A *P*-value of less than 0.05 was considered statistically significant.

Acknowledgments

We thank Dr. Georg Auburger for providing the PINK1 knockout mice.

This work was supported by the National Institutes of Health [GM082828 and GM103613 to L.L. and AG034126 to L.S.C.] and the Emory University Research Committee [SK38167 to L.S.C.]. We thank Emory Integrated Cellular Imaging Core Facility for providing instrumentation and support.

Abbreviations list

OMM, outer mitochondrial membrane; IMM, inner mitochondrial membrane; IMS, intermembrane space; PINK1, PTEN induced kinase 1; Cyt *c.*, cytochrome *c.*, PD, Parkinson's disease, TRAP1, TNF receptor associated protein 1; 3D-SIM, Three-dimensional structured illumination microscopy; MTS, mitochondrial targeting sequence.

References

1. de Rijk, M.C., et al., Prevalence of parkinsonism and Parkinson's disease in Europe: the EUROPARKINSON Collaborative Study. European Community Concerted Action on the Epidemiology of Parkinson's disease. 1997. *J Neurol Neurosurg Psychiatry*, **62**(1): 10-5.
2. Lang, A.E. and A.M. Lozano, Parkinson's disease. First of two parts. 1998. *N Engl J Med*, **339**(15): 1044-53.
3. Lang, A.E. and A.M. Lozano, Parkinson's disease. Second of two parts. 1998. *N Engl J Med*, **339**(16): 1130-43.
4. Braak, H., et al., Stages in the development of Parkinson's disease-related pathology. 2004. *Cell & Tissue Research*, **318**(1): 121-34.
5. Dauer, W. and S. Przedborski, Parkinson's disease: mechanisms and models. 2003. *Neuron*, **39**(6): 889-909.
6. Goedert, M., et al., 100 years of Lewy pathology. 2013. *Nat Rev Neurol*, **9**(1): 13-24.
7. Hawkes, C.H., et al., A timeline for Parkinson's disease. 2010. *Parkinsonism Relat Disord*, **16**(2): 79-84.
8. Schapira, A.H., et al., Mitochondrial complex I deficiency in Parkinson's disease. 1989. *Lancet*, **1**(8649): 1269.
9. Abou-Sleiman, P.M., et al., Expanding insights of mitochondrial dysfunction in Parkinson's disease. 2006. *Nature Reviews Neuroscience*, **7**(3): 207-19.
10. Schapira, A.H., Mitochondrial dysfunction in Parkinson's disease. 2007. *Cell Death & Differentiation*, **14**(7): 1261-6.
11. Schon, E.A. and S. Przedborski, Mitochondria: the next (neurode)generation. 2011. *Neuron*, **70**(6): 1033-53.
12. Bossy-Wetzell, E., et al., Molecular pathways to neurodegeneration. 2004. *Nat Med*, **10 Suppl**: S2-9.
13. Cookson, M.R. and O. Bandmann, Parkinson's disease: insights from pathways. 2010. *Human Molecular Genetics*, **19**(R1): R21-7.
14. Valente, E.M., et al., Hereditary early-onset Parkinson's disease caused by mutations in PINK1. 2004. *Science*, **304**(5674): 1158-60.
15. Hatano, Y., et al., Novel PINK1 mutations in early-onset parkinsonism.[erratum appears in *Ann Neurol*. 2004 Oct;56(4):603]. 2004. *Annals of Neurology*, **56**(3): 424-7.
16. Bonifati, V., et al., Early-onset parkinsonism associated with PINK1 mutations: frequency, genotypes, and phenotypes. 2005. *Neurology*, **65**(1): 87-95.
17. Tan, E.K. and L.M. Skipper, Pathogenic mutations in Parkinson disease. 2007. *Human Mutation*, **28**(7): 641-53.
18. Godeiro, C., Jr., et al., PINK1 polymorphism IVS1-7 A-->G, exposure to environmental risk factors and anticipation of disease onset in Brazilian patients with early-onset Parkinson's Disease. 2010. *Neurosci Lett*, **469**(1): 155-8.
19. Toft, M., et al., PINK1 mutation heterozygosity and the risk of Parkinson's disease. 2007. *J Neurol Neurosurg Psychiatry*, **78**(1): 82-4.

20. Abou-Sleiman, P.M., et al., Genetic association studies of complex neurological diseases. 2006. *J Neurol Neurosurg Psychiatry*, **77**(12): 1302-4.
21. Hedrich, K., et al., Clinical spectrum of homozygous and heterozygous PINK1 mutations in a large German family with Parkinson disease: role of a single hit? 2006. *Arch Neurol*, **63**(6): 833-8.
22. Klein, C., et al., Deciphering the role of heterozygous mutations in genes associated with parkinsonism. 2007. *Lancet Neurol*, **6**(7): 652-62.
23. Ricci, J.E., et al., Mitochondrial functions during cell death, a complex (I-V) dilemma. 2003. *Cell Death Differ*, **10**(5): 488-92.
24. Hansen, J.M., et al., Nuclear and mitochondrial compartmentation of oxidative stress and redox signaling. 2006. *Annu Rev Pharmacol Toxicol*, **46**: 215-34.
25. Jin, S.M., et al., Mitochondrial membrane potential regulates PINK1 import and proteolytic destabilization by PARL. 2010. *J Cell Biol*, **191**(5): 933-42.
26. Zhou, C., et al., The kinase domain of mitochondrial PINK1 faces the cytoplasm. 2008. *Proc Natl Acad Sci U S A*, **105**(33): 12022-7.
27. Lin, W. and U.J. Kang, Structural determinants of PINK1 topology and dual subcellular distribution. 2010. *BMC Cell Biol*, **11**: 90.
28. Gandhi, S., et al., PINK1 protein in normal human brain and Parkinson's disease. 2006. *Brain*, **129**(Pt 7): 1720-31.
29. Silvestri, L., et al., Mitochondrial import and enzymatic activity of PINK1 mutants associated to recessive parkinsonism. 2005. *Hum Mol Genet*, **14**(22): 3477-92.
30. Muqit, M.M., et al., Altered cleavage and localization of PINK1 to aggresomes in the presence of proteasomal stress. 2006. *J Neurochem*, **98**(1): 156-69.
31. Vives-Bauza, C., et al., PINK1-dependent recruitment of Parkin to mitochondria in mitophagy. 2010. *Proc Natl Acad Sci U S A*, **107**(1): 378-83.
32. Pridgeon, J.W., et al., PINK1 protects against oxidative stress by phosphorylating mitochondrial chaperone TRAP1. 2007. *PLoS Biol*, **5**(7): e172.
33. Narendra, D.P., et al., PINK1 is selectively stabilized on impaired mitochondria to activate Parkin. 2010. *PLoS Biol*, **8**(1): e1000298.
34. Mills, R.D., et al., Biochemical aspects of the neuroprotective mechanism of PTEN-induced kinase-1 (PINK1). 2008. *J Neurochem*, **105**(1): 18-33.
35. Becker, D., et al., Pink1 kinase and its membrane potential ($\Delta\psi$)-dependent cleavage product both localize to outer mitochondrial membrane by unique targeting mode. 2012. *J Biol Chem*, **287**(27): 22969-87.
36. Yamano, K. and R.J. Youle, PINK1 is degraded through the N-end rule pathway. 2013. *Autophagy*, **9**(11): 1758-69.
37. Schermelleh, L., et al., Subdiffraction multicolor imaging of the nuclear periphery with 3D structured illumination microscopy. 2008. *Science*, **320**(5881): 1332-6.
38. Huang, B., et al., Super-resolution fluorescence microscopy. 2009. *Annu Rev Biochem*, **78**: 993-1016.
39. Kim, Y., et al., PINK1 controls mitochondrial localization of Parkin through direct phosphorylation. 2008. *Biochem Biophys Res Commun*, **377**(3): 975-80.
40. Frey, T.G. and C.A. Mannella, The internal structure of mitochondria. 2000. *Trends Biochem Sci*, **25**(7): 319-24.

41. Perkins, G., et al., Electron tomography of neuronal mitochondria: three-dimensional structure and organization of cristae and membrane contacts. 1997. *J Struct Biol*, **119**(3): 260-72.
42. Schulke, N., et al., In vivo zippering of inner and outer mitochondrial membranes by a stable translocation intermediate. 1997. *Proc Natl Acad Sci U S A*, **94**(14): 7314-9.
43. Reichert, A.S. and W. Neupert, Contact sites between the outer and inner membrane of mitochondria-role in protein transport. 2002. *Biochim Biophys Acta*, **1592**(1): 41-9.
44. Banci, L., et al., Mitochondrial copper(I) transfer from Cox17 to Sco1 is coupled to electron transfer. 2008. *Proc Natl Acad Sci U S A*, **105**(19): 6803-8.
45. Cechetto, J.D. and R.S. Gupta, Immunoelectron microscopy provides evidence that tumor necrosis factor receptor-associated protein 1 (TRAP-1) is a mitochondrial protein which also localizes at specific extramitochondrial sites. 2000. *Exp Cell Res*, **260**(1): 30-9.
46. Vives-Bauza, C. and S. Przedborski, PINK1 points Parkin to mitochondria. 2010. *Autophagy*, **6**(5): 674-5.
47. Geisler, S., et al., PINK1/Parkin-mediated mitophagy is dependent on VDAC1 and p62/SQSTM1. 2010. *Nat Cell Biol*, **12**(2): 119-31.
48. Kawajiri, S., et al., PINK1 is recruited to mitochondria with parkin and associates with LC3 in mitophagy. 2010. *FEBS Lett*, **584**(6): 1073-9.
49. Matsuda, N., et al., PINK1 stabilized by mitochondrial depolarization recruits Parkin to damaged mitochondria and activates latent Parkin for mitophagy. 2010. *J Cell Biol*, **189**(2): 211-21.
50. Grenier, K., et al., Parkin- and PINK1-Dependent Mitophagy in Neurons: Will the Real Pathway Please Stand Up? 2013. *Front Neurol*, **4**: 100.
51. Park, J., et al., Mitochondrial dysfunction in *Drosophila* PINK1 mutants is complemented by parkin. 2006. *Nature*, **441**(7097): 1157-61.
52. Clark, I.E., et al., *Drosophila* pink1 is required for mitochondrial function and interacts genetically with parkin. 2006. *Nature*, **441**(7097): 1162-6.
53. Exner, N., et al., Loss-of-function of human PINK1 results in mitochondrial pathology and can be rescued by parkin. 2007. *J Neurosci*, **27**(45): 12413-8.
54. Zhang, L., et al., TRAP1 rescues PINK1 loss-of-function phenotypes. 2013. *Hum Mol Genet*, **22**(14): 2829-41.
55. Costa, A.C., et al., *Drosophila* Trap1 protects against mitochondrial dysfunction in a PINK1/parkin model of Parkinson's disease. 2013. *Cell Death Dis*, **4**: e467.
56. Shiba-Fukushima, K., et al., PINK1-mediated phosphorylation of the Parkin ubiquitin-like domain primes mitochondrial translocation of Parkin and regulates mitophagy. 2012. *Sci Rep*, **2**: 1002.
57. Okatsu, K., et al., PINK1 autophosphorylation upon membrane potential dissipation is essential for Parkin recruitment to damaged mitochondria. 2012. *Nat Commun*, **3**: 1016.
58. Gispert, S., et al., Parkinson phenotype in aged PINK1-deficient mice is accompanied by progressive mitochondrial dysfunction in absence of neurodegeneration. 2009. *PLoS One*, **4**(6): e5777.

59. Giles, L.M., et al., Dystonia-associated mutations cause premature degradation of torsinA protein and cell-type-specific mislocalization to the nuclear envelope. 2008. *Hum Mol Genet*, **17**(17): 2712-22.
60. Chen, J., et al., Parkinson disease protein DJ-1 converts from a zymogen to a protease by carboxyl-terminal cleavage. 2010. *Hum Mol Genet*, **19**(12): 2395-408.
61. Rodal, A.A., et al., A presynaptic endosomal trafficking pathway controls synaptic growth signaling. 2011. *J Cell Biol*, **193**(1): 201-17.
62. Bolte, S. and F.P. Cordelieres, A guided tour into subcellular colocalization analysis in light microscopy. 2006. *J Microsc*, **224**(Pt 3): 213-32.

FIGURES AND LEGENDS

A

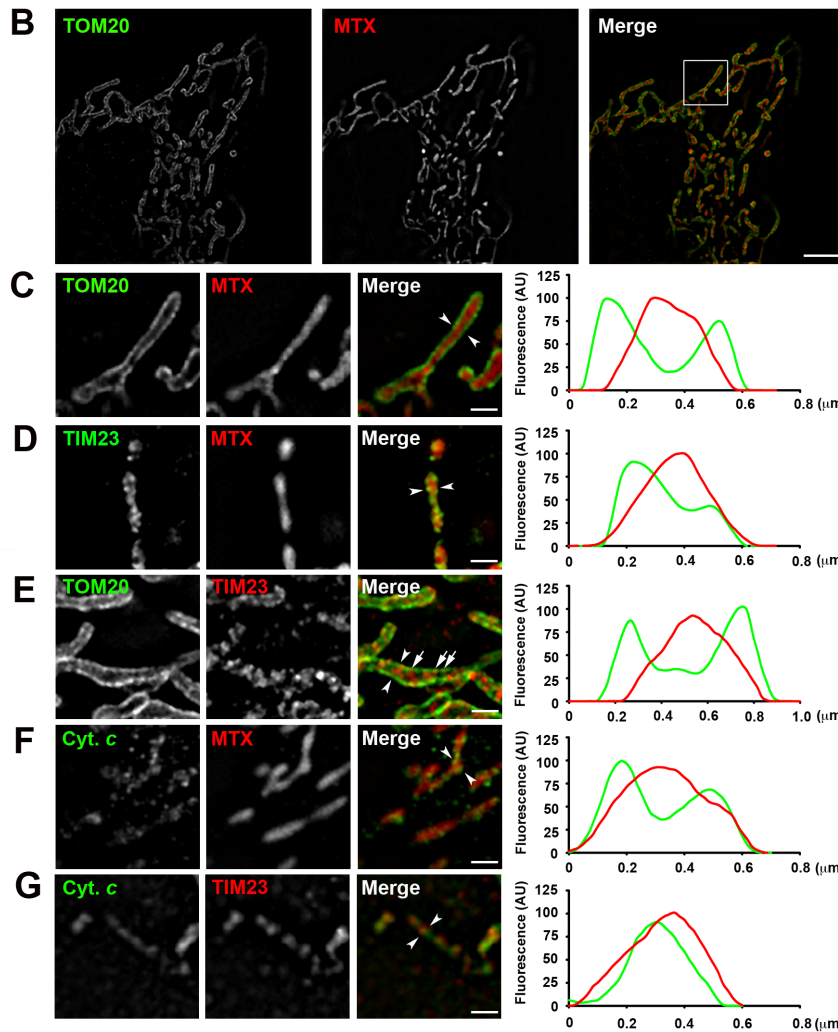
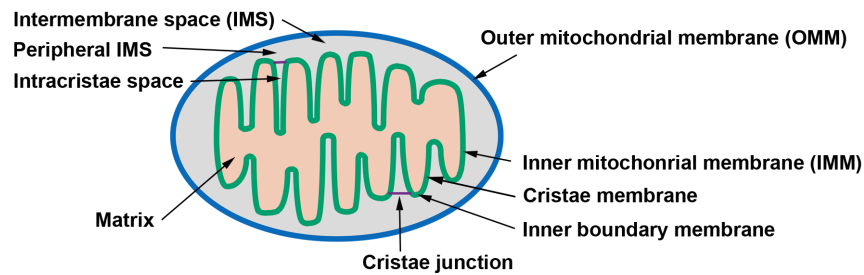


Figure II-1: Super-resolution imaging of submitochondrial compartments by dual color 3D-SIM fluorescence microscopy. (A) Diagram depicting the compartments and subdomain structures of the mitochondria. (B-G) Dual color 3D-SIM fluorescence imaging analysis of HeLa cells labeled with the mitochondrial matrix (MTX) marker mito-dsRed and antibodies against the OMM marker TOM20, the IMM marker TIM23, or the IMS marker Cytochrome *c* (Cyt. *c*). Enlarged view (C) of the boxed region in (B) shows that the TOM20-positive OMM and the mito-dsRed-labeled MTX can clearly be distinguished from each other. The arrows in (E) indicate the sites where the TIM23-labeled IMM appears in close proximity to the TOM20-positive OMM. Scale bars, 5 μm (B) or 1 μm (C-E). Line scans show the fluorescence intensity profiles of each labeling along a line drawn through the mitochondria between the two arrowheads indicated in (C-G).

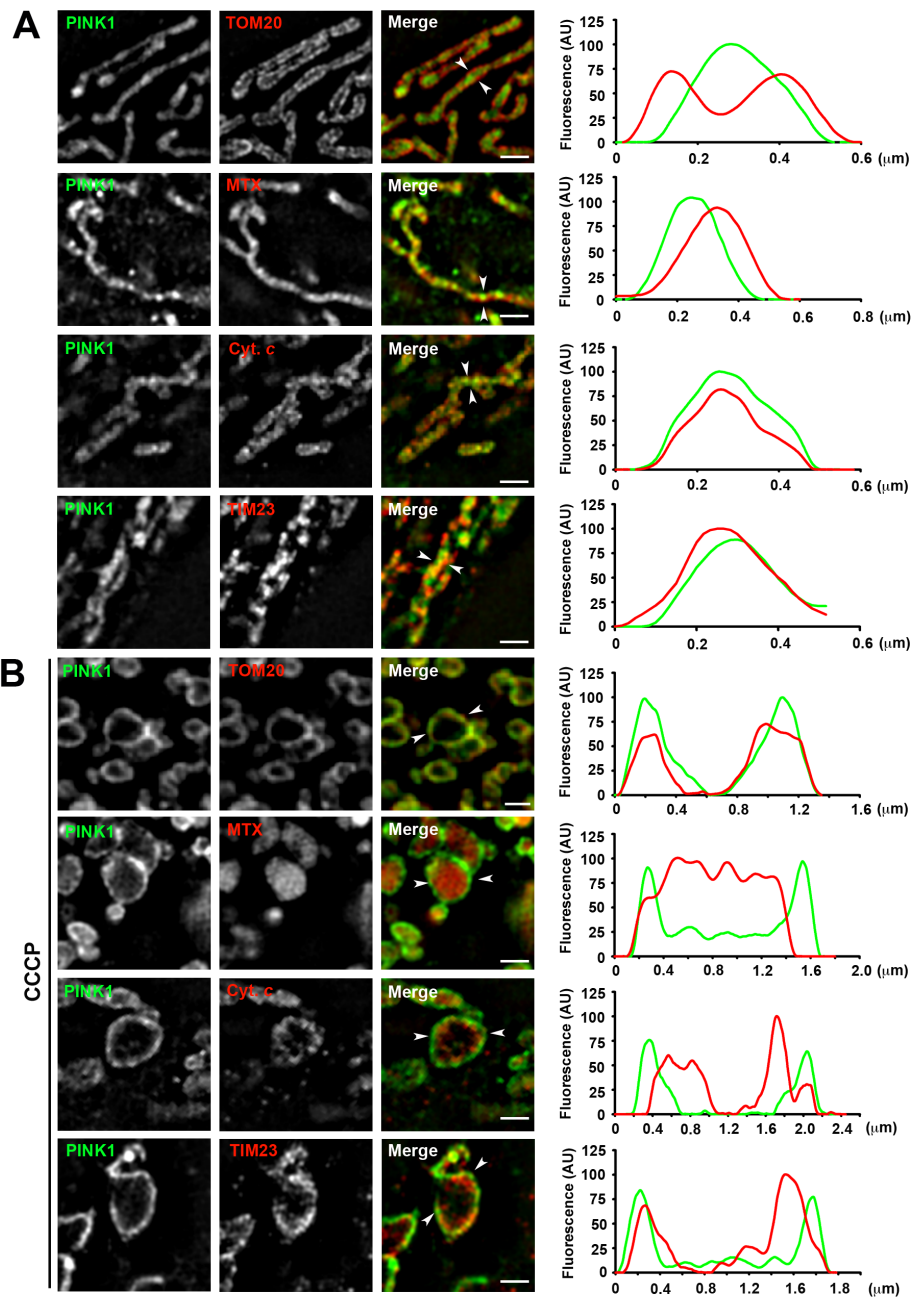


Figure II-2. PINK1 resides in the cristae membrane/intracristae space under normal conditions and translocates to the OMM following mitochondrial depolarization. (A and B) HeLa cells expressing PINK1-GFP were either untreated (A) or treated with 10 μ M CCCP for 2 h (B) followed by staining with the indicated antibodies and 3D-SIM imaging. The MTX was visualized using mito-dsRed, and the OMM, IMM, and IMS using antibodies against TOM20, TIM23, and Cyt. *c*, respectively. Line scans show the fluorescence intensity profiles of each labeling along a line drawn through the mitochondria between the two arrowheads. Scale bars, 1 μ m. (C) Quantification of the percentage of mitochondria with PINK1 localized to the OMM following CCCP or other treatments as indicated. Data represent mean \pm SEM (error bars; $n = 90$ mitochondria) from three independent experiments. *, $P < 0.05$ versus the untreated control, one-way analysis of variance with a Tukey's *post hoc* test.

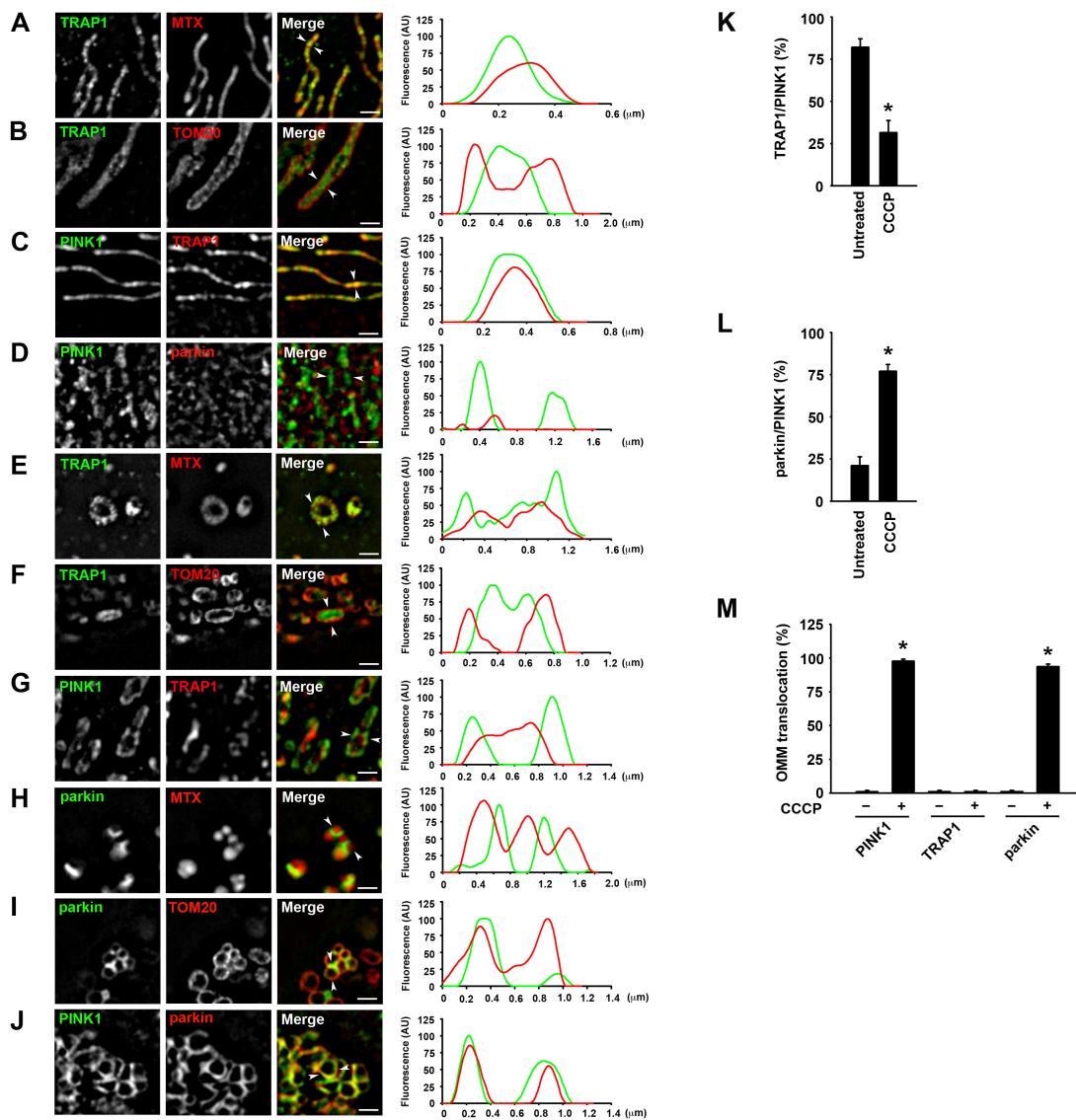


Figure II-3. PINK1 colocalizes with TRAP1 in the IMM/IMS of healthy mitochondria and colocalizes with parkin on the OMM following mitochondrial depolarization. (A-J) HeLa cells were either untransfected (B and F) or transfected with mito-dsRed (A and E), PINK1-GFP (C and G), or GFP-parkin (H and I) or co-transfected with PINK1-GFP and mCherry-parkin (D and J). Cells were either untreated (A-D) or treated with 10 μ M CCCP for 2 h (E-J) followed by staining with anti-TRAP (A-C and

E-G) and/or anti-TOM20 (B, F, and I) antibodies and 3D-SIM imaging. (B). Line scans show the fluorescence intensity profiles of each signal along a line drawn through the mitochondria between the two arrowheads. Scale bars, 1 μm . (K-M) Quantification shows the percentage of PINK1 colocalized with TRAP1 (K), the percentage of PINK1 colocalized with parkin (L), and the percentage of mitochondria with OMM-localized PINK1, TRAP1 or parkin under the basal or CCCP-treated conditions. Data represent mean \pm SEM (error bars; $n = 90$ mitochondria) from three independent experiments. *, $P < 0.05$ versus the corresponding untreated control, one-way analysis of variance with a Tukey's *post hoc* test.

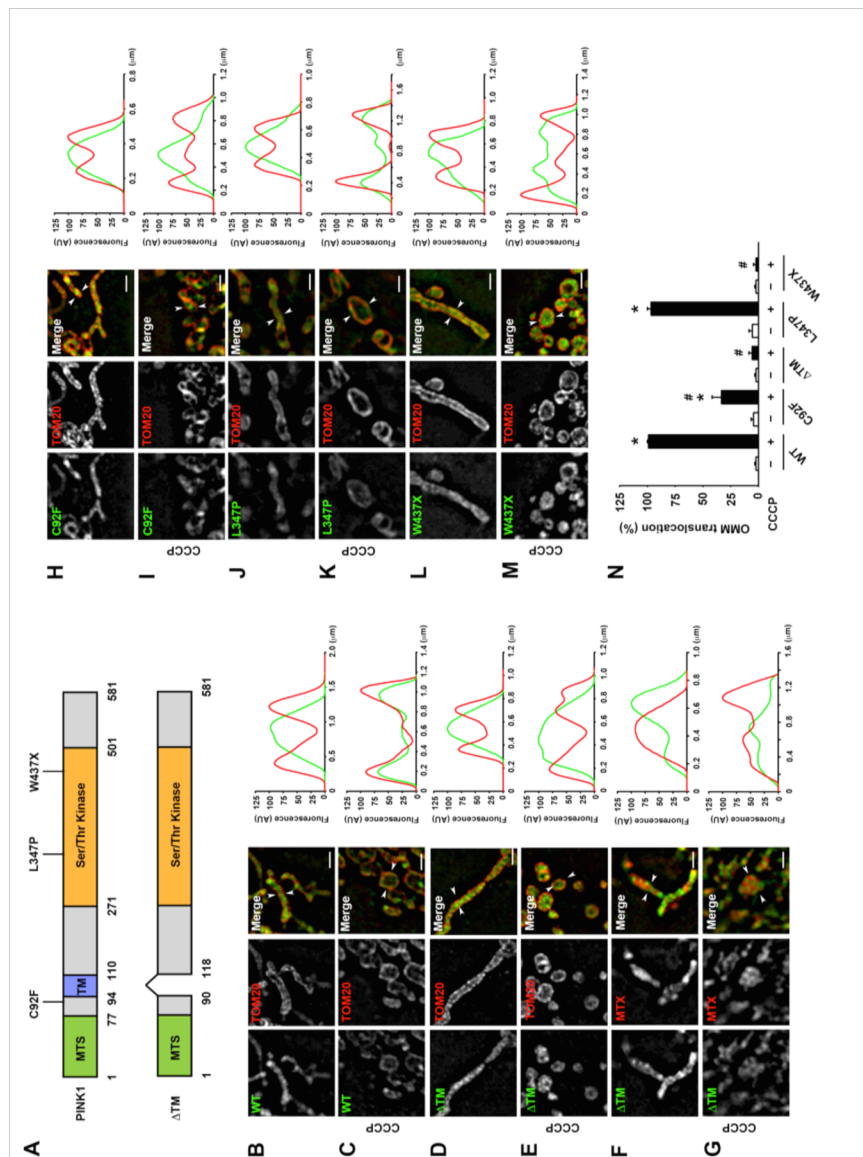


Figure II-4. Mitochondrial depolarization-induced PINK1 OMM translocation is impaired by PINK1 Δ TM, C92F and W437X mutations. (A) Domain structure of PINK1. The locations of mitochondrial targeting sequence (MTS), transmembrane domain (TM), Kinase domain, and PD-linked PINK1 point mutations are indicated. (B-M) HeLa cells expressing C-terminal GFP-tagged PINK1 WT (B, C) or indicated PINK1 mutants (D-M) were either untreated or treated with 10 μ M CCCP for 2 h as indicated

followed by staining with anti-TOM20 antibodies and 3D-SIM imaging. The MTX was visualized using mito-dsRed. Line scans show the fluorescence intensity profiles of each signal along a line drawn through the mitochondria between the two arrowheads. Scale bars, 1 μm . (N) Quantification shows the percentage of mitochondria with OMM-localized PINK1 under the basal or CCCP-treated conditions. Data represent mean \pm SEM (error bars; $n = 90$ mitochondria) from three independent experiments. *, $P < 0.05$ versus the corresponding untreated control; #, $P < 0.05$ versus the CCCP-treated PINK1 WT, two -way analysis of variance with a Tukey's *post hoc* test.

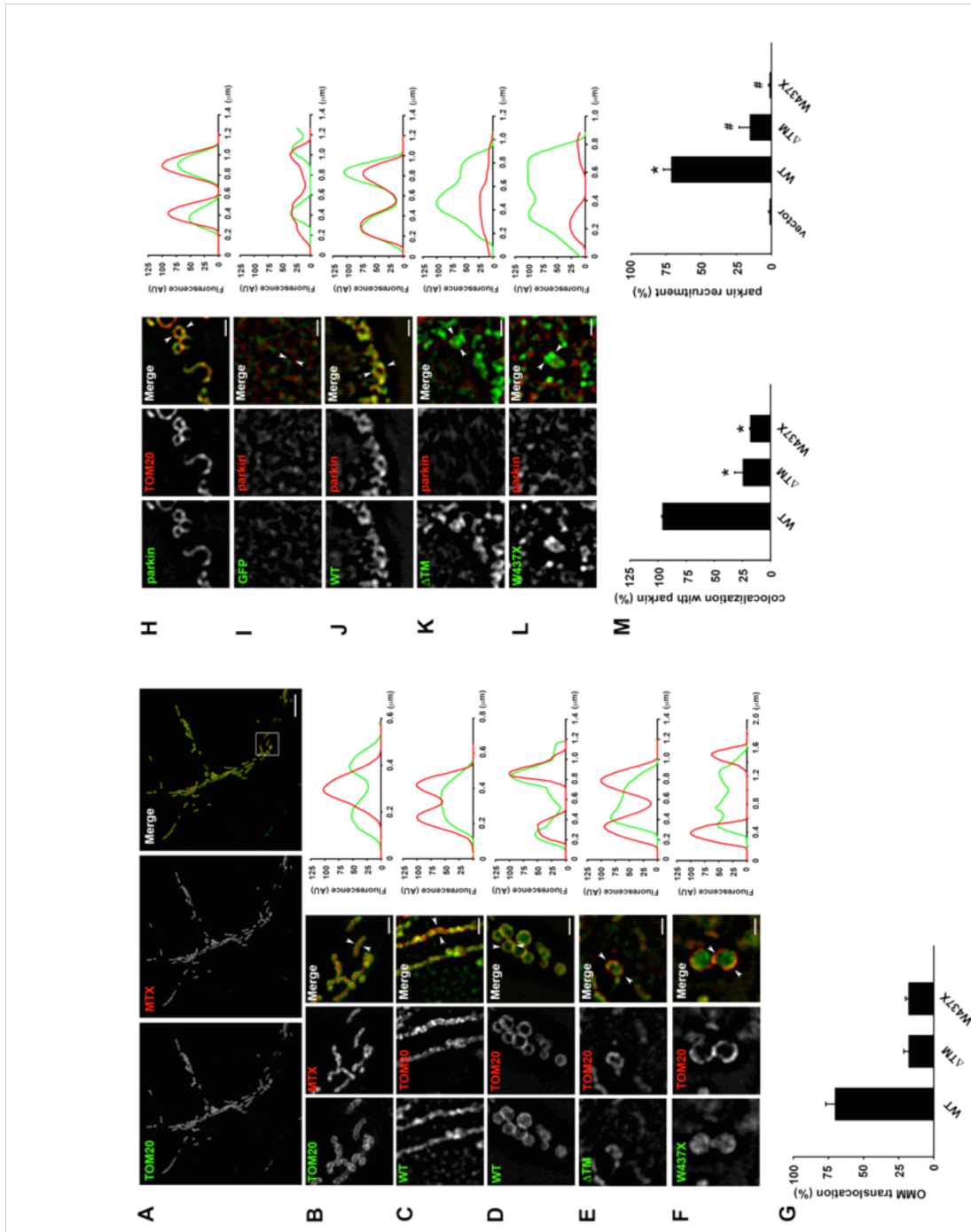
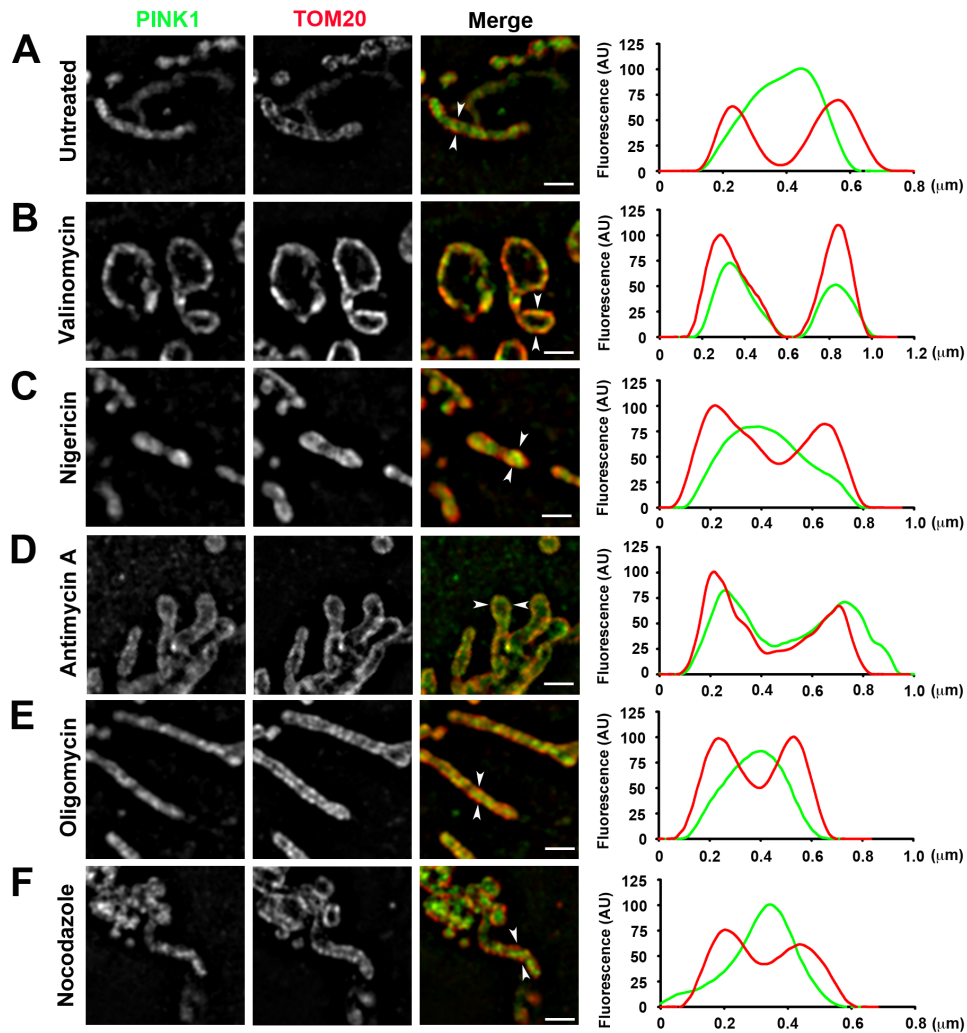


Figure II-5. The transmembrane domain and C-terminal region are required for OMM translocation and parkin recruitment in neurons. (A) Full panel and (B) inset SIM images of primary cortical neurons transfected with mito-dsRed and stained with an antibody against TOM20. (C-F) SIM images of primary cortical neurons PINK1-GFP

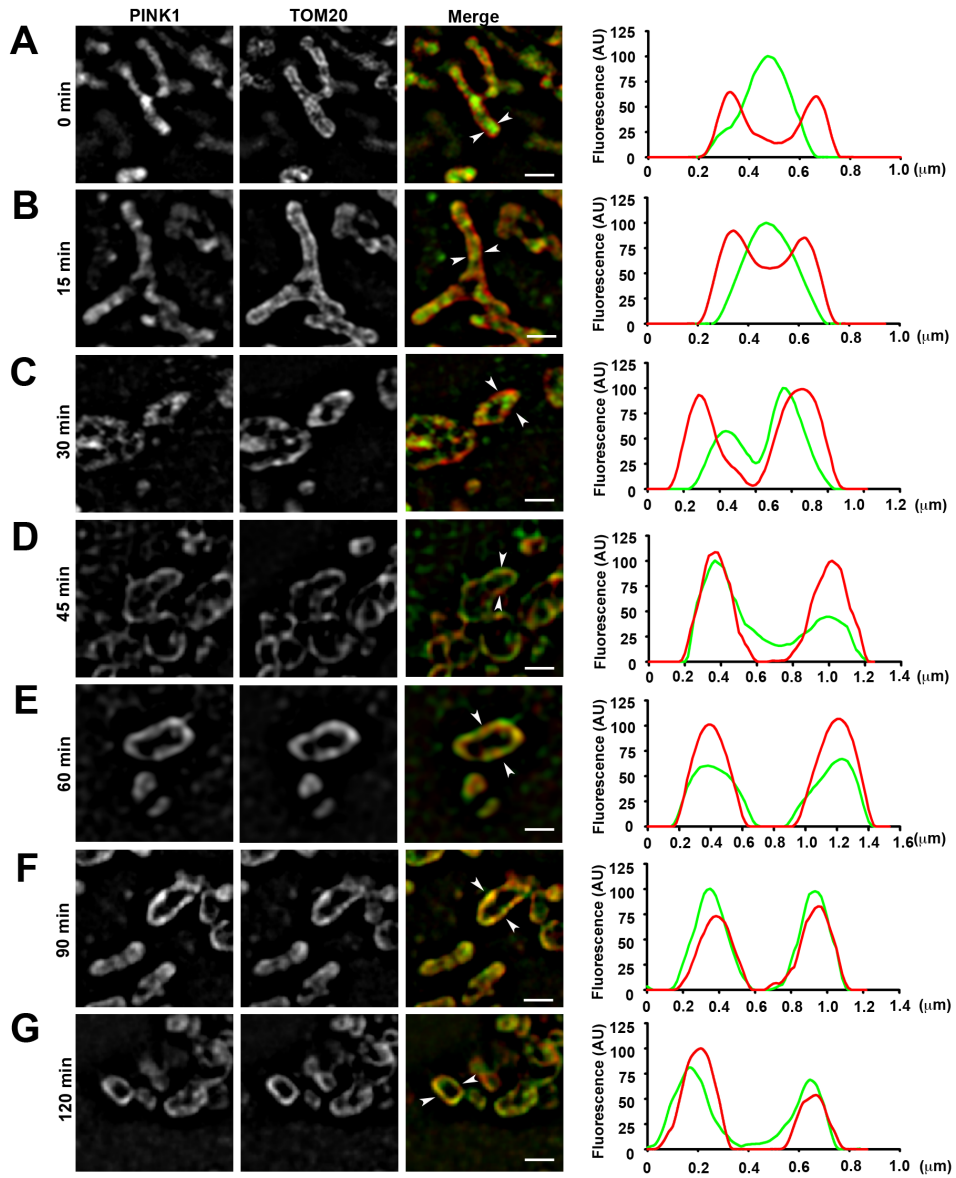
wild type (C, D), or PD-linked PINK1 mutants Δ TM (E) or W437X (F) and stained with the OMM marker TOM20. Neurons were either untreated (C) or treated with 10 μ M CCCP (D-F). (G) Quantification of the percentage of mitochondria with PINK1 localized to the OMM following CCCP or other treatments as indicated. Data represent mean \pm SEM (error bars; $n = 90$ mitochondria) from three independent experiments. (H) Wild-type neurons were transfected with mcherry-parkin and (I-L) PINK1 deficient neurons transfected with PINK1 WT or indicated PINK1 mutants and treated with CCCP to observe parkin recruitment (H) or colocalization with parkin (I-L). Line scans were acquired using ImageJ and indicate the fluorescence intensity of each signal over a line (AU). Arrowheads indicate where the line was drawn through the mitochondria. Scale bars, 0.1 μ M. (M) Colocalization of WT PINK1 or the indicated PINK1 mutant with parkin. (N) Quantification of the percentage of mitochondria with parkin recruited to mitochondria or colocalized with PINK1. Data represent mean \pm SEM (error bars; $n = 90$ mitochondria) from three independent experiments. *, $P < 0.05$ versus the corresponding untreated control, one-way analysis of variance with a Tukey's *post hoc* test.

Supplementary material

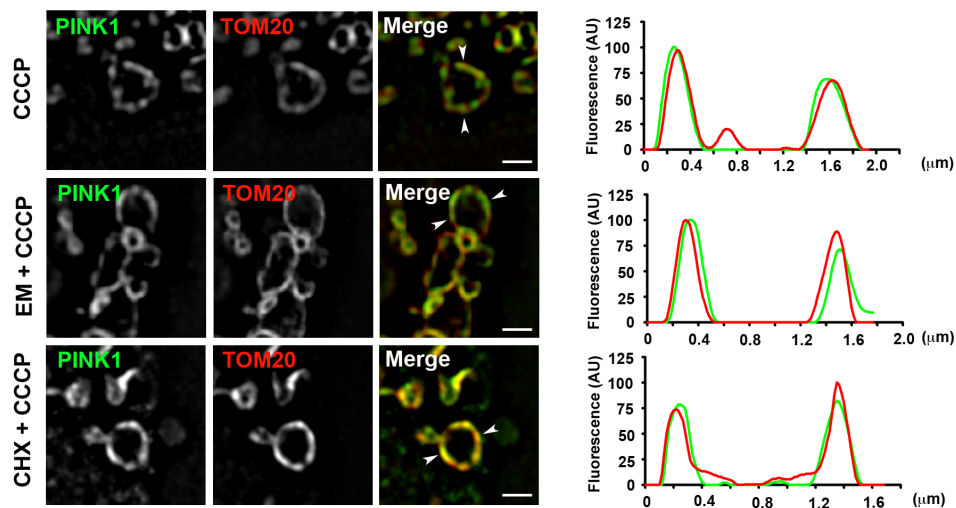


Supplementary Figure II-S1. PINK1 translocates to the OMM following loss of $\Delta\Psi$ but not loss of ΔpH , ATP, or microtubule integrity. (A-G) HeLa cells expressing PINK1-GFP were either untreated (A) or treated with valinomycin (B), nigericin (C), antimycin A (D), oligomycin (E), or nocodazole (F) for 2 h followed by staining with

anti-TOM20 antibodies and 3D-SIM imaging. Line scans show the fluorescence intensity profiles of each signal along a line drawn through the mitochondria between the two arrowheads. Scale bars, 1 μm .



Supplementary Figure II-S2. Timecourse of mitochondrial depolarization-induced PINK1 translocation to the OMM. HeLa cells expressing PINK1-GFP were treated with 10 μ M CCCP for the indicated lengths of time followed by staining with anti-TOM20 antibodies and 3D-SIM imaging. Line scans show the fluorescence intensity profiles of each signal along a line drawn through the mitochondria between the two arrowheads. Scale bars, 1 μ m.



Supplementary Figure II-S3. Mitochondrial depolarization-induced PINK1 OMM translocation does not require new protein synthesis. HeLa cells expressing PINK1-GFP were pretreated with protein synthesis inhibitor emetine (EM) or cycloheximide (CHX) or vesicle (DMSO) for 1 h followed by addition of CCCP and co-incubation for 2 h. Cells were then stained with anti-TOM20 antibodies and imaged by 3D-SIM. Line scans show the fluorescence intensity profiles of each signal along a line drawn through the mitochondria between the two arrowheads. Scale bars, 1 μ m.

CHAPTER III

**SPONGIFORM NEURODEGENERATION LINKED E3 LIGASE MGRN1 IS
LOCALIZED TO MITOCHONDRIA WHERE IT REGULATES
MITOCHONDRIAL MORPHOLOGY**

Abstract

Spongiform neurodegeneration, or the degeneration of neuronal cells accompanied by vacuolation of nervous tissue, represents the neuropathological hallmark of prion diseases and is also seen as a pathological consequence in other neurodegenerative diseases. Because multiple diseases present with a similar pathology, this implicates a common underlying mechanism of pathogenesis yet this mechanism remains undefined. Previous reports revealed that mice with a null mutation in the gene encoding Mahogunin RING (really interesting new gene) finger 1 (Mgrn1), an E3 ubiquitin-protein ligase, exhibit age-dependent spongiform neurodegeneration, but interestingly, these mice lacked typical proteinase K prion aggregation. Mitochondrial dysfunction and oxidative stress is observed in brains of Mgrn1 mutant mice prior to development of spongiform change; however, the precise mechanism by which these mice experience mitochondrial dysfunction remains undefined. We have determined that Mgrn1 is primarily localized to mitochondria through *N*-myristoylation. In Mgrn1 deficient cells, we observe severe defects in the mitochondrial network and ultrastructure via confocal microscopy and electron microscopy, respectively. Taken together, this suggests that Mgrn1 may regulate mitochondrial dynamics. Loss of Mgrn1 increases susceptibility to oxidative stress induced cell death. These findings further support mitochondrial dysfunction as a mechanism for the pathogenesis of spongiform neurodegenerative disorders.

Introduction

Spongiform neurodegeneration, the pathological hallmark of prion diseases and also seen as a pathological consequence to HIV encephalitis, Alzheimer's disease (AD), and diffuse Lewy body disease (DLBD), is characterized by the accumulation of large vacuoles, deposition of protein aggregation, and neuronal and/or glial cell death (reviewed in [1]). Spongiform neurodegenerative diseases are seen in humans and other mammals and can be familial, sporadic, or caused by an infection. While each specific spongiform neurodegenerative disease has its own unique clinical presentation, they all present with rapidly progressive dementia. Since such a wide range of diseases present with similar pathology, it has been suggested that a common mechanism is involved; however, this mechanism remains undefined.

Mitochondrial dysfunction is implicated as an underlying cause of neurodegeneration, including spongiform neurodegenerative disorders (reviewed in [2]). Mitochondrial dysfunction leads to increased generation of reactive oxygen species (ROS), which in turn, can oxidize proteins, lipids, and nucleic acids, affecting their functions [3]. Mitochondrial dysfunction and increased vulnerability to oxidative stress are seen in several spongiform neurodegenerative disorders including models of prion disease [4-8], AD [9-11], and HIV encephalitis [12]. Mitochondria are highly dynamic organelles that readily break apart (fission) and recombine (fusion) in order to protect themselves from stress and respond to energy needs [13]. Mitochondrial dynamics are highly regulated and dysregulation of the balance between fission and fusion results in either elongation or fragmentation of the mitochondrial network and both result in disease

[14-16]. For instance, patients suffering from prion diseases and prion infected animal models exhibit altered mitochondrial morphology [4,17]. Mitochondrial fission is required for distribution of mitochondria according to energy demands and degradation of damaged mitochondria [20]. Fusion is also important to allow complementation of mitochondrial DNA and dilution deleterious substances [21]. A group of proteins regulate the shape of the mitochondrial network by directly affecting mitochondrial dynamics. Dynamin-related protein 1 (Drp1) is a GTPase required for mitochondria fission [24]. GTPases mitofusins1 and 2 (Mfn1 and Mfn2, respectively) regulate outer mitochondrial membrane (OMM) fusion, while inner mitochondrial membrane (IMM.) fusion is mediated by OPA1 [18]. The activity of mitochondrial fission and fusion proteins is regulated by posttranslational modifications such as ubiquitination, phosphorylation, and sumoylation [19-22].

Mice with a spontaneous null frameshift mutation in Mahogunin RING (really interesting new gene) finger 1 (*Mgrn1*^{mg-nc}) develop age dependent spongiform neurodegeneration that strikingly resembles the pathology observed in models of prion diseases [23]. *Mgrn1* is an ubiquitously expressed C3HC4 RING finger protein that has been previously shown to mediate ubiquitination of TSG101 [24], melanocortin receptor [25], and indirectly, α -tubulin [26]. Cytosolically exposed prion sequesters *Mgrn1* [27], suggesting that in the presence of pathogenic prion (PrP^{Sc}), *Mgrn1* is mislocalized abolishing neuroprotective function. Prior to neurodegeneration, *Mgrn1* mice exhibit mitochondrial dysfunction and oxidative stress [28]; therefore, it is likely that mitochondrial dysfunction contributes to the pathogenesis of spongiform

neurodegeneration. The mitochondrial role of Mgrn1 remains undefined and the mechanism by which Mgrn1 protects against neurodegeneration remains unclear.

In this study, we investigated the potential role(s) of Mgrn1 at mitochondria. We observed a large pool of Mgrn1 is localized to mitochondria and targeted to the OMM via *N*-myristoylation. We sought to determine the role of Mgrn1 in maintaining mitochondrial homeostasis and examine the precise effects of Mgrn1 loss on mitochondria. Overexpression of Mgrn1 in HeLa cells promotes mitochondrial elongation. Neurons cultured from Mgrn1 mutant mice exhibited fragmented mitochondria and reduced mitochondrial health. Mgrn1-mediated cytoprotection is dependent on its *N*-myristoylation and E3 ligase activity. This study further defines the mechanism by which loss of Mgrn1 leads to mitochondrial dysfunction and cell death.

Results

Mgrn1 mutant mice suffer from spongiform neurodegeneration

A spontaneous mutation arose in the C3H/HeJ mouse strain resulting in a coat color phenotype [29]. It wasn't until much later that Mgrn1 mutant mice were also shown to exhibit spongiform neurodegeneration [23]. Before we began our studies, we wanted to first confirm spongiform neurodegeneration observed in Mgrn1 mutant mice. Based on previous studies, the neurodegeneration exhibited by Mgrn1 mutant mice is age dependent, so in order to make sure that we observed these mice at the right point in their lives, we subjected mice that were 12 months of age to both histology and electron microscopic analysis. In the 12-month-old wild type mice, we observed healthy tissue throughout the brain including the cortex (Fig. 1A). No vacuolation, protein deposits, or any trace of neurodegeneration was observed in wild type mice. On the other hand, we observed large vacuoles in the tissue in Mgrn1 mutant animals throughout the brain, but most severe was in the cortex (pictured) (Fig. 1B). This confirms what others had seen in that Mgrn1 mutant mice exhibit spongiform neurodegeneration. We also wanted to observe these structures via electron microscopic analysis to see these vacuolation structures in greater detail. In addition to observing vacuolation in Mgrn1 mutant mouse brains using electron microscopy, we also observed curled membrane fragments inside the vacuole, typical of spongiform neurodegeneration [30,31] (Fig. 1C). Taken together, this confirms the presence of spongiform neurodegeneration in aged Mgrn1 mutant mice.

Mgrn1 is primary localized to mitochondria

While we previously determined that Mgrn1 is partially localized to early endosomes, where Mgrn1 ubiquitinates the ESCRT component, TSG101 [24], the subcellular localization of Mgrn1 remains mostly uncharacterized. Because Mgrn1 mutant mice exhibit mitochondrial dysfunction, Mgrn1 likely must be localized to mitochondria to play a direct role in mitochondrial biology. To further characterize the subcellular localization of Mgrn1, we first generated a rabbit polyclonal anti-Mgrn1 antibody against residues 255-283 of human Mgrn1. We confirmed that this antibody specifically recognizes both human and mouse endogenous and recombinant Mgrn1 for western blotting and immunocytochemistry (data not shown).

Once we confirmed the reliability of our anti-Mgrn1 polyclonal antibody, we performed immunofluorescence confocal microscopic analysis to determine the subcellular distribution of endogenous Mgrn1 in HeLa cells. We observed a cytosolic punctate pattern accompanied by nuclear staining most likely from the two isoforms of Mgrn1 that contain nuclear localization signals [32,33] (Fig. 2A). We observed extensive colocalization between Mgrn1 and the mitochondrial marker, HSP60 (Fig. 2A), indicating that a large pool of Mgrn1 is localized to mitochondria. We also observed significant colocalization between Mgrn1 and the early endosome marker Rab5, consistent with our previously published data [24]. We observed some colocalization with the lysosomal marker, LAMP2, which may be explained to the endosome-to-lysosome trafficking role of Mgrn1 as previously published [24]. There was very little colocalization between endogenous Mgrn1 and the marker of the medial golgi, GM130. Together these findings indicate that Mgrn1 is associated with both mitochondria and

early endosomes (Fig. 2A,B). Because Mgrn1 is primarily localized to mitochondria, this suggests Mgrn1 has a direct role in mitochondrial biology.

Once we had characterized the subcellular localization of Mgrn1 in HeLa cells, we wanted to characterize the distribution of Mgrn1 expression in neurons. Since Mgrn1 mutant mice exhibit neuronal cell death and vacuolation, it is likely Mgrn1 is expressed in neurons and localized to the cellular structures in which it acts. We stained primary cortical neurons with anti-Mgrn1 and an antibody against the presynaptic neuronal marker, synaptophysin (SVP38). We observed that Mgrn1 was distributed in the cell body and dendrites of cortical neurons and partially colocalizes with synaptophysin (Fig. 2 C). We then wanted to determine if Mgrn1 localized to mitochondria in neurons. Cortical neurons were stained with anti-Mgrn1 and the mitochondrial marker TOM20. We observed extensive colocalization between endogenous Mgrn1 and mitochondria in cortical neurons (Fig. 2D). This suggests that Mgrn1 may have functions in the mitochondria and/or synapses of neurons.

The putative *N*-myristoylation motif is required for mitochondrial localization of Mgrn1

Because we observed that a large pool of Mgrn1 localizes to mitochondria, we wanted to determine the mechanism by which Mgrn1 may be targeted to mitochondria. We first determined that Mgrn1 lacks a canonical mitochondrial targeting sequence, a common way that nuclear encoded proteins are targeted to the mitochondria (data not shown). In addition, Mgrn1 does not have any predicted transmembrane domains, which would have been a potential mechanism by which Mgrn1 could anchor into the

mitochondrial membranes. To determine the mechanism by which Mgrn1 localizes to mitochondria, we first performed a motif search using the eukaryotic linear motif (ELM) search from ExPASy and determined that Mgrn1 has a predicted *N*-myristoylation motif (MGXXXSXXX) (Fig. 3A). *N*-myristoylation is a lipid modification in which myristic acid is conjugated to the glycine residue via *N*-myristoyltransferase allowing protein-lipid interactions. After comparing orthologs of Mgrn1, we determined that this is a well-conserved motif, indicating the importance of this motif in Mgrn1 function (Fig. 3A). To determine the role of the putative *N*-myristoylation motif in the subcellular localization of Mgrn1, we designed and created a mutant, Mgrn1G2A in which the N-terminal glycine residue, to which myristic acid is attached, was mutated to an alanine. We transfected HeLa cells with Mgrn1-myc and Mgrn1G2A-myc and purified mitochondria from cell lysates. We observed that Mgrn1-myc but not Mgrn1G2A-myc partially cofractionated with the mitochondrial marker TOM20 (Fig. 3B). To confirm our subcellular fractionation and western blotting analysis, the subcellular distribution of Mgrn1-myc and Mgrn1G2A-myc was examined visually by immunocytochemistry confocal microscopic analysis (Fig 3C). We observed extensive colocalization between Mgrn1-myc and the mitochondrial protein, TRAP1. This confirms our observation that Mgrn1 significantly localizes to mitochondria. Interestingly, we observed that Mgrn1G2A-myc was cytosolically distributed and not localized to the mitochondria (Fig. 3C). This suggests that *N*-myristoylation is required for mitochondrial localization.

Since mitochondrial functions are highly compartmentalized, it is important to determine the submitochondrial localization of Mgrn1. Because addition of myristic acid to the N-terminus of proteins allows proteins to associate with membranes, we first

assumed that Mgrn1 interacts with one of the mitochondrial membranes. We have previously shown the ability to differentiate submitochondrial compartments (Chapter II) using 3D-SIM. HeLa cells were transfected with of the mitochondrial matrix marker, Mito-dsRed (MTX), and Mgrn1-myc or Mgrn1G2A-myc. Using 3D-SIM imaging analysis, we observed that Mgrn1 resides outside the mitochondrial matrix (Fig. 3D). Line scan analysis indicates that there is very little overlap between Mgrn1 and the matrix marker fluorescent signals, suggesting that Mgrn1 is localized to the OMM (Fig. 3D). Additionally, we examined the distribution of Mgrn1G2A-myc in HeLa cells using 3D-SIM imaging analysis and we confirmed that mutation of the putative *N*-myristoylation motif abolishes mitochondrial localization.

Mgrn1 regulates mitochondrial morphology

When we were examining the submitochondrial localization of endogenous and overexpressed Mgrn1 and the *N*-myristoylation mutant Mgrn1G2A-myc, we observed alterations in mitochondrial morphology. Specifically, we observed that the mitochondrial network appeared to be elongated in the WT Mgrn1-myc overexpressing cells compared to the cells overexpressing Mgrn1G2A-myc or untransfected cells. Since we also determined that Mgrn1 is localized to the OMM, we hypothesized that Mgrn1 may regulate mitochondrial dynamics.

To determine the effect of Mgrn1 expression on mitochondrial morphology, we overexpressed WT Mgrn1-myc, Mgrn1G2A-myc, or Mgrn1mtE3-myc in HeLa cells. Mgrn1mtE3-myc is a catalytically inactive mutant of Mgrn1 previously characterized by our lab [24]. We examined mitochondrial morphology through the direct visualization of

Mito-dsRed or by staining cells with an antibody against the mitochondrial protein, TIM23. We observed elongation of the mitochondrial network in cells overexpressing WT Mgrn1 compared to cells not overexpressing Mgrn1, overexpressing Mgrn1G2A-myc, or overexpressing Mgrn1mtE3-myc (Fig. 4A-D). And interestingly, we also observed swollen mitochondria near the cell periphery in Mgrn1 overexpressing cells and not in the untransfected cells (Fig. 4E,F). Reflecting on the literature, our observations are similar to what is seen when the mitochondrial fission protein, Drp1, is depleted in cells [34]. The elongation of the mitochondrial network and the presence of mitochondrial “balloons” suggest that Mgrn1 either promotes mitochondrial fusion or inhibits mitochondrial fission. Comparing overexpression of the mislocalized Mgrn1G2A or the enzymatically inactive Mgrn1mtE3 to untransfected cells, we did not see a significant difference in the number of cells with elongated mitochondria or balloon structures (Fig 4 G,H). This suggests these two mutants have a negligible effect on the mitochondrial network. Additionally, we saw a significant decrease in the number of cells with elongated mitochondria in Mgrn1G2A and Mgrn1mtE3 compared to overexpression of WT Mgrn1. This suggests that *N*-myristoylation and E3 ubiquitin-protein ligase activity are both required but neither is sufficient to promote elongation of the mitochondrial network.

Since altered mitochondrial dynamics is a common underlying cause of multiple neurodegenerative diseases [35-37], and we have determined overexpression of Mgrn1 results in elongation of the mitochondrial network, we wanted to determine if loss of Mgrn1 also affects mitochondrial morphology. Cortical neurons cultured from Mgrn1 mutant and wild type mice were stained with MitoTracker Green (Invitrogen), a

mitochondrial dye that allows visualization of mitochondria, and imaged live (Fig. 5A). In wild type neurons, the mitochondrial network is branched and interconnected in the cell body and tubular structures in the neuronal processes (Fig. 5A). In the cell body and neuronal processes of Mgrn1 mutant neurons, mitochondria appear as rounded, donut shaped structures and with very little interconnection. In addition, the mitochondria appeared more clustered in the cell body than in the processes in Mgrn1 mutant neurons, indicative of a potential trafficking defect.

We observed a significant decrease in the average mitochondrial length of mitochondria in Mgrn1 mutant neurons compared to the average mitochondrial length in wild type neurons (Fig 5B). In addition, we also observed a significant increase in the number of neurons with fragmented mitochondria compared to wild type controls (Fig. 5C). This suggests that Mgrn1 expression is required for proper regulation of the mitochondrial network and that loss of Mgrn1 expression can result in mitochondrial fragmentation.

Mgrn1 is required for mitochondrial health

As previously stated, regulation of mitochondrial fusion and fission are required for the proper maintenance of mitochondrial health [38]. Without a balance of fusion and fission, the mitochondrial network can either become elongated or fragmented, but in either case, trafficking is disrupted and damaged mitochondria accumulate. Because we observed altered mitochondrial morphology in Mgrn1 mutant neurons compared to wild type, we sought to determine the effect of this altered morphology on mitochondrial health. To determine if mitochondria in Mgrn1 mutant neurons had reduced membrane

potential compared to wild type controls, we stained these cells with MitoTracker Green, which labels all mitochondria, and tetramethylrhodamine ethyl ester (TMRE), a red dye that requires membrane potential in order to be imported into mitochondria; therefore, it only labels healthy mitochondria [39]. We observed a striking loss of TMRE fluorescence in the mitochondria from Mgrn1 mutant neurons compared to their wild type controls (Fig. 6A). The MitoTracker Green fluorescence appeared consistent between wild type and Mgrn1 mutant neurons, suggesting no change in mitochondrial mass (Fig. 6A). Normalized TMRE fluorescence was significantly reduced in the mitochondria in Mgrn1 mutant neurons compared to wild type (Fig. 6B). This indicates that the dysregulation in mitochondrial dynamics in Mgrn1 mutant mice can result in mitochondrial damage. In addition, this suggests that loss of Mgrn1 expression is sufficient to cause mitochondrial dysfunction.

Mitochondria from aged Mgrn1 mutant mice exhibit ultrastructural defects as shown by electron microscopy.

Our evidence suggests that Mgrn1 may regulate mitochondrial dynamics in both HeLas and cortical neurons. Because Mgrn1 mutant mice exhibit mitochondrial dysfunction and age dependent spongiform neurodegeneration, we wanted to examine mitochondrial ultrastructure in aged Mgrn1 mutant mice. We perfused wild type and Mgrn1 mutant mice aged 12 months and the cortices were subjected to negative staining and electron microscopy. We observed that mitochondria from wild type mice had regular mitochondrial structure (Fig. 7A). Specifically, mitochondria exhibited organized cristae and fully intact IMMs and OMMs. On the other hand, mitochondria from Mgrn1

mutant mice had discontinuous cristae and OMM vesiculation (Fig. 7B,C). The significance of these two phenotypes is not fully understood; however, similar mitochondrial ultrastructure is other instances of spongiform neurodegeneration [40,41]. We determined that there was a significant increase in mitochondria observed with discontinuous cristae, vesiculation, or both in *Mgrn1* mutant mouse brains compared to wild type controls (Fig. 7D). This suggests that loss of *Mgrn1*-mediated regulation of mitochondrial dynamics and health causes structural defects in mitochondria.

***Mgrn1* is cytoprotective against mitochondrial dysfunction**

Although it has been previously shown that *Mgrn1* is cytoprotective against various stressors [42], we wanted to further determine if *Mgrn1* protects against neuronal cell death associated with mitochondrial dysfunction. To determine the effect of *Mgrn1* on cytoprotection in neurons, wild type and *Mgrn1* mutant neurons were treated with rotenone. Because rotenone inhibits complex I of the electron transport chain, treatment with rotenone causes mitochondrial dysfunction and cell death. We observed that *Mgrn1* mutant cortical neurons exhibited increased susceptibility to rotenone-induced cell death compared to the wild type controls (Fig. 8A-C). Because rotenone is a mitochondrial toxin, this suggests that *Mgrn1* is cytoprotective against mitochondrial dysfunction.

To determine if mitochondrial localization or E3 ligase activity were required for *Mgrn1*-mediated cytoprotective function, we transfected *Mgrn1* mutant cortical neurons with myc tagged empty vector, WT *Mgrn1*-myc, *Mgrn1*G2A-myc, or *Mgrn1*mtE3-myc constructs and treated with 100 nM rotenone for 24 hours. We observed that overexpression of WT *Mgrn1* rescues the susceptibility of *Mgrn1* mutant cortical neurons

to rotenone-induced apoptosis (Fig. 8D,E). This effect was abrogated by Mgrn1G2A and Mgrn1mtE3 mutations, suggesting that mitochondrial localization and E3 ubiquitin-protein ligase activity are required for Mgrn1 mediated cytoprotection against mitochondrial toxins. Together, these findings suggest that Mgrn1 can protect cells against deleterious effects associated with mitochondrial dysfunction, and Mgrn1-mediated cytoprotection is dependent on mitochondrial localization and E3 ligase activity.

Discussion

The pathogenesis of spongiform neurodegenerative diseases is poorly understood; however, mitochondrial dysfunction and increased susceptibility to oxidative stress have been implicated as potential causative factors. The relationship between spongiform neurodegenerative disorders and mitochondrial dysfunction remains unclear. Mgrn1 is an E3 ubiquitin-protein ligase that interacts with cytosolically exposed of the prion protein and this interaction has been shown to alter the subcellular localization of Mgrn1 [27]. Although there is evidence that Mgrn1 mutant mice exhibit mitochondrial dysfunction and oxidative stress prior to the onset of neurodegeneration [28], the role of Mgrn1 in regulating mitochondrial health remained undefined. In this study, we determined that Mgrn1 is primarily localized to mitochondria. Mgrn1 contains a putative *N*-myristoylation motif, which we show is required for mitochondrial localization and targets Mgrn1 to the OMM.

Mgrn1 is not unique in the fact that *N*-myristoylation targets the protein to interact with the OMM [43-45]; however, the precise mechanisms that target Mgrn1 to the OMM

as opposed to other membranous structures remain unclear. Aside from mitochondrial membranes, it has been shown that *N*-myristoylation can also target proteins to the ER [46,47], plasma membrane [48-52], and endosomes [47,53]. So in theory, *N*-myristoylation may also be required for localization to early endosomes. From our immunocytochemistry confocal microscopic analysis, it appears Mgrn1G2A-myc is completely cytosolic, and is unlikely to be significantly localized to early endosomes. Potentially, in order for Mgrn1 to localize to early endosomes, the protein must be *N*-myristoylated and also interact with TSG101. In the same token, an interaction between Mgrn1 and a mitochondrial substrate protein may drive mitochondrial localization. At this point, the precise requirements for early endosome localization or mitochondrial localization remain unclear. It is critical to understand the individual contributions of endosomally-localized Mgrn1 and mitochondrially-localized Mgrn1 to neuroprotection.

Other E3 ubiquitin protein ligases localized to the OMM have been shown to regulate mitochondrial dynamics [22,54,55]. We observed elongation and ballooning of the mitochondrial network while overexpressing WT Mgrn1, suggesting that Mgrn1 regulates mitochondrial morphology. Interestingly, *N*-myristoylation, and therefore, mitochondrial localization and E3 ubiquitin-protein ligase activity are required for Mgrn1-mediated mitochondrial elongation. This suggests that Mgrn1-mediated ubiquitination of a mitochondrial substrate causes mitochondrial elongation. In addition, we observed mitochondrial fragmentation in Mgrn1 mutant neurons, suggesting that loss of Mgrn1 results in dysregulation of mitochondrial dynamics. Taken together, this likely suggests that Mgrn1 promotes mitochondrial fusion or inhibits fission through the ubiquitination of a mitochondrial substrate. At this point, we cannot say for certain if

Mgrn1 positively regulates fusion or negatively regulates fission. In order to determine the precise function of Mgrn1, a mitochondrial substrate should be identified. Then the ubiquitin linkage and ultimate fate of the substrate following Mgrn1-mediated ubiquitination should be determined. Elucidation of the precise role of Mgrn1 in the regulation of the mitochondrial network is important to determining the role of Mgrn1 in mitochondrial health and neuroprotection. In addition, the effect of Mgrn1 expression on the individual rates of mitochondrial fusion and fission should be examined.

We observed defects in mitochondrial ultrastructure in the brains of Mgrn1 mutant mice compared to their wild type controls. Since mitochondrial structure is tightly tied to its functions, defects in mitochondrial structure likely affect mitochondrial activity. It is likely that the discontinuous cristae and defects in cristae structure can affect mitochondrial transport via the electron transport chain [56]. This might support the previously published data that Mgrn1 mutant mice have defects in the ETC and reduced ATP production [28]. Taken together, this suggests that loss of Mgrn1-mediated regulation of the mitochondrial network can cause the mitochondrial dysfunction observed in Mgrn1 mutant mice. Because cytochrome *c* resides in the intercrisatiae space and the mitochondrial cristae are disorganized in Mgrn1 mutant mouse brains, there may be uncontrolled cytochrome *c* release. This could lead to aberrant apoptotic signaling in Mgrn1 mutant mouse brains, resulting in neurodegeneration. Taken together, defects in mitochondrial ultrastructure may further clarify the role of mitochondrial dysfunction in cell death and the pathogenesis of spongiform neurodegeneration in Mgrn1 mutant mice.

Our data suggest that Mgrn1 plays a direct role in regulating mitochondrial dynamics and health in response to mitochondrial stress. Therefore, loss of Mgrn1 can

cause loss of the mechanisms mitochondria require to respond to stress. As a result, Mgrn1 mutant mice are more susceptible to age related mitochondrial stresses and suffer spongiform neurodegeneration. Future studies to identify mitochondrial substrate(s) of Mgrn1-mediated ubiquitination and understand Mgrn1-mediated alterations in mitochondrial morphology should provide additional understanding to the role of Mgrn1 in regulating mitochondrial health and in protection from spongiform neurodegeneration.

Materials and Methods

Expression constructs and antibodies

Human Mgrn1cDNA was obtained from Kasuza DNA institute (Chiba, Japan). Mgrn1 was subsequently subcloned into various modified expression vectors including with tags such as myc, HA, and FLAG. Mgrn1G2A and Mgrn1mtE3 were constructed using PCR and subcloned into modified expression vectors with myc, HA, and FLAG tags.

Polyclonal antibodies were generated against synthetic peptides corresponding to amino acid residues 255-283 of human Mgrn1 (anti-Mgrn1 antibody). Anti-Mgrn1 was affinity purified using the antigen conjugated to a SulfoLink column (Thermo Fisher Scientific) according to the manufacturer's instructions. Anti-TOM20 (FL-145) was purchased from Santa Cruz. Antibodies against TIM23 and native cytochrome *c* (Clone 6H2.B4) were purchased from BD biosciences. Other antibodies include anti-active caspase 3 (Cell Signaling), anti-Myc (9E10.3, Neomarkers), and anti-TRAP1 (BD biosciences), SVP38

(Santa Cruz). All secondary antibodies (FITC, TRITC, and Cy5) were purchased from Jackson ImmunoResearch Laboratories, Inc.

Cell transfection and treatment

HeLa cells were cultured in Dulbecco's Modified Eagle Medium supplemented with 5% fetal bovine serum, 100 IU/ml penicillin, and 100 mg/ml streptomycin. HeLa cells were transfected with the indicated plasmids using Lipofectamine 2000 (Invitrogen) by following the manufacturer's instructions. For analysis of the role of Mgrn1 in cytoprotection, cells were either untreated or treated for 24 hours with 100 nM rotenone. purchased from Sigma-Aldrich.

Mgrn1 mutant mice and primary cell cultures

Mgrn1 mutant mice (*Mgrn1^{md-nc}*) were obtained from Dr. Gregory Barsh of Stanford University, who originally obtained the mice from the Frozen Embryo and Sperm Archive at the Harwell Mammalian Genetics Unit (Harwell, UK). Colonies are maintained through heterozygote breeding; however, homozygote breeding is performed for primary culture of cortical neurons. Genotypes of animals were determined by PCR. Primary cortical neurons were harvested from embryonic day 18 (E18) from wild type and Mgrn1 mutant mice as described previously [57,58]. Cells were plated on poly-L-lysine coated 35mm glass bottom dishes (MatTek, Ashland, MA). Neurons were cultured in Neurobasal Media (Invitrogen) supplemented with 0.5 mM L-glutamine, B27 (Invitrogen), 100 IU/ml penicillin, and 100 mg/ml streptomycin. Neurons were

transfected with the indicated constructs on day *in vitro* 4 using Lipofectamine 2000 (Invitrogen).

Hematoxylin and eosin staining

Blocks of the cortex from 12-month-old wild type and *Mgrn1* mutant mice were fixed for 48 hours in 4% paraformaldehyde and embedded in paraffin. Paraffin-embedded blocks were cut into 8 μ m sections. Sections were stained with hematoxylin-eosin (H&E) and mounted on slides. Whole slides were scanned using Nanozoomer (Hamamatsu) and compiled as tifs. Images were acquired using Aperio Spectrum.

Immunofluorescence confocal microscopy

Cells were fixed in 4% paraformaldehyde (Electron Microscopy Sciences) and were processed as described previously [59]. In brief, cells were fixed with 4% paraformaldehyde in culture media for 10 min, permeabilized with a solution containing 0.1% saponin (Sigma-Aldrich) and 2% horse serum (Lonza) in 1 \times PBS, stained with the indicated primary antibodies followed by secondary antibodies conjugated to FITC, TRITC, or Cy5 (Jackson ImmunoResearch Laboratories, Inc.), and then mounted in ProLong Gold antifade reagent with DAPI (Life Technologies) as directed by the manufacturer. For immunofluorescence confocal microscopic analyses, cell images were acquired in room temperature with a confocal microscope (Eclipse Ti; Nikon) equipped with Plan-Apochromat 40 \times /1.3 NA or 60 \times /1.4 NA oil immersion objective lenses; filter sets for FITC, TRITC, DAPI, and Cy5; and the EZ-C1 acquisition software (Nikon). For oil immersion, type A immersion oil (Nikon) was used. The acquired 16-bit RGB images

were converted into 8-bit RGB images with the EZ-C1 acquisition software (Nikon), and the brightness was adjusted using Volocity Software (Perkin-Elmer). Figures were compiled using Photoshop CS4 software (Adobe Systems).

3D-Structured illumination microscopy

HeLa cells were transfected as indicated, fixed in 4% PFA in culture media and permeabilized with 0.1% saponin as described in the previous section. Images were acquired at room temperature using a CFI Apo TIRF 100x oil immersion lens (N.A. 1.49), CCD camera (DU-897; Nikon), Perfect Focus System, and SIM Illuminator (Nikon Instruments Inc., Melville, NY) using 488 and 561 lasers. All images were acquired and reconstructed using NIS Elements software. Image stacks were acquired in 100 nm intervals for 8-15 Z planes. In each plane, 15 images were acquired with a rotating illumination pattern (5 phases, 3 angles) in 488 and 561 channels independently. The series of images were reconstructed using NIS-Elements software to yield an image with resolution beyond the limit of diffraction. Each image represents a single Z section of a three dimensional image and measurements were performed on the image shown. Brightness was adjusted using NIS-Elements software (Nikon Instruments) and figures were compiled using Photoshop CS4 software (Adobe Systems).

Purification of mitochondria

To purify mitochondria, cells were pelleted at 500g for 5 minutes and were resuspended in buffer containing 250 mM sucrose, 20 mM Hepes, 10 mM KCl, 1.5 mM MgCl₂, 0.1 mM EDTA, and 1 mM EGTA, pH 7.5. Cell suspension was dounced 30 times in a loose

dounce. Unbroken cells and nuclei were pelleted at 1000g for 5 minutes. The resulting supernatant was centrifuged at 10,000g for 15 minutes to pellet mitochondria. The mitochondrial pellet was washed 3 times in subsequent 15-minute 10000g spins, in the previously mentioned buffer. Cytosolic and mitochondrial fractions were subjected to SDS-PAGE and western blotting. Briefly, protein extracts were prepared in 1.1% SDS, and extracts were subjected to SDS-PAGE electrophoresis and transferred to nitrocellulose membranes. Blots were incubated in 5% milk in TBST with the indicated primary antibodies and horseradish peroxidase-conjugated secondary antibodies. Antibody binding to the nitrocellulose membrane was detected using ECL.

Live imaging of mitochondria

Primary cortical neurons were incubated with the indicated dye for 30 minutes, followed by two washes, and 30 minutes at 37°C to allow for equilibration, removal of excess dye, and stabilization of mitochondrial morphology as described previously [39]. Concentrations used were as follows: MitoTracker green (Invitrogen, M7514): 20nM and tetramethylrhodamine (TMRE) (Invitrogen, T-669): 600nM. Cells were placed on a temperature and CO₂ controlled stage and images were captured using an inverted confocal microscope (C-1, Nikon Instruments) with a 40x or 60x oil immersion objective. For all neuronal experiments, images are maximum projections, and mitochondrial length measurements were performed on these maximum projections. For experiments with TMRE staining, the same laser power, gain, and pinhole size was the same between samples. In addition, all manipulations to these images (such as enhancing contrast for better visual results) were consistent between wild type and Mgrn1 mutant samples.

Mitochondria were depolarized by incubation with 20 μ M carbonyl cyanide m-chlorophenyl hydrazone (CCCP) for 2h at 37°C.

Perfusion of mice and electron microscopy

Wild type and Mgrn1 mutant mice of 12 months of age were perfusion fixed with 2.5% glutaraldehyde buffered with 0.1M sodium phosphate (pH 7.2). Fixative was delivered at the rate of 10mL/min. Brains were removed from the skulls, and stored overnight in the same fixative to insure complete fixation. With a vibrating microtome, the fixed brain was sliced into 100 μ M sections. Sections were washed in the same buffer and post-fixed in 1% buffered osmium tetroxide and subsequently dehydrated through a graded ethanol series to 100%. Dehydrated sections were flat embedded in Eponate 12 resin (Ted pella In, Redding, CA). The embedded sections containing cortex were cut out and re-embedded in resin for ultrathin sectioning on a Leica UC6rt ultramicrotome (Leica Microsystems, Bannockburn, IL) and 70 nm. Sections were counter-stained with 4% aqueous uranyl acetate and 2% lead citrate. Sections were examined using a Hitachi H-7500 transmission electron microscope (Hitachi High Technologies of America, Inc., Pleasanton, CA) and a Gatan BioScan CCD camera.

Cell viability and apoptosis assays

Wild type and Mgrn1 mutant primary cortical neurons were transfected with Mgrn1-myc, Mgrn1G2A-myc, of Mgrn1mtE3-myc using Lipofectamine2000 (Invitrogen) for 24 hours and treated with 100 nM rotenone for the following 24 hours, and subsequently fixed in 4% paraformaldehyde and stained with labeled with caspase 3 and myc (9E10) (red).

Nuclei were stained with DAPI and directly visualized for the assessment of nuclear morphology. The percentages of transfected neurons with active caspase-3 staining or apoptotic nuclei were scored as described [57,60,61]. Thirty cells were randomly selected for each of three experiments. The data shown represents the mean \pm S.E.M. for these three independent experiments. Contrast of images was adjusted using Volocity Software (Perkin-Elmer). Graphs were drawn using SigmaPlot software (Systat, Inc.) and figures were made using Photoshop CS4.

Image analysis

Quantification of colocalization

Quantification of colocalization was performed on single channel, unprocessed images. Quantification was performed on the Z plane adjacent to the coverslip interface. Using the JACOP plugin for ImageJ, the images were individually thresholded and Mander's coefficients [62,63] were determined for each condition as indicated. The percentage of overlap was quantified from 3 separate experiments. Graphs were generated with SigmaPlot 11.0 software (Systat Software, Inc.) and Photoshop CS4 software was used to produce figures.

Mitochondrial Length

Mitochondrial length in neurons was determined using the length function in NIS-Elements (Nikon Instruments). An ROI was selected of each individual cell and the software was thresholded to specifically detect mitochondria in the cell body and processes. The length of every individual mitochondrion was calculated via NIS-

Elements software length function. The data was imported into Excel (Microsoft Office Suite, Microsoft) and the average mitochondria length was determined per cell. The average mitochondrial length was determined from 30 cells per each of three independent experiments. The average mitochondrial length was then determined from each condition. Graphs were generated with SigmaPlot 11.0 software (Systat Software, Inc.) and Photoshop CS4 software was used to produce figures

Mitochondrial membrane potential

Mitochondria in wild type and *Mgrn1* mutant neurons were stained with MitoTracker Green and TMRE as described in a previous section. The laser power, pinhole, gain, and exposure time remained constant throughout all conditions and all trials of this experiment. An ROI of each individual cell was selected and total fluorescence was determined in each channel on unaltered images per each cell per condition using NIS-Elements software (Nikon Instruments). The ratio of TMRE:MitoTracker Green fluorescence was determined per cell. The average TMRE:MitoTracker Green was determined from 30 cells per each of three independent experiments. Graphs were generated with SigmaPlot 11.0 software (Systat Software, Inc.) and Photoshop CS4 software was used to produce figures.

Statistical analysis

All experiments were repeated at least three times. Data were subjected to statistical analyses by one- or two-way analysis of variance (ANOVA) with a Tukey's *post hoc* test

using the SigmaPlot software (Systat Software, Inc.) Results are expressed as mean \pm S.E.M. A *P*-value of less than 0.05 was considered statistically significant.

Acknowledgments

We thank Greg Barsh for providing the *Mgrn1* mutant mice.

This work was supported by the National Institutes of Health [GM082828 and GM103613 to L.L. and AG034126 to L.S.C.] and the Emory University Research Committee [SK38167 to L.S.C.]. We thank Emory Integrated Cellular Imaging Core Facility for providing instrumentation and support.

References

1. Whatley, B.R., et al., The ubiquitin-proteasome system in spongiform degenerative disorders. 2008. *Biochim Biophys Acta*, **1782**(12): 700-12.
2. Filosto, M., et al., The role of mitochondria in neurodegenerative diseases. 2011. *J Neurol*, **258**(10): 1763-74.
3. Olzmann, J.A., et al., Aggresome formation and neurodegenerative diseases: therapeutic implications. 2008. *Curr Med Chem*, **15**(1): 47-60.
4. Liberski, P.P., et al., Ultrastructural pathology of prion diseases revisited: brain biopsy studies. 2005. *Neuropathol Appl Neurobiol*, **31**(1): 88-96.
5. Siskova, Z., et al., Morphological and functional abnormalities in mitochondria associated with synaptic degeneration in prion disease. 2010. *Am J Pathol*, **177**(3): 1411-21.
6. Choi, S.I., et al., Mitochondrial dysfunction induced by oxidative stress in the brains of hamsters infected with the 263 K scrapie agent. 1998. *Acta Neuropathol*, **96**(3): 279-86.
7. Brown, D.R., Neurodegeneration and oxidative stress: prion disease results from loss of antioxidant defence. 2005. *Folia Neuropathol*, **43**(4): 229-43.
8. Kim, J.I., et al., Oxidative stress and neurodegeneration in prion diseases. 2001. *Ann N Y Acad Sci*, **928**: 182-6.
9. Bobba, A., et al., Alzheimer's proteins, oxidative stress, and mitochondrial dysfunction interplay in a neuronal model of Alzheimer's disease. 2010. *Int J Alzheimers Dis*, **2010**.
10. Du, H., et al., Early deficits in synaptic mitochondria in an Alzheimer's disease mouse model. 2010. *Proc Natl Acad Sci U S A*, **107**(43): 18670-5.
11. Pratico, D., Evidence of oxidative stress in Alzheimer's disease brain and antioxidant therapy: lights and shadows. 2008. *Ann N Y Acad Sci*, **1147**: 70-8.
12. Turchan, J., et al., Oxidative stress in HIV demented patients and protection *ex vivo* with novel antioxidants. 2003. *Neurology*, **60**(2): 307-14.
13. Chen, H. and D.C. Chan, Mitochondrial dynamics--fusion, fission, movement, and mitophagy--in neurodegenerative diseases. 2009. *Hum Mol Genet*, **18**(R2): R169-76.
14. Han, X.J., et al., Regulation of mitochondrial dynamics and neurodegenerative diseases. 2011. *Acta Med Okayama*, **65**(1): 1-10.
15. Alexander, C., et al., OPA1, encoding a dynamin-related GTPase, is mutated in autosomal dominant optic atrophy linked to chromosome 3q28. 2000. *Nat Genet*, **26**(2): 211-5.
16. Zuchner, S., et al., Mutations in the mitochondrial GTPase mitofusin 2 cause Charcot-Marie-Tooth neuropathy type 2A. 2004. *Nat Genet*, **36**(5): 449-51.
17. Park, J.H., et al., Association of endothelial nitric oxide synthase and mitochondrial dysfunction in the hippocampus of scrapie-infected mice. 2010. *Hippocampus*.
18. Song, Z., et al., Mitofusins and OPA1 mediate sequential steps in mitochondrial membrane fusion. 2009. *Mol Biol Cell*, **20**(15): 3525-32.

19. Harder, Z., et al., Sumo1 conjugates mitochondrial substrates and participates in mitochondrial fission. 2004. *Curr Biol*, **14**(4): 340-5.
20. Wasiak, S., et al., Bax/Bak promote sumoylation of DRP1 and its stable association with mitochondria during apoptotic cell death. 2007. *J Cell Biol*, **177**(3): 439-50.
21. Braschi, E., et al., MAPL is a new mitochondrial SUMO E3 ligase that regulates mitochondrial fission. 2009. *EMBO Rep*, **10**(7): 748-54.
22. Li, W., et al., Genome-wide and functional annotation of human E3 ubiquitin ligases identifies MULAN, a mitochondrial E3 that regulates the organelle's dynamics and signaling. 2008. *PLoS One*, **3**(1): e1487.
23. He, L., et al., Spongiform degeneration in mahoganoid mutant mice. 2003. *Science*, **299**(5607): 710-2.
24. Kim, B.Y., et al., Spongiform neurodegeneration-associated E3 ligase Mahogunin ubiquitylates TSG101 and regulates endosomal trafficking. 2007. *Mol Biol Cell*, **18**(4): 1129-42.
25. Cooray, S.N., et al., The E3 ubiquitin ligase Mahogunin ubiquitinates the melanocortin 2 receptor. 2011. *Endocrinology*, **152**(11): 4224-31.
26. Srivastava, D. and O. Chakrabarti, Mahogunin-mediated alpha-tubulin ubiquitination via noncanonical K6 linkage regulates microtubule stability and mitotic spindle orientation. 2014. *Cell Death Dis*, **5**: e1064.
27. Chakrabarti, O. and R.S. Hegde, Functional depletion of mahogunin by cytosolically exposed prion protein contributes to neurodegeneration. 2009. *Cell*, **137**(6): 1136-47.
28. Sun, K., et al., Mitochondrial dysfunction precedes neurodegeneration in mahogunin (*Mgrn1*) mutant mice. 2007. *Neurobiol Aging*, **28**(12): 1840-52.
29. Phan, L.K., et al., The mouse mahoganoid coat color mutation disrupts a novel C3HC4 RING domain protein. 2002. *J Clin Invest*, **110**(10): 1449-59.
30. Lampert, P.W., et al., Experimental spongiform encephalopathy (Creutzfeldt-Jakob disease) in chimpanzees. Electron microscopic studies. 1971. *J Neuropathol Exp Neurol*, **30**(1): 20-32.
31. Mancardi, G.L., et al., Spongiform-like changes in Alzheimer's disease. An ultrastructural study. 1982. *Acta Neuropathol*, **56**(2): 146-50.
32. Perez-Oliva, A.B., et al., Mahogunin ring finger-1 (MGRN1) E3 ubiquitin ligase inhibits signaling from melanocortin receptor by competition with Galphas. 2009. *J Biol Chem*, **284**(46): 31714-25.
33. Jiao, J., et al., Transgenic analysis of the physiological functions of Mahogunin Ring Finger-1 isoforms. 2009. *Genesis*, **47**(8): 524-34.
34. Lee, Y.J., et al., Roles of the mammalian mitochondrial fission and fusion mediators Fis1, Drp1, and Opa1 in apoptosis. 2004. *Mol Biol Cell*, **15**(11): 5001-11.
35. Itoh, K., et al., Mitochondrial dynamics in neurodegeneration. 2013. *Trends Cell Biol*, **23**(2): 64-71.
36. Cho, D.H., et al., Mitochondrial dynamics in cell death and neurodegeneration. 2010. *Cell Mol Life Sci*, **67**(20): 3435-47.
37. Lu, B., Mitochondrial dynamics and neurodegeneration. 2009. *Curr Neurol Neurosci Rep*, **9**(3): 212-9.

38. Chan, D.C., Mitochondrial fusion and fission in mammals. 2006. *Annu Rev Cell Dev Biol*, **22**: 79-99.
39. Mitra, K. and J. Lippincott-Schwartz, Analysis of mitochondrial dynamics and functions using imaging approaches. 2010. *Curr Protoc Cell Biol*, **Chapter 4**: Unit 4 25 1-21.
40. Sandbach, J.M., et al., Ocular pathology in mitochondrial superoxide dismutase (Sod2)-deficient mice. 2001. *Invest Ophthalmol Vis Sci*, **42**(10): 2173-8.
41. Baloyannis, S.J., Mitochondrial alterations in Alzheimer's disease. 2006. *J Alzheimers Dis*, **9**(2): 119-26.
42. Chhangani, D. and A. Mishra, Mahogunin ring finger-1 (MGRN1) suppresses chaperone-associated misfolded protein aggregation and toxicity. 2013. *Sci Rep*, **3**: 1972.
43. Borgese, N., et al., A role for N-myristoylation in protein targeting: NADH-cytochrome b5 reductase requires myristic acid for association with outer mitochondrial but not ER membranes. 1996. *J Cell Biol*, **135**(6 Pt 1): 1501-13.
44. Utsumi, T., et al., C-terminal 15 kDa fragment of cytoskeletal actin is posttranslationally N-myristoylated upon caspase-mediated cleavage and targeted to mitochondria. 2003. *FEBS Lett*, **539**(1-3): 37-44.
45. Bentham, M., et al., Role of myristoylation and N-terminal basic residues in membrane association of the human immunodeficiency virus type 1 Nef protein. 2006. *J Gen Virol*, **87**(Pt 3): 563-71.
46. Colombo, S., et al., N-myristoylation determines dual targeting of mammalian NADH-cytochrome b5 reductase to ER and mitochondrial outer membranes by a mechanism of kinetic partitioning. 2005. *J Cell Biol*, **168**(5): 735-45.
47. Santonico, E., et al., Multiple modification and protein interaction signals drive the Ring finger protein 11 (RNF11) E3 ligase to the endosomal compartment. 2010. *Oncogene*, **29**(41): 5604-18.
48. Hermida-Matsumoto, L. and M.D. Resh, Localization of human immunodeficiency virus type 1 Gag and Env at the plasma membrane by confocal imaging. 2000. *J Virol*, **74**(18): 8670-9.
49. Song, K.S., et al., Targeting of a G alpha subunit (Gi1 alpha) and c-Src tyrosine kinase to caveolae membranes: clarifying the role of N-myristoylation. 1997. *Cell Mol Biol (Noisy-le-grand)*, **43**(3): 293-303.
50. Koutelou, E., et al., Neuralized-like 1 (Neurl1) targeted to the plasma membrane by N-myristoylation regulates the Notch ligand Jagged1. 2008. *J Biol Chem*, **283**(7): 3846-53.
51. Baticic, O., et al., Dual fatty acyl modification determines the localization and plasma membrane targeting of CBL/CIPK Ca²⁺ signaling complexes in Arabidopsis. 2008. *Plant Cell*, **20**(5): 1346-62.
52. Rowe, D.C., et al., The myristoylation of TRIF-related adaptor molecule is essential for Toll-like receptor 4 signal transduction. 2006. *Proc Natl Acad Sci U S A*, **103**(16): 6299-304.
53. McCabe, J.B. and L.G. Berthiaume, Functional roles for fatty acylated amino-terminal domains in subcellular localization. 1999. *Mol Biol Cell*, **10**(11): 3771-86.

54. Tang, F., et al., RNF185, a novel mitochondrial ubiquitin E3 ligase, regulates autophagy through interaction with BNIP1. 2011. *PLoS One*, **6**(9): e24367.
55. Nagashima, S., et al., Roles of mitochondrial ubiquitin ligase MITOL/MARCH5 in mitochondrial dynamics and diseases. 2014. *J Biochem*, **155**(5): 273-9.
56. Zick, M., et al., Cristae formation-linking ultrastructure and function of mitochondria. 2009. *Biochim Biophys Acta*, **1793**(1): 5-19.
57. Chen, J., et al., Parkinson disease protein DJ-1 converts from a zymogen to a protease by carboxyl-terminal cleavage. 2010. *Hum Mol Genet*, **19**(12): 2395-408.
58. Giles, L.M., et al., Dystonia-associated mutations cause premature degradation of torsinA protein and cell-type-specific mislocalization to the nuclear envelope. 2008. *Hum Mol Genet*, **17**(17): 2712-22.
59. Olzmann, J.A., et al., Parkin-mediated K63-linked polyubiquitination targets misfolded DJ-1 to aggresomes via binding to HDAC6. 2007. *J Cell Biol*, **178**(6): 1025-38.
60. Young, J.E., et al., Polyglutamine-expanded androgen receptor truncation fragments activate a Bax-dependent apoptotic cascade mediated by DP5/Hrk. 2009. *J Neurosci*, **29**(7): 1987-97.
61. Sherer, T.B., et al., Subcutaneous rotenone exposure causes highly selective dopaminergic degeneration and alpha-synuclein aggregation. 2003. *Exp Neurol*, **179**(1): 9-16.
62. Bolte, S. and F.P. Cordelieres, A guided tour into subcellular colocalization analysis in light microscopy. 2006. *J Microsc*, **224**(Pt 3): 213-32.
63. Rodal, A.A., et al., A presynaptic endosomal trafficking pathway controls synaptic growth signaling. 2011. *J Cell Biol*, **193**(1): 201-17.

FIGURES AND LEGENDS

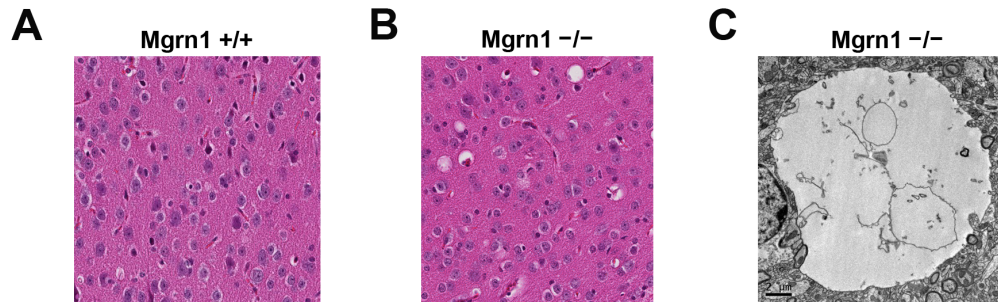


Figure III-1: Neuropathology of Mgrn1 mutant mice. (A, B) Hematoxylin and eosin-stained brain sections from the cortical region of 12 month old wild type (A) and Mgrn1 mutant (B) mice illustrating spongiform neurodegeneration in mice lacking Mgrn1 expression. (C) Vacuolar ultrastructure from the cortex of Mgrn1 mutant mice. Observed is a vacuole containing curled membrane fragments. Scale bars (A, B) 25 μm . Scale bar (C) 2 μm .

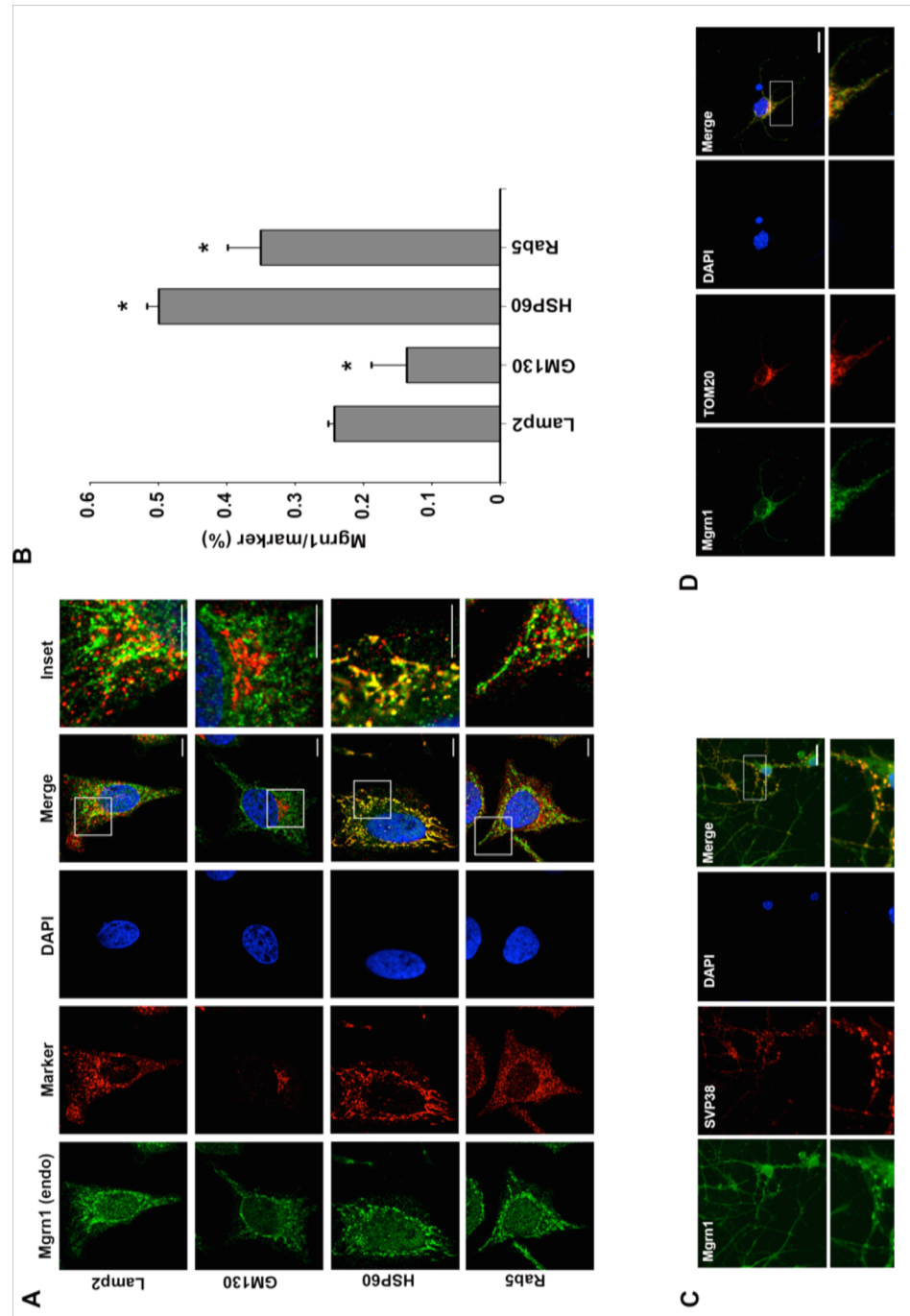


Figure III-2: Endogenous localization of Mgrn1. (A) HeLa cells were double-immunostained using an anti-Mgrn1, anti-Lamp2, anti-GM130, anti-HSP60, and anti-Rab5 antibodies. Scale bar, 10 μ m. (B) Quantification of Mgrn1 localization in HeLa

cells. Images were processed and analyzed as described in the Materials and Methods section. The percentage of overlap between Mgrn1 and the indicated marker is represented as the average \pm S.E.M. *, $P < 0.05$. (C) Mgrn1 is expressed in the cell body and processes of neurons and partially colocalizes with presynaptic markers. (D) Endogenous Mgrn1 partially colocalizes with mitochondrial marker in neurons. Scale bar, 10 μ m.

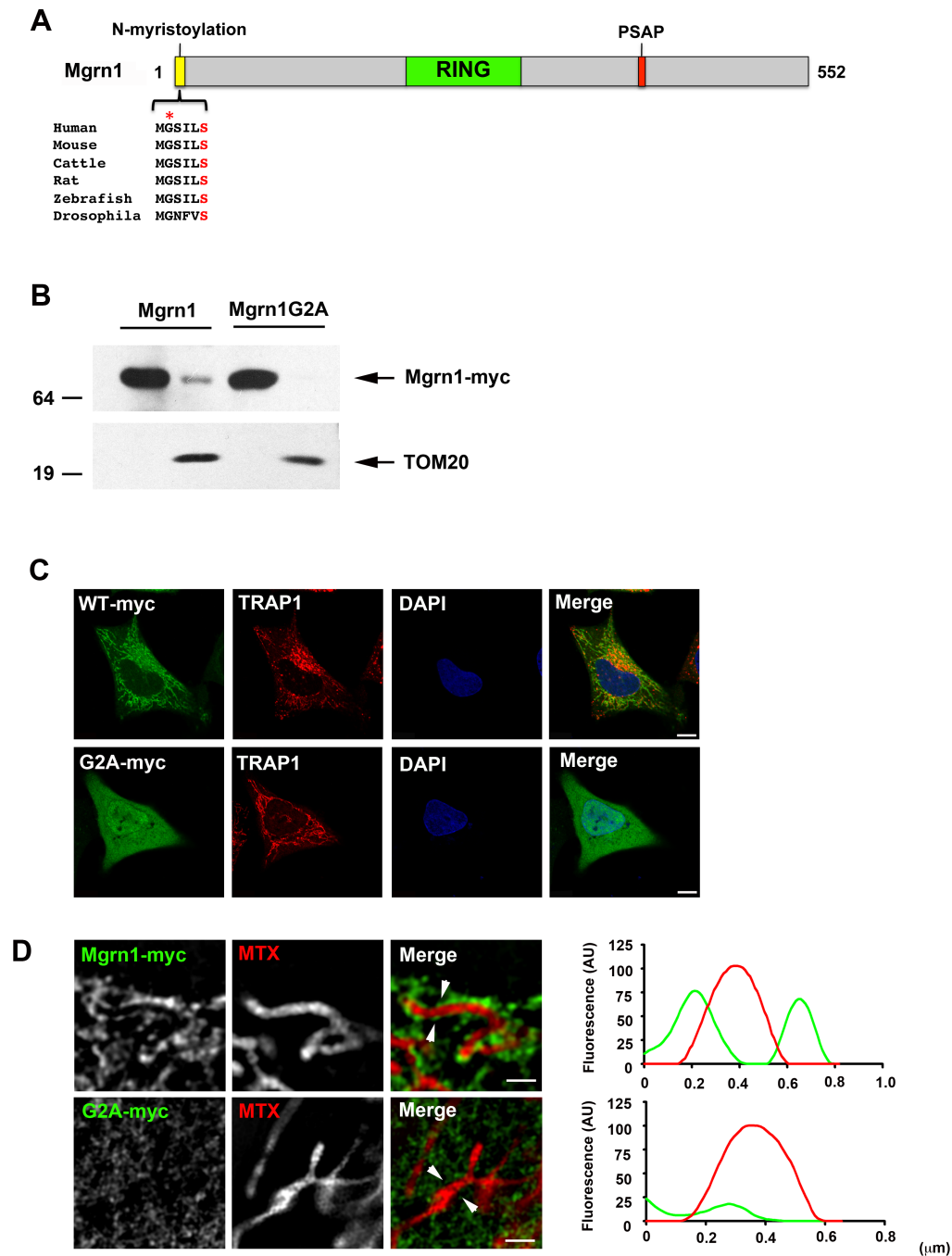


Figure III-3: *N*-myristoylation targets Mgrn1 to the outer mitochondrial membrane.

(A) Sequence alignment of the N-terminal region of Mgrn1. Residues implicated in *N*-myristoylation are indicated in red. The asterisk indicates the glycine residue in which myristic acid is conjugated. (B) Cytosol/mitochondria fractionations indicating that

Mgrn1-myc and not Mgrn1G2A-myc is partially localized to the mitochondria. (C) Immunofluorescence confocal microscopic analysis of HeLa cells transfected with Mgrn1-myc or Mgrn1G2A-myc and stained with an antibody against the mitochondrial protein, TRAP1. This shows mitochondrial localization of Mgrn1-myc and cytosolic localization of Mgrn1G2A-myc. (D) Dual color 3D-SIM fluorescence imaging analysis of HeLa transfected with Mgrn1-myc and Mgrn1G2A-myc cells labeled with the mitochondrial matrix marker mito-dsRed (MTX) and stained with an anti-myc antibody (9E10). Scale bars, 10 μm (C) or 1 μm (D). Line scans were acquired using ImageJ and indicate the fluorescence intensity of each signal over a line (AU). Arrowheads indicate where the line was drawn through the mitochondrion.

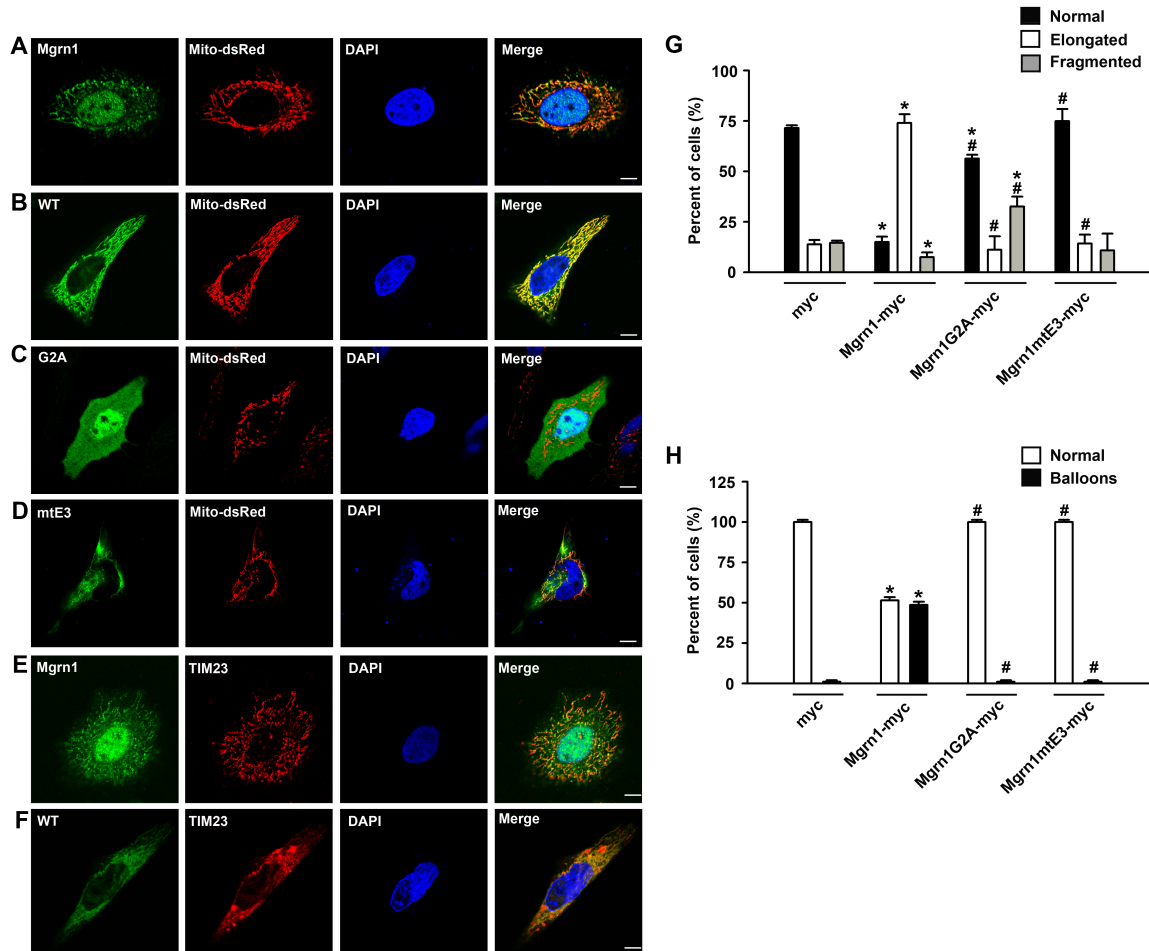


Figure III-4: Overexpression of Mgrn1 promotes mitochondrial elongation.

(A-E) HeLa cells transfected with Mgrn1-myc, Mgrn1G2A-myc, or Mgrn1mtE3 were stained with antibodies against the mitochondrial marker, TOM20 or transfected with the mitochondrial matrix marker, Mito-dsRed. Cells were stained with anti-myc (9E10) to detect transfected cells. Immunofluorescence confocal microscopic analysis shows that overexpression of Mgrn1-myc (B, F) but not Mgrn1G2A-myc (C) or Mgrn1mtE3-myc (D) promotes mitochondrial elongation compared to untransfected (A, E). Scale bars, 10

μm . (G) Number of cells with observed mitochondrial phenotypes: normal, elongated, or fragmented. (H) Number of cells with mitochondrial balloon phenotype. Data represent mean \pm SEM (error bars; $n = 75\text{-}90$ mitochondria) from three independent experiments. *, $P < 0.05$ versus the corresponding untransfected control; #, $P < 0.05$ versus the corresponding wild type overexpressing control, two-way analysis of variance with a Tukey's *post hoc* test.

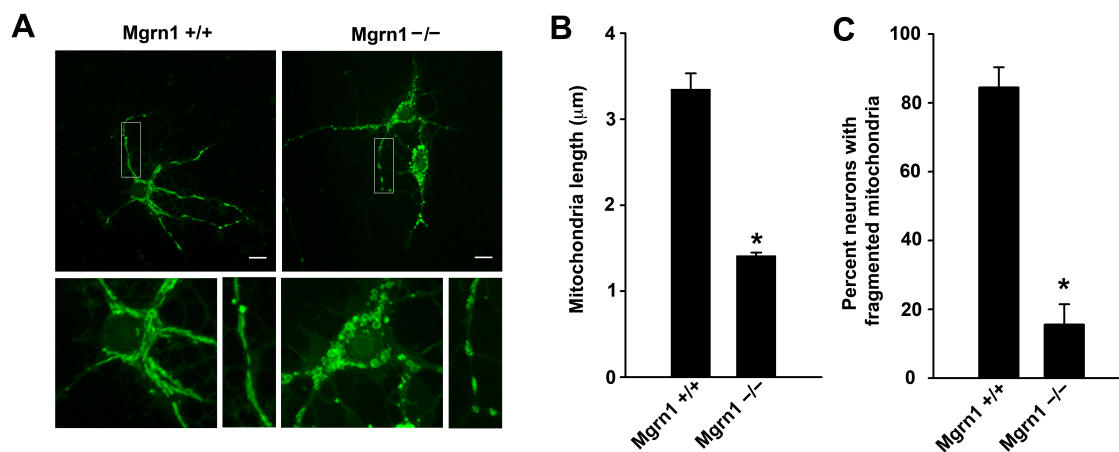


Figure III-5: Loss of Mgrn1 expression affects mitochondrial morphology

(A) Cortical neurons cultured from wild type and Mgrn1 mutant mouse embryos were stained with Mitotracker Green and directly imaged using live cell confocal microscopy. Fluorescence confocal imaging analysis was performed on wild type and Mgrn1 mutant cortical neurons. Scale bars, 10 μm . (B) Quantification of the average mitochondrial length per cell. (C) Quantification of the percent of neurons that exhibit fragmented mitochondria. Error bars = \pm S.E.M. *, $P < 0.05$ one-way ANOVA with a Tukey's *post hoc* test.

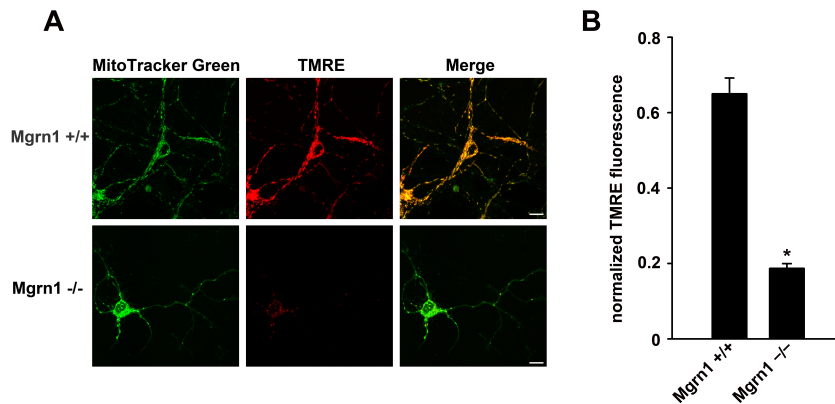


Figure III-6: Mgrn1 mutant neurons exhibit reduced mitochondrial membrane potential. Cortical neurons from wild type and Mgrn1 mutant mice were cultured from mouse embryos and were stained with mitochondrial markers Mitotracker Green and TMRE. The microscope settings and image adjustments were all kept consistent throughout the experiment between both sets of cells. (A) TMRE and MitoTracker Green fluorescence in wild type and Mgrn1 mutant cortical neurons. Scale bars, 10 μ m. (B) Quantification of mitochondrial membrane potential in wild type and Mgrn1 mutant neurons. The fluorescence intensity was measured for each channel (red and green) of each individual cell. The TMRE fluorescence for each cell was normalized to MitoTracker Green fluorescence. Error bars = \pm S.E.M. *, $P < 0.05$ one-way ANOVA with a Tukey's *post hoc* test.

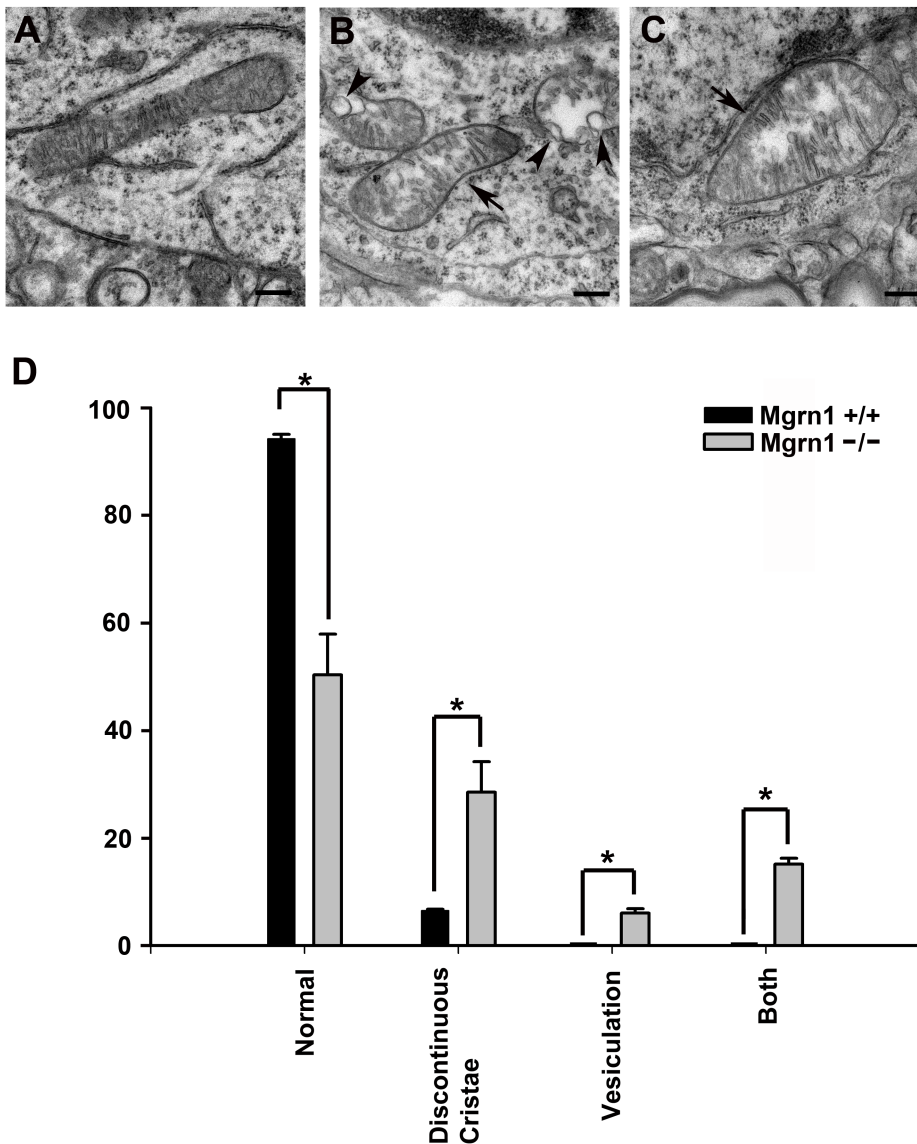


Figure III-7: Mitochondrial ultrastructural defects observed in aged *Mgrn1* mutant mouse brains. Perfusion fixed cortices from 12-month-old wild type (A) and *Mgrn1* mutant (B,C) mice were subjected to negative staining and electron microscopy. (A) Mitochondria in wild type mouse maintained a regular structure. (B) Mitochondria in *Mgrn1* mutant mouse brains were observed with discontinuous cristae (arrows) and vesiculation (arrowheads). (D) Quantification of mitochondrial abnormalities in wild type

and Mgrn1 mutant mice. Error bars = \pm S.E.M. *, $P < 0.05$ one-way ANOVA with a Tukey's *post hoc* test

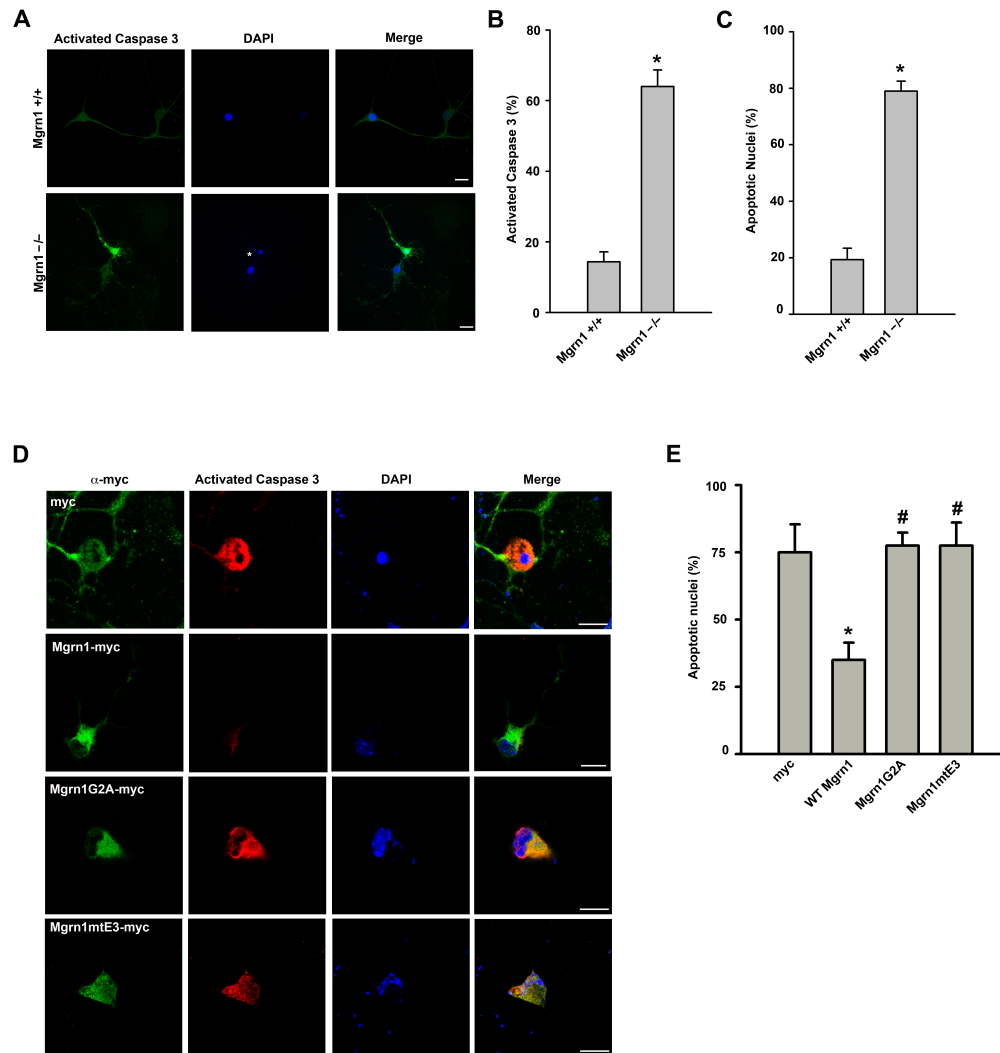


Figure III-8: Mitochondrially localized Mgrn1 is cytoprotective against oxidative stress and mitochondrial dysfunction

Cortical neurons from wild type and Mgrn1 mutant mice were primary cultured from mouse embryos and treated with 100 nM rotenone. (A) Cells were fixed 24 hours after

treatment and analyzed for caspase 3 cleavage and apoptotic nuclei. Scale bars, 10 μm . (B) Quantification of caspase 3 cleavage. Cells were scored according to the presence of caspase 3 staining. (C) Quantification of apoptotic nuclei in rotenone treated wild type and Mgrn1 mutant primary cortical neurons. Cells were scored on whether their nuclei were apoptotic (condensed or fragmented) or normal. (D) Mgrn1 mutant cortical neurons were transfected with myc vector, Mgrn1-myc, Mgrn1G2A-myc, and Mgrn1mE3-myc constructs. After 24 hours transfection, cells were treated with 100 nM rotenone. (E) Quantification of apoptotic nuclei in Mgrn1 mutant cortical neurons transfected with myc vector, Mgrn1-myc, Mgrn1G2A-myc, and Mgrn1mE3-myc and treated with rotenone. Cells were scored on whether their nuclei were apoptotic (condensed or fragmented) or normal. Error bars = \pm S.E.M. *, $P < 0.05$ one-way ANOVA with a Tukey's *post hoc* test.

CHAPTER IV

DISCUSSION AND FUTURE DIRECTIONS

Summary of Findings

In this dissertation, I investigated the role and targeting of two proteins implicated in regulating mitochondrial health related to neurodegenerative diseases. Using super-resolution, 3D-Structured Illumination Microscopy (3D-SIM) I was able to better define the spatiotemporal dynamics of two proteins as they function to regulate mitochondrial health. The findings presented in chapters II-III demonstrate:

1. Using 3D-SIM, I show that PINK1 is dual-targeted to the inner mitochondrial membrane (IMM) or outer mitochondrial membrane (OMM) depending on the health of mitochondria so that PINK1 can differentially colocalize with two substrates. Mistargeting of PD-linked mutations of PINK1 suggests incorrect submitochondrial localization of PINK1 may be implicated in disease.
2. Mgrn1, a spongiform neurodegeneration-linked E3 ubiquitin-protein ligase, is targeted to mitochondria via *N*-myristoylation where it regulates mitochondrial dynamics and protects against mitochondrial dysfunction and cell death.

These findings contribute to a better understanding of mitochondrial signaling in mitochondrial health and disease. Provided in this section is a discussion of the implications of these findings.

PINK1 DISCUSSION AND FUTURE DIRECTIONS

3D-SIM analyses provide insights into PINK1 spatiotemporal dynamics

3D-SIM can differentiate submitochondrial compartments

As our understanding of the mechanisms underlying mitochondrial health and dynamics grows and we are faced with more difficult questions to elucidate the role of mitochondrial dysfunction in disease, the methods by which we study mitochondria have mostly remained unchanged. Mitochondrial functions are highly compartmentalized, so correct identification of the submitochondrial localization of proteins is essential to characterizing their function and role in mitochondrial health.

The two most commonly used methods to study the localization of mitochondrial proteins, transmission electron microscopy (TEM) coupled with immunogold labeling and biochemical subcellular and submitochondrial fractionation, were first described in 1971 and 1968, respectively [1,2]. While much has been learned from the utilization of these techniques, they each have limitations and caveats. The lack of further technique development to study substructures within mitochondria is causing the field to remain stagnant and ambiguous. As more diseases are linked to mitochondrial dysfunction, it will be difficult to achieve breakthrough findings without the development of new methods.

There are several reasons why artifacts arise from TEM/immunogold labeling linked to the fixation and labeling of samples and interpretation of results. To examine

the submitochondrial localization of proteins, researchers must balance fixation to preserve ultrastructures while still achieving robust labeling. The harsh fixation conditions required for the preservation of mitochondrial ultrastructure reduce the antigenicity of proteins, making immunolabeling much less efficient. There is a limit to the number of proteins that can be examined at one time resulting in the lack of a control within the same mitochondrial compartment. Using TEM without a geographic control, results can easily be misinterpreted. Moreover, without a geographic control, there are few ways to quantitatively analyze the data obtained. Instead, the electron dense nature of mitochondrial membranes is used to interpret where labeled proteins of interest are located. However, in many disease states, mitochondrial ultrastructure is severely impacted, making it difficult to visually identify submitochondrial compartments.

Subcellular and submitochondrial fractionation has been performed extensively since its development; however, biochemical fractionations have consistently produced conflicting results. Biochemical fractionation relies on the lysing of membranes with detergents or physical or osmotic stress coupled with centrifugation to separate the components. Cells are lysed and the cytosol is separated from heavy organelles based on differential density. The majority of studies use this resulting fraction as a “crude mitochondrial fraction” although this mixture also contains lysosomes, the ER, and other membranous structures. If your protein of interest is localized to multiple organelles, the interpretation of subsequent submitochondrial fractionations can be quite confusing. While most people use the crude mitochondrial fraction to represent mitochondria, some use mitochondria that have been further purified using a gradient. The mitochondrial membranes are lysed in two steps and mixtures are subjected to centrifugation to separate

membranous structures from aqueous compartments. Throughout this procedure, there are several steps that can result in contamination from incomplete separation of compartments or incomplete or excessive lysing of membranes. The harsh conditions required to lyse membranes and separate cellular compartments damage mitochondria, which can affect protein localization [3]. In addition, the amount of starting material required for submitochondrial fractionations is limiting.

We show that super-resolution fluorescence microscopy, specifically 3D-SIM, can differentiate submitochondrial compartments without many of the challenges of other methods. Fluorescent markers can be used to indicate the submitochondrial compartments providing researchers with additional controls and more options for quantification than TEM. In addition to immunostaining with fluorophore conjugated antibodies, fluorescent-tagged fusion proteins or organelle specific dyes can also be used to detect proteins and mitochondrial structures providing additional options for visualization. Cells can be gently fixed so as not to affect the mitochondrial ultrastructure, health, or network so results obtained are more physiologically relevant. Because 3D-SIM can be performed with limited starting material, there are many applications in which 3D-SIM would be a better option than biochemical fractionation.

In this study, we demonstrated that 3D-SIM has the resolution capacity required to analyze the spatial dynamics of proteins within the mitochondria. Although super-resolution microscopy, or techniques in fluorescence microscopy yielding a level of resolution beyond the limit of diffraction, has been described in detail for 10 years, there are limited applications of these methods described in the literature. 3D-SIM can achieve a lateral resolution of about 100 nm and an axial resolution of less than 300 nm,

approximately a 2-fold increase in resolution compared to confocal microscopy [4]. Because the average width of a mitochondrion in mammalian cells is between 0.5 to 1.0 μm divided amongst the 4 submitochondrial compartments, the resolution provided by 3D-SIM is sufficient to study substructures within the mitochondria.

We were able to differentiate markers of the individual submitochondrial compartments: the outer mitochondrial membrane (OMM), intermembrane space (IMS), inner mitochondrial membrane (IMM.), and mitochondrial matrix. In addition, we could also tell the difference between the subdomains of the IMS and IMM. Specifically, we could distinguish between the inner boundary membrane and the cristae membrane of the IMM as parallel to the OMM signal or striations along the length of the mitochondrion, respectively. We could also differentiate the IMS into the peripheral IMS and the intercristae space using the same visual cues. This newfound ability to differentiate submitochondrial compartments using super-resolution fluorescence microscopy provides novel methods of acquiring and analyzing structural data.

While we were able to differentiate submitochondrial compartments in fixed cells, we were unable to resolve submitochondrial compartments using 3D-SIM in living cells. As mitochondria are highly dynamic and rapidly moving in living cells, we were unable to acquire images that showed clear differentiation of submitochondrial compartments. The reconstructed images to lack the clearly defined boundaries required for the determination of submitochondrial compartments as was achieved with our 3D-SIM imaging analysis on fixed samples. Improvements in the 3D-SIM imaging system or the dyes and fluorescent tags used to label mitochondrial proteins or compartments may overcome this limitation.

PINK1 is dual targeted depending on the health of mitochondria

The submitochondrial localization of PINK1, a serine/threonine kinase in which loss of function mutations result in recessively inherited forms of early onset PD [5-7], has been studied using various techniques causing inconsistencies throughout the literature. Due to the lack of a reliable method to examine the submitochondrial localization of proteins using fluorescence microscopy, the majority of studies that sought to determine the submitochondrial localization of PINK1 used either electron microscopy (EM) [8-10] or biochemical fractionation [11-14]. While some groups observed that PINK1 resides within the interior structures of the mitochondria [8,9,11,15-17], others have demonstrated PINK1 being anchored to the OMM [10,14,18]. Conflicting reports on PINK1 submitochondrial localization, coupled with the unreliability of previously established methods, underscores the importance of developing a novel reliable method to detect proteins within a particular submitochondrial compartment.

Because dysregulated PINK1 signaling has been implicated in the pathogenesis of PD and PINK1 substrates are located in separate membrane-isolated regions of the mitochondria, it was imperative to clarify PINK1 submitochondrial localization. Previously established methods identified PINK1 to be localized on the OMM or in the IMM/IMS causing confusion in the field. We determined that PINK1 was dual targeted depending on the health of mitochondria. PINK1 is located in the IMM/IMS of healthy mitochondria and located on the OMM of depolarized mitochondria.

The significance of PINK1 dual targeting is just beginning to be elucidated. The role of PINK1 on the OMM has been studied extensively and shown to involve the phosphorylation and activation of parkin and recruiting parkin to mitochondria [19-21].

Because the major focus of PINK1 function has been studying its role on the OMM, this has significantly downplayed the role of PINK1 inside the mitochondria. In addition, prior models of PINK1 mitochondrial signaling either suggest that PINK1 is rapidly degraded inside the mitochondria or that PINK1 remains on the OMM and is not imported into mitochondria. These models ignore the role of PINK1-mediated phosphorylation inside mitochondria that we among others have observed [15].

PINK1 differentially colocalizes with its substrates depending on mitochondrial health

Under healthy, energized conditions, PINK1 resides in the IMM and IMS. Following loss of mitochondrial membrane potential, PINK1 is translocated to the OMM. This dual targeting allows PINK1 to differentially colocalize with, interact with, and phosphorylate substrates localized in different compartments based on mitochondrial health. Thus, we defined PINK1 to be a “molecular switch” that can initiate two separate signaling cascades to maintain mitochondrial homeostasis and protect cells mitochondrial dysfunction. After low levels of mitochondrial stress, PINK1 phosphorylates TRAP1 in the IMM/IMS and phosphorylated TRAP1 protects against oxidative stress induced cell death [15]. PINK1-mediated phosphorylation of TRAP1 rescues mitochondria from dysfunction. In contrast, after high levels of mitochondrial damage and depolarization, PINK1 is translocated to the OMM, where it recruits parkin to damaged mitochondria, initiating mitophagy [16,21,22].

Like PINK1, submitochondrial localization of TRAP1 has also been controversial. We observed TRAP1 in the IMM/IMS while others observed TRAP1 in the matrix [15,23]. Using 3D-SIM, we confirmed our previous study and observed TRAP1 to be

localized to the IMM/IMS [15]. Interestingly, while we observed robust translocation to the OMM of PINK1 following loss of mitochondrial membrane potential, we did not observe any changes in the submitochondrial localization of TRAP1. In both healthy and depolarized conditions, TRAP1 was localized to the IMM/IMS. It has been suggested that PINK1 accumulates on the OMM because protein import is blocked when mitochondria are depolarized [16,19]; however, TRAP1 submitochondrial localization remains unchanged following depolarization. This suggests that the mechanism by which PINK1 localizes to the OMM in depolarized mitochondria is specific to PINK1. The structural determinants required for PINK1 OMM protein translocation following loss of membrane potential should be further investigated.

PINK1 phosphorylation of TRAP1 is likely the first line of defense for mitochondrial damage. PINK1 phosphorylates TRAP1 in response to oxidative stress to protect against mitochondrial dysfunction and oxidative stress induced cell death [15,24-26]. TRAP1 also ameliorates PD-associated α -synuclein induced mitochondrial phenotypes and cell death, suggesting a role for PINK1-mediated phosphorylation of TRAP1 in neuroprotection [27]. Since PINK1-mediated phosphorylation of TRAP1 is required for its cytoprotective function, proper mitochondrial targeting of PINK1 is likely required for TRAP1-mediated cytoprotection. Therefore, although we have not yet identified a PINK1 mutant that does not localize to the IMM/IMS under basal conditions, incorrect PINK1 targeting could be a potential mechanism of pathogenesis due to errors in signaling via reduced TRAP1-mediated cytoprotection.

We demonstrated that loss of mitochondrial membrane potential triggers translocation of PINK1 to the OMM, where it colocalizes with parkin. In this case,

mitochondria are past the point of repair, and in an effort to protect the cell against any deleterious effects caused by the damaged mitochondrion; the damaged mitochondrion is degraded by mitophagy [16,28,29]. Because mitochondria are highly compartmentalized, correct targeting is essential to the functions of mitochondrial proteins. Several disease-linked PINK1 mutants have also been shown to be unable to initiate mitophagy [16,30]; however, prior to this study, the only suggested mechanism was through loss of kinase activity. Using 3D-SIM, we have better characterized the spatiotemporal dynamics of PINK1 in relation to its previously reported substrates.

Reduced OMM-translocation of PINK1 as a novel mechanism of PD pathogenesis

PD-linked mutants of PINK1 are not translocated to the OMM following loss of membrane potential

Once we clearly showed the submitochondrial localization of PINK1, we wanted to determine the significance of PINK1 targeting. We examined the submitochondrial localization of 3 disease linked proteins, C92F, L347P, and W437X, and a mutant lacking the transmembrane domain (Δ TM). While L347P and the W437X truncation mutation both occur within the kinase domain, L347P causes loss of kinase activity, while W437X does not. We demonstrated that the W437X mutation results in loss of OMM-translocation. Interestingly, dual targeting was not affected in the L347P mutant. This suggests that the C-terminal domain, but not kinase activity is required for OMM translocation. The PD-linked mutant PINK1 C92F showed a reduction in OMM translocation, while PINK1 Δ TM OMM translocation was abolished. This suggests that

the transmembrane domain is required for PINK1 OMM-translocation, and PINK1 C92F may have a partially disrupted transmembrane domain. Taken together, this suggests that reduced or inability of PINK1 OMM translocation may be implicated in the pathogenesis of PD.

Translocation-defective PINK1 mutants are unable to recruit parkin to damaged mitochondria

In order to determine the role of PINK1 translocation in neurons, we had to first confirm our ability to distinguish submitochondrial compartments in neurons. We sought to determine if the resolution provided by 3D-SIM was sufficient to differentiate submitochondrial compartments in primary neurons, since mitochondria in neuronal processes are thinner than those in immortalized cells. We were able to easily differentiate OMM and matrix markers, further confirming the power of 3D-SIM super-resolution microscopy in studying submitochondrial localization of proteins in neurons.

Initial difficulties in studying mitophagy in primary neurons have resulted in poor understanding of the dynamics of neuronal mitophagy. Using 3D-SIM, we observed that PINK1 is translocated from the IMM/IMS to the OMM following CCCP treatment in neurons. Confirming our observations in HeLa cells, PINK1 Δ TM and W437X mutants were defective in OMM translocation. Examining the ability of wild type PINK1 and OMM translocation defective mutants Δ TM and W437X to recruit parkin, we observed that only the wild type was able to efficiently recruit parkin. Taken together, this suggests that in neurons, PINK1 translocation may be affected by PD-linked mutations. Following loss of membrane potential and mitochondrial damage, translocation defective mutants

are unable to recruit parkin to damaged mitochondria and mitochondrial localization is necessary for initiation of mitophagy. The failure of PINK1 OMM-translocation by PINK1 W437X or Δ TM likely results in the accumulation of damaged mitochondria, accumulation of reactive oxygen species, loss of efficient mitochondrial respiration, and eventually, cell death. Identification that the PD-linked mutant PINK1 W437X fails to translocate to the OMM following depolarization and recruit parkin suggests that defects in OMM-translocation may be a causative link to PD.

This study clearly establishes that PINK1 is dual targeted depending on the health of the mitochondria; specifically, PINK1 colocalizes with TRAP1 in the IMM/IMS of healthy mitochondria and colocalizes with parkin on the OMM in damaged mitochondria. Because TRAP1 and parkin signaling have been implicated in the maintenance and removal of damaged mitochondria and cytoprotection, PINK1 is likely a molecular switch between these two signaling cascades depending on the degree of mitochondrial damage. Since TRAP1 is localized inside the mitochondria and parkin is located outside the mitochondria, the submitochondrial localization of PINK1 must be tightly regulated for proper mitochondrial signaling. Therefore, we hypothesize that PINK1 mistargeting may result in the dysregulation of mitochondrial signaling required for maintaining a healthy population of mitochondria. PINK1 mistargeting likely causes increased mitochondrial dysfunction, accumulation of ROS, and eventually neuronal dysfunction and death.

Using 3D-SIM to investigate the submitochondrial localization of PINK1 has provided us with a new understanding of the spatiotemporal dynamics of PINK1 related to mitochondrial health. We elucidated new insights about PINK1-mediated

mitochondrial signaling in immortalized cells and primary neurons. Examination of PD-linked mutants suggests that incorrect PINK1 targeting may contribute to mitochondrial dysfunction associated with PD pathogenesis. Further understanding of the role of PINK1 targeting in neuronal mitochondria will provide novel insights into the mechanisms by which PINK1 is neuroprotective.

PINK1 Future Directions

Determine the structural determinants of PINK1 dual targeting

We clearly show that PINK1 dual targeting is dependent on mitochondrial health; however, the mechanism(s) underlying PINK1 dual targeting remains undefined. We have determined that both the transmembrane domain and the C-terminal domain are required for OMM translocation of PINK1, but the mechanism by which PINK1 is mistargeted remains unclear. To determine the necessary regions of PINK1 for OMM translocation, various truncation mutants can be examined. Since W437X affects the C-terminal region of the kinase domain and also the remaining C-terminal of the protein, it is unclear whether the disruption of the kinase domain and/or the C-terminal region results in OMM translocation defects. In addition to removing regions of PINK1 to determine the structural determinants of OMM translocation, we could also attach domains of PINK1 to fluorescent tags to examine their effect on protein submitochondrial targeting. For instance, further investigation should be performed to determine if the mitochondrial targeting sequence, the transmembrane domain, and the C-terminal region

(437-581) are sufficient to direct PINK1 dual targeting. In addition, a BLAST search should then be performed to find other proteins with similar motifs/domains to PINK1. The submitochondrial localization of any candidate proteins should be determined to see if other proteins that undergo similar mitochondrial targeting.

What are the physiological triggers of PINK1 translocation?

Although treatment with CCCP has become a common cellular model to study the effect of mitochondrial depolarization on cells and proteins, the physiological relevance of this model is debated. In cells, and particularly neurons, it is unlikely that the entire mitochondrial network will be depolarized at once. In addition, the rapid changes in mitochondrial biology that occur following CCCP treatment likely do not occur under physiological conditions. However, CCCP is still widely used due to the well-characterized effects and reliable depolarization.

To determine if PINK1 dual targeting has a physiological role in maintaining mitochondrial health and cytoprotection, PINK1 submitochondrial localization should be characterized using a milder agent to depolarize mitochondria. Additional studies should include more subtle mitochondrial insults such as the use of Mito-KillerRed (Evrogen), a fluorescent-tagged protein that localizes to the mitochondrial matrix. The tag can be stimulated to release ROS via a short pulse with a 561 nm laser and damage only the selected mitochondrion within the selected ROI [31]. Following depolarization of an individual mitochondrion via laser activation, PINK1 submitochondrial localization should be characterized.

In addition, PINK1 OMM-translocation should be characterized using *in vivo Drosophila* models. A recent study revealed that wild type flies exhibit regular turnover of mitochondrial proteins, while parkin and PINK1 mutant expressing flies had much slower turnover [32]. This suggests that regular mitophagy is occurring *in vivo* under normal conditions and *in vivo* mitophagy is disrupted by disease-linked mutations in PINK1 or parkin. By placing OMM translocation defective mutants of PINK1 into a *PINK1* deficient fly, we can determine the effect of mistargeting PINK1 on mitophagy rates *in vivo*. Understanding the significance of PINK1 translocation *in vivo* and how that relates to the kinetics of mitochondrial turnover is important to understand PINK1 function and the role of PINK1 translocation dysfunction in PD pathogenesis.

How does PINK1 translocate?

Throughout this study, we show PINK1 resides inside healthy mitochondria and on the OMM of depolarized mitochondria; however, origin of the OMM-localized PINK1 remains undefined. Previous models suggest PINK1 is normally imported into the mitochondria, rapidly degraded, and mitochondrial depolarization blocks protein import and causes PINK1 accumulation on the OMM [16,33]. Our data, however, suggest otherwise. For instance, the OMM-translocation defective mutations are imported into the mitochondria at the same rate as wild type. But when mitochondria are depolarized, OMM-translocation mutants remain inside the mitochondria. If the previously suggested models were true, this would mean that not only was degradation of those mutants impeded, but also, the protein was still able to get imported into the mitochondria. It is unlikely that PINK1 W437X or Δ TM are defective in both rapid degradation and OMM

retention following loss of mitochondrial membrane potential. I suggest a new model in which PINK1 is directly targeted to the OMM following mitochondrial depolarization.

Further studies are needed in order to confirm this new model. The effect of protease inhibitors and proteasome inhibitors on the submitochondrial localization of PINK1 WT and OMM translocation negative mutants should be examined. For instance, by using protease and proteasome inhibitors, we can better determine the fate of the intramitochondrial population of PINK1. If the intramitochondrial PINK1 were rapidly degraded as previously proposed, potentially we would observe a population of PINK1 in both the IMM/IMS and OMM regions following CCCP treatment when blocking protein degradation. Another potential study to determine the source of OMM localized PINK1 is by using PINK1-Dendra. Photoswitchable fluorophore Dendra-labeled PINK1 wild type and OMM-translocation defective PINK1 mutants should be photoswitched from green to red before starting the CCCP treatment. Two hours later, if the PINK1 on the OMM is red, it was specifically translocated. If PINK1 localized on the OMM is green, this would indicate that it's newly translated and transported to the mitochondrion.

Determine the effect of translocation defective PINK1 mutants in cell death and neurodegeneration

To understand the significance of OMM translocation in neuroprotection, the role of PINK1 mitochondrial targeting in cytoprotection needs to be further characterized. Translocation defective mutants C92F, W437X, and Δ TM should be expressed in PINK1 deficient neurons and subjected to mitochondrial insults associated with PD such as rotenone and paraquat. These cells should then be investigated using caspase 3 cleavage

and nuclear fragmentation assays for viability. Interestingly, overexpression of W437X worsens the effects of α -synuclein induced cell death [34], which suggests a toxic gain-of-function. The effects of W437X expression on neuroprotection should be determined in both PINK1-expressing and PINK1-deficient backgrounds to clarify the effects of W437X. Taking this a step further, transgenic mice expressing the translocation defective mutants can be made on a PINK1 knockout background. These mice should be tracked over the course of their lifetime and evaluated for behavioral, pathological, and mitochondrial defects. Moreover, these mice should be subjected to MPTP to see if they have increased susceptibility to mitochondrial toxins compared to the wild type controls.

Determining the submitochondrial localization of PINK1 in patient samples and animal models of PD would provide additional insight into the role of PINK1 submitochondrial targeting in PD pathology. PD patient fibroblasts and neurons derived from induced pluripotent stem cells have been studied extensively as a PD model to get more clinically relevant data [35-40]. Using patient fibroblasts, the spatiotemporal dynamics of PINK1 can be characterized under basal and treated conditions. PINK1 translocation in patients without any mutations in the gene may suggest severe mitochondrial damage while patients with PD that do not exhibit PINK1 OMM-translocation may indicate errors in PINK1 submitochondrial targeting.

MGRN1 DISCUSSION

Mgrn1 is targeted to the outer mitochondrial membrane via *N*-myristoylation

Mgrn1 is primarily localized to mitochondria

Because *Mgrn1* loss results in mitochondrial dysfunction preceding neurodegeneration, this suggests that mitochondrial dysfunction may have a causative link to the pathogenesis of spongiform neurodegeneration [41]. In addition, accumulation of oxidative stress and mitochondrial dysfunction is seen in a wide range of spongiform neurodegenerative disorders, which underscores the relationship between mitochondrial dysfunction and disease [42]. While it has been observed that *Mgrn1* deficient mice exhibit mitochondrial dysfunction, a specific role of *Mgrn1* at the mitochondria was not defined prior to this study. We sought to better understand the role of *Mgrn1* at the mitochondria and characterize the effects of *Mgrn1* loss on mitochondrial health and cytoprotection.

The localization of *Mgrn1* is relevant to its function because as an E3-ubiquitin protein ligase, the proximity of *Mgrn1* to its substrate proteins is crucial to its activity. Errors in *Mgrn1* localization has been implicated in the pathogenesis of spongiform neurodegeneration observed in *Mgrn1* mutant mice [43]. In this study, we confirmed *Mgrn1* endosomal localization, as we have previously reported [44], but also see a large pool of *Mgrn1* localized to mitochondria. Since *Mgrn1* is significantly localized to mitochondria, this suggests that *Mgrn1* might play an active role in mitochondrial biology.

***N*-myristoylation targets Mgrn1 to the OMM**

Since Mgrn1 lacks a mitochondrial targeting sequence and transmembrane domain, we wanted to determine the mechanism(s) behind its mitochondrial targeting. After establishing that Mgrn1 has a putative *N*-myristoylation motif, we determined that wild type Mgrn1, but not the myristoylation negative mutant Mgrn1G2A, is significantly localized to mitochondria suggesting for the first time a direct role in mitochondrial function. Using 3D-SIM we showed that Mgrn1 is localized to the OMM. Because mitochondrial functions are highly compartmentalized, localization of Mgrn1 to the OMM suggests that Mgrn1 does not have a direct role in mitochondrial functions such as respiration, calcium buffering, or redox control. On the other hand, Mgrn1 could play a role in the biology of the OMM including regulation of membrane dynamics or mitochondrial protein import, like other OMM localized E3 ubiquitin-protein ligases [45-47].

Interestingly, when we overexpressed Mgrn1 in HeLa cells we observed altered mitochondrial morphology in the Mgrn1 overexpressing cells compared to the cells overexpressing Mgrn1G2A, Mgrn1mtE3, or a vector control. Specifically, in Mgrn1 WT overexpressing cells we observed elongated and swollen mitochondria. Reflecting on the literature, this “balloon” phenotype is reminiscent of phenotypes seen when overexpressing the fusion proteins Mfn1 or Mfn2 or in fission protein Drp1 depleted cells [48]. This suggests that Mgrn1 might have a role in the regulation of the mitochondrial network, specifically the inhibition of mitochondrial fission or promotion of mitochondrial fusion. Because Mgrn1G2A or Mgrn1mtE3 do not cause the same phenotype, mitochondrial localization and E3 ubiquitin-protein ligase activity are

required for Mgrn1-mediated mitochondrial elongation. Since mitochondrial morphology is so closely tied to mitochondrial function, altered morphology of the mitochondrial network may be closely tied to the mitochondrial dysfunction observed in Mgrn1 mutant mice.

Mgrn1 maintains mitochondrial health

Loss of Mgrn1 results in mitochondrial fragmentation

Although Mgrn1 mutant mice exhibit mitochondrial dysfunction, the mechanisms by which mitochondria become damaged in Mgrn1 mutant mice remain unclear. Since altered mitochondrial dynamics is heavily implicated in the pathogenesis of many neurodegenerative diseases, we sought to characterize the mitochondrial network in primary cortical neurons cultured from wild type and Mgrn1 mutant mice. Mgrn1 mutant primary cortical neurons exhibited a very pronounced mitochondrial fragmentation phenotype when imaging using live cell confocal microscopy. Instead of a reticular mitochondrial network with a tubular structure as seen in wild type neurons Mgrn1 mutant cortical neurons had mitochondria shorter in length with a “donut” shape. Since the function of mitochondria is so closely tied to its structure, this altered structure could be indicative of mitochondrial dysfunction. In addition, these mitochondria were more clustered in the cell body as opposed to in the processes of the neurons, suggesting a mitochondrial trafficking defect. Dysregulated mitochondrial trafficking can result in energy deficits in subdomains of neurons and neuronal death. Fragmented and clustered

mitochondria observed in Mgrn1 mutant cortical neurons are similar to what is seen in patients and animal models of spongiform neurodegenerative disorders [49-52]. Dysregulation of the mitochondrial network and distribution of mitochondria in neurons may contribute to mitochondrial dysfunction and neurodegeneration in Mgrn1 mutant mice.

Loss of Mgrn1 results in mitochondrial dysfunction

After observing fragmented mitochondria in Mgrn1 mutant neurons, we wanted to further characterize the mitochondrial health in wild type and mutant neurons. Mitochondria in Mgrn1 mutant neurons exhibit reduced mitochondrial membrane potential as seen when staining cells with TMRE compared to wild type neurons, suggesting these mitochondria are severely damaged. Loss of membrane potential can affect multiple functions of the mitochondria including respiration, protein import, calcium sensing, and calcium signaling. The mitochondrial localization of Mgrn1 and mitochondrial defects observed in Mgrn1-deficient cells suggest that Mgrn1 regulates mitochondrial health.

Time-lapse confocal fluorescence microscopy revealed that the mitochondria in Mgrn1 mutant neurons were static and did not exhibit anterograde or retrograde movement. Mitochondrial movement is essential to respond to energy demands in the cell. Neurons are especially sensitive to defects in mitochondrial trafficking because of their complicated architecture, long distances between the cell body, where mitochondria are made *de novo*, and distal regions of the neuron with high-energy demands. Taken together, this suggests that Mgrn1 is essential for regulating the mitochondrial network,

and that loss of mitochondrial trafficking has a direct effect on maintaining mitochondrial morphology and homeostasis.

Ubiquitination of Mgrn1 mitochondrial substrate(s) may confer cytoprotection

Since mitochondria play several essential roles in the cell and mitochondrial dysfunction is associated with the accumulation of toxic ROS, mitochondrial dysfunction and cell death are closely linked. Mgrn1 deficient neurons are more susceptible to oxidative stress induced cell death. This is interesting for a few reasons. First, we determined that Mgrn1 mutant neurons exhibit mitochondrial dysfunction. Once there are increased ROS, Mgrn1 deficient neurons have an increased susceptibility to cell death. This suggests that Mgrn1 might not just have a role in preventing accumulation of ROS in the cell through regulating mitochondrial dynamics, but also in cytoprotection against cell death. This suggests that Mgrn1 may have a role in regulating mitochondrial dynamics and health in response to oxidative stress. This effect can be rescued with expression of the wild type Mgrn1, but not Mgrn1G2A or Mgrn1mtE3. Taken together, this suggests that Mgrn1 plays an essential role in cytoprotection of neurons and that loss of Mgrn1 is clearly linked to increased death of neurons in Mgrn1 mutant mice. Because neurodegeneration observed in Mgrn1 mutant mice is age dependent and mitochondrial dysfunction and oxidative stress accumulates with age, Mgrn1 likely plays a role in the maintenance of mitochondria against age related stress.

Mgrn1 Future Directions

Identification of mitochondrial substrates of Mgrn1-mediated ubiquitination

To date, no mitochondrial substrates of Mgrn1-mediated ubiquitination have been identified. Without a mitochondrially-localized substrate, the precise role of Mgrn1-mediated ubiquitination on mitochondrial dynamics remains unclear. To find a mitochondrial substrate of Mgrn1, mitochondrially localized Mgrn1 can be subjected to mass spectrometry. Briefly, epitope tagged-Mgrn1 can be exogenously expressed in cells, mitochondria can be purified from the cell lysates, lysed, and Mgrn1 can be pulled down from the resulting mitochondrial fraction. The resulting pulldown can be subjected to mass spectrometry. To verify the candidate substrate(s) of Mgrn1-mediated ubiquitination, the interaction can be tested via coimmunoprecipitation. *In vivo* and *in vitro* ubiquitination assays using wild type Mgrn1 and mtE3 Mgrn1 can be performed under various conditions to determine if Mgrn1 does indeed ubiquitinate the substrate(s) of interest.

If mitochondrially localized substrates of Mgrn1-mediated ubiquitination cannot be determined using mass spectrometry methods, proteins involved in mitochondrial fusion and fission would be ideal candidates to test. While ubiquitination is most known for its role in tagging proteins to be delivered to the proteasome for degradation, ubiquitination can also regulate the activity of proteins. Since our data suggest that

Mgrn1 promotes mitochondrial elongation, Mgrn1 may ubiquitinate Drp1 to reduce its expression or activity, or it could ubiquitinate mitofusins in order to increase their activity. To test if Mgrn1 ubiquitinates any of the fusion or fission proteins, coimmunoprecipitation assays and ubiquitination assays can be performed.

If neither mass spectrometry nor coimmunoprecipitation with the fusion and fission proteins reveals a substrate of Mgrn1-mediated ubiquitination at the mitochondria, potentially Mgrn1 regulates another protein that regulates mitochondrial fission and/or fusion. Some other potential substrates to check via coimmunoprecipitation and ubiquitination would be March5, MULAN, or the kinases and phosphatases that regulate Drp1 function. Once a mitochondrial substrate of Mgrn1-mediated ubiquitination is identified, the ubiquitin linkage should be determined. Then the fate of the ubiquitinated substrate should be investigated to define the precise role that Mgrn1 has on mitochondrial dynamics.

Does Mgrn1 inhibit mitochondrial fission or promote mitochondrial fusion?

We observed elongation of the mitochondrial network with overexpression of Mgrn1 and fragmentation in Mgrn1 deficient neurons. But since mitochondrial morphology is a balance between mitochondrial fusion and fission, we do not know if Mgrn1 expression affects mitochondrial fusion or mitochondrial fission. Aside from the identification of substrates of Mgrn1-mediated ubiquitination, the effect of Mgrn1 on mitochondrial fusion and fission can be observed. Mitochondrial dynamics can be tracked using time-lapse fluorescence confocal microscopic analysis in various conditions overexpressing and depleting Mgrn1 expression. In addition, mitochondrial dynamics can

be observed in wild type and Mgrn1 mutant cortical neurons. There are a few ways to evaluate mitochondrial fusion utilizing the mixing of mitochondrial contents during fusion events. One potential method would be using the photoswitchable fluorophore, Mito-Dendra and watching the spread of red fluorescent mitochondria over time [53]. In addition, watching the spread of fluorescence from two separate cells with differentially fluorescent mitochondria joined through polyethylene glycol (PEG) – cell fusion. Both mitochondrial fusion and fission events can be manually tracked over time.

How do the mitochondrial and endosomal roles of Mgrn1 contribute to neuronal health?

Mgrn1 is significantly localized to two separate subcellular compartments, mitochondria and early endosomes and the precise cytoprotective role of Mgrn1 at either site remains unclear. In order to truly understand the role that Mgrn1 dysfunction has on spongiform neurodegenerative disease pathogenesis, the contribution of Mgrn1 localization to endosomes and mitochondria must each be investigated separately.

First, the mechanism by which Mgrn1 is targeted to each subcellular compartment must be determined. We have previously shown that Mgrn1 localization is dependent on its interaction with TSG101 [44]. Interestingly, it also appears that mutating the PSAP tetrapeptide motif responsible for the TSG101 interaction also disrupts the localization to mitochondria because the cellular distribution Mgrn1ASAA appears to be entirely cytosolic [44]. To determine targeting signals required for Mgrn1 localization to endosomes and mitochondria, mapping studies should be performed. The subcellular localization of the truncations should be evaluated and compared to see which truncations

yield more or less localization to either endosomes or mitochondria. If there are particular regions that seem important for targeting, those regions can be investigated more closely by creating point mutations within those regions of the protein.

Like Mgrn1 localization to early endosomes, mitochondrial localization of Mgrn1 may be dependent on its interaction with its mitochondrial substrate(s). Once a mitochondrial substrate of Mgrn1-mediated ubiquitination has been discovered, the interaction between Mgrn1 and its mitochondrial substrate can be mapped to determine if mutation of that site disrupts mitochondrial localization. Potentially, mutations of the residues required for the interaction between Mgrn1 and its substrate could affect mitochondrial localization.

After the regions and domains of Mgrn1 required for endosomal and mitochondrial localization are determined, isoforms of mitochondrially localized and endosome localized Mgrn1 can be constructed. Then, the effect of each isoform of Mgrn1 on cell function and health should be determined. Overexpressing each in a Mgrn1 deficient background, such as Mgrn1 mutant neurons, and then examining the endosome, lysosome, and mitochondrial morphology, rates of respiration, rates of cellular replication, and sensitivity to various cell stressors should be determined. This would clarify the specific roles that Mgrn1 localization to endosomes and mitochondria have on the onset of neurodegenerative diseases. In addition, quantification of Mgrn1 localization to endosomes and mitochondria should be determined in primary neuronal cells and brain tissue to determine the contribution of Mgrn1 activity at either subcellular site.

What is the link between Mgrn1 deficiency and spongiform neurodegenerative diseases?

Although the neurodegeneration exhibited by Mgrn1 mutant mice closely resembles the neurodegeneration exhibited by mouse models of prion disease, neurodegeneration occurs without deposition of protease resistant prion and Mgrn1 expression has no effect on prion pathogenesis [54,55]. On the other hand, cytosolically exposed prion (PrP^{ctm}) can sequester Mgrn1 where it is assumed Mgrn1 cannot ubiquitinate its substrates leading to functional depletion of Mgrn1 [43]. Taken together, the role of Mgrn1 in prion pathogenesis is controversial. We must consider that loss of Mgrn1 may serve as a better model for a different neurodegenerative disease.

We have preliminary data (not shown) that Mgrn1 mutant mice exhibit lysosomal defects and accumulation of lipids similar in morphology to lysosome storage diseases such as Neimann Pick Disease Type C and interestingly, lysosomal storage disorders also exhibit mitochondrial dysfunction. In order to use Mgrn1 mutant mice as an effective model for spongiform neurodegenerative diseases, the disease(s) that Mgrn1 deficiency most closely resembles should be identified. Specifically, Mgrn1 mutant mice should be compared more closely to various spongiform neurodegenerative diseases in pathology and behavioral phenotypes. The levels, subcellular localization, and activity of Mgrn1 should be investigated in other spongiform neurodegenerative diseases. In addition, the effect of Mgrn1 expression on the pathogenesis of other types of spongiform neurodegenerative diseases should be investigated in animal models.

FINAL WORDS

Mitochondria are essential organelles involved in many important cellular processes. Without properly functioning mitochondria, cells, especially neurons, are susceptible to cell dysfunction and death. The two proteins examined in this study, PINK1 and Mgrn1, play important roles in maintaining mitochondrial health. The dual targeting of PINK1 depending on the health of mitochondria serves as a molecular switch in that it can initiate two separate signaling cascades depending on the extent of mitochondrial damage. In low levels of mitochondrial damage, PINK1 colocalizes with TRAP1 in the IMM/IMS where it can phosphorylate TRAP1 in an effort to save the mitochondria. Following severe mitochondrial damage, PINK1 translocates to the OMM where it colocalizes with parkin to phosphorylate parkin to initiate mitophagy. Since we observed mitochondrial elongation with Mgrn1 overexpression and fragmentation with loss of Mgrn1 expression, Mgrn1 is likely involved in regulating mitochondrial dynamics. The OMM localization of Mgrn1 suggests that Mgrn1 is likely directly involved with either promoting mitochondrial fusion or inhibiting mitochondrial fission. Mitochondrial fusion is essential for maintaining mitochondrial homeostasis because it allows damaged mitochondria to recombine their mtDNA and dilute toxic material within a single mitochondrion over the entire network suggesting Mgrn1 may respond to mitochondrial stress. Loss of Mgrn1 results in fragmented mitochondria, which is associated with mitochondrial dysfunction and disease.

Understanding the roles of PINK1 and Mgrn1 in regulating mitochondrial health, morphology, and function is essential for understanding the roles that these proteins have

in protection against cell death and disease. As the link between mitochondrial dysfunction and neurodegenerative diseases is becoming more defined, the role of these proteins in mitochondrial signaling becomes of higher interest. Novel methods to study the proteins involved in mitochondrial signaling and health, such as 3D-SIM, are needed to be able to answer the increasingly difficult questions regarding mitochondrial dysfunction in neurodegenerative diseases. More focus needs to be placed on asking questions about mitochondrial function and therapeutic approaches to neurodegenerative disorders associated with mitochondrial dysfunction. The application of 3D-SIM to investigate the role of PINK1 spatiotemporal dynamics in mitochondrial health and disease has provided novel insights into PINK1 function in neuroprotection.

References

1. Schnaitman, C. and J.W. Greenawalt, Enzymatic properties of the inner and outer membranes of rat liver mitochondria. 1968. *J Cell Biol*, **38**(1): 158-75.
2. Faulk, W.P. and G.M. Taylor, An immunocolloid method for the electron microscope. 1971. *Immunochemistry*, **8**(11): 1081-3.
3. Venditti, P., et al., Functional and biochemical characteristics of mitochondrial fractions from rat liver in cold-induced oxidative stress. 2004. *Cell Mol Life Sci*, **61**(24): 3104-16.
4. Somekh, M.G., et al., Resolution in structured illumination microscopy: a probabilistic approach. 2008. *J Opt Soc Am A Opt Image Sci Vis*, **25**(6): 1319-29.
5. Bonifati, V., et al., Early-onset parkinsonism associated with PINK1 mutations: frequency, genotypes, and phenotypes. 2005. *Neurology*, **65**(1): 87-95.
6. Hatano, Y., et al., Novel PINK1 mutations in early-onset parkinsonism. 2004. *Ann Neurol*, **56**(3): 424-7.
7. Valente, E.M., et al., PINK1 mutations are associated with sporadic early-onset parkinsonism. 2004. *Ann Neurol*, **56**(3): 336-41.
8. Muqit, M.M., et al., Altered cleavage and localization of PINK1 to aggresomes in the presence of proteasomal stress. 2006. *J Neurochem*, **98**(1): 156-69.
9. Silvestri, L., et al., Mitochondrial import and enzymatic activity of PINK1 mutants associated to recessive parkinsonism. 2005. *Hum Mol Genet*, **14**(22): 3477-92.
10. Vives-Bauza, C., et al., PINK1-dependent recruitment of Parkin to mitochondria in mitophagy. 2010. *Proc Natl Acad Sci U S A*, **107**(1): 378-83.
11. Gandhi, S., et al., PINK1 protein in normal human brain and Parkinson's disease. 2006. *Brain*, **129**(Pt 7): 1720-31.
12. Jin, S.M., et al., Mitochondrial membrane potential regulates PINK1 import and proteolytic destabilization by PARL. 2010. *J Cell Biol*, **191**(5): 933-42.
13. Lin, W. and U.J. Kang, Structural determinants of PINK1 topology and dual subcellular distribution. 2010. *BMC Cell Biol*, **11**: 90.
14. Zhou, C., et al., The kinase domain of mitochondrial PINK1 faces the cytoplasm. 2008. *Proc Natl Acad Sci U S A*, **105**(33): 12022-7.
15. Pridgeon, J.W., et al., PINK1 protects against oxidative stress by phosphorylating mitochondrial chaperone TRAP1. 2007. *PLoS Biol*, **5**(7): e172.
16. Narendra, D.P., et al., PINK1 is selectively stabilized on impaired mitochondria to activate Parkin. 2010. *PLoS Biol*, **8**(1): e1000298.
17. Mills, R.D., et al., Biochemical aspects of the neuroprotective mechanism of PTEN-induced kinase-1 (PINK1). 2008. *J Neurochem*, **105**(1): 18-33.
18. Becker, D., et al., Pink1 kinase and its membrane potential ($\Delta\psi$)-dependent cleavage product both localize to outer mitochondrial membrane by unique targeting mode. 2012. *J Biol Chem*, **287**(27): 22969-87.
19. Lazarou, M., et al., Role of PINK1 binding to the TOM complex and alternate intracellular membranes in recruitment and activation of the E3 ligase Parkin. 2012. *Dev Cell*, **22**(2): 320-33.
20. Kane, L.A., et al., PINK1 phosphorylates ubiquitin to activate Parkin E3 ubiquitin ligase activity. 2014. *J Cell Biol*.

21. Kondapalli, C., et al., PINK1 is activated by mitochondrial membrane potential depolarization and stimulates Parkin E3 ligase activity by phosphorylating Serine 65. 2012. *Open Biol*, **2**(5): 120080.
22. Narendra, D., et al., Parkin-induced mitophagy in the pathogenesis of Parkinson disease. 2009. *Autophagy*, **5**(5): 706-8.
23. Cechetto, J.D. and R.S. Gupta, Immunoelectron microscopy provides evidence that tumor necrosis factor receptor-associated protein 1 (TRAP-1) is a mitochondrial protein which also localizes at specific extramitochondrial sites. 2000. *Exp Cell Res*, **260**(1): 30-9.
24. Costa, A.C., et al., Drosophila Trap1 protects against mitochondrial dysfunction in a PINK1/parkin model of Parkinson's disease. 2013. *Cell Death Dis*, **4**: e467.
25. Hua, G., et al., Heat shock protein 75 (TRAP1) antagonizes reactive oxygen species generation and protects cells from granzyme M-mediated apoptosis. 2007. *J Biol Chem*, **282**(28): 20553-60.
26. Zhang, L., et al., TRAP1 rescues PINK1 loss-of-function phenotypes. 2013. *Hum Mol Genet*, **22**(14): 2829-41.
27. Butler, E.K., et al., The mitochondrial chaperone protein TRAP1 mitigates alpha-Synuclein toxicity. 2012. *PLoS Genet*, **8**(2): e1002488.
28. Darios, F., et al., Parkin prevents mitochondrial swelling and cytochrome c release in mitochondria-dependent cell death. 2003. *Hum Mol Genet*, **12**(5): 517-26.
29. Narendra, D., et al., Parkin is recruited selectively to impaired mitochondria and promotes their autophagy. 2008. *J Cell Biol*, **183**(5): 795-803.
30. Geisler, S., et al., The PINK1/Parkin-mediated mitophagy is compromised by PD-associated mutations. 2010. *Autophagy*, **6**(7): 871-8.
31. Bulina, M.E., et al., Chromophore-assisted light inactivation (CALI) using the phototoxic fluorescent protein KillerRed. 2006. *Nat Protoc*, **1**(2): 947-53.
32. Vincow, E.S., et al., The PINK1-Parkin pathway promotes both mitophagy and selective respiratory chain turnover in vivo. 2013. *Proc Natl Acad Sci U S A*, **110**(16): 6400-5.
33. Matsuda, N., et al., PINK1 stabilized by mitochondrial depolarization recruits Parkin to damaged mitochondria and activates latent Parkin for mitophagy. 2010. *J Cell Biol*, **189**(2): 211-21.
34. Marongiu, R., et al., Mutant Pink1 induces mitochondrial dysfunction in a neuronal cell model of Parkinson's disease by disturbing calcium flux. 2009. *J Neurochem*, **108**(6): 1561-74.
35. Rakovic, A., et al., Effect of endogenous mutant and wild-type PINK1 on Parkin in fibroblasts from Parkinson disease patients. 2010. *Hum Mol Genet*, **19**(16): 3124-37.
36. Seibler, P., et al., Mitochondrial Parkin recruitment is impaired in neurons derived from mutant PINK1 induced pluripotent stem cells. 2011. *J Neurosci*, **31**(16): 5970-6.
37. Mortiboys, H., et al., Mitochondrial function and morphology are impaired in parkin-mutant fibroblasts. 2008. *Ann Neurol*, **64**(5): 555-65.
38. Rakovic, A., et al., Mutations in PINK1 and Parkin impair ubiquitination of Mitofusins in human fibroblasts. 2011. *PLoS One*, **6**(3): e16746.

39. Exner, N., et al., Loss-of-function of human PINK1 results in mitochondrial pathology and can be rescued by parkin. 2007. *J Neurosci*, **27**(45): 12413-8.
40. Hoepken, H.H., et al., Parkinson patient fibroblasts show increased alpha-synuclein expression. 2008. *Exp Neurol*, **212**(2): 307-13.
41. Sun, K., et al., Mitochondrial dysfunction precedes neurodegeneration in mahogunin (*Mgrn1*) mutant mice. 2007. *Neurobiol Aging*, **28**(12): 1840-52.
42. Beal, M.F., Mitochondria take center stage in aging and neurodegeneration. 2005. *Ann Neurol*, **58**(4): 495-505.
43. Chakrabarti, O. and R.S. Hegde, Functional depletion of mahogunin by cytosolically exposed prion protein contributes to neurodegeneration. 2009. *Cell*, **137**(6): 1136-47.
44. Kim, B.Y., et al., Spongiform neurodegeneration-associated E3 ligase Mahogunin ubiquitylates TSG101 and regulates endosomal trafficking. 2007. *Mol Biol Cell*, **18**(4): 1129-42.
45. Fang, L., et al., Inactivation of MARCH5 prevents mitochondrial fragmentation and interferes with cell death in a neuronal cell model. 2012. *PLoS One*, **7**(12): e52637.
46. Tang, F., et al., RNF185, a novel mitochondrial ubiquitin E3 ligase, regulates autophagy through interaction with BNIP1. 2011. *PLoS One*, **6**(9): e24367.
47. Li, W., et al., Genome-wide and functional annotation of human E3 ubiquitin ligases identifies MULAN, a mitochondrial E3 that regulates the organelle's dynamics and signaling. 2008. *PLoS One*, **3**(1): e1487.
48. Lee, Y.J., et al., Roles of the mammalian mitochondrial fission and fusion mediators Fis1, Drp1, and Opa1 in apoptosis. 2004. *Mol Biol Cell*, **15**(11): 5001-11.
49. Choi, S.I., et al., Mitochondrial dysfunction induced by oxidative stress in the brains of hamsters infected with the 263 K scrapie agent. 1998. *Acta Neuropathol*, **96**(3): 279-86.
50. Walis, A., et al., Ultrastructural changes in the optic nerves of rodents with experimental Creutzfeldt-Jakob Disease (CJD), Gerstmann-Straussler-Scheinker disease (GSS) or scrapie. 2003. *J Comp Pathol*, **129**(2-3): 213-25.
51. Park, J.H., et al., Association of endothelial nitric oxide synthase and mitochondrial dysfunction in the hippocampus of scrapie-infected mice. 2011. *Hippocampus*, **21**(3): 319-33.
52. Siskova, Z., et al., Morphological and functional abnormalities in mitochondria associated with synaptic degeneration in prion disease. 2010. *Am J Pathol*, **177**(3): 1411-21.
53. Magrane, J., et al., Mitochondrial dynamics and bioenergetic dysfunction is associated with synaptic alterations in mutant SOD1 motor neurons. 2012. *J Neurosci*, **32**(1): 229-42.
54. Silviu, D., et al., Levels of the Mahogunin Ring Finger 1 E3 ubiquitin ligase do not influence prion disease. 2013. *PLoS One*, **8**(1): e55575.
55. He, L., et al., Spongiform degeneration in mahoganoid mutant mice. 2003. *Science*, **299**(5607): 710-2.